NATIONAL ADVISORY COMMITTEE FOR AERONAUTICS

TECHNICAL NOTE 3235

LOW-SPEED YAWED-ROLLING AND SOME OTHER ELASTIC

CHARACTERISTICS OF TWO 56-INCH-DIAMETER,

24-PLY-RATING AIRCRAFT TIRES

By Walter B. Horne, Bertrand H. Stephenson,
and Robert F. Smiley

Langley Aeronautical Laboratory
Langley Field, Va.

Washington

August 1954

H.

NATIONAL ADVISORY COMMITTEE FOR AERONAUTI

TECHNICAL NOTE 3235

LOW-SPEED YAWED-ROLLING AND SOME OTHER ELASTIC

CHARACTERISTICS OF TWO 56-INCH-DIAMETER,

24-PLY-RATING AIRCRAFT TIRES

By Walter B. Horne, Bertrand H. Stephenson,
and Robert F. Smiley

SUMMARY

The low-speed (up to 4 miles per hour) cornering characteristics of two 56 × 16, type VII, extra-high-pressure, 24-ply-rating tires were determined for a range of vertical loadings, yaw angles, and tire inflation pressures. Locked-wheel drag tests were also made for one vertical-load condition. The quantities measured included cornering force, drag force, self-alining torque, pneumatic caster, vertical tire deflection, rolling radius, and relaxation length. Some supplementary tests were made which included measurements of tire footprint area, vertical-load-deflection characteristics, and the variation of tire radius and width with inflation pressure.

Results indicated that the normal force reached a maximum at between 14° and 18° yaw. The self-alining torque increased with yaw angle up to between 5° and 8° yaw where a maximum was reached. Increasing the yaw angle beyond this point tended to decrease the self-alining torque considerably. The pneumatic caster was a maximum at small yaw angles and tended to decrease in value with increasing yaw angle. The yawed-rolling and sliding drag coefficients of friction both tended to decrease in magnitude with increasing average bearing pressure. In general, the test results indicate that the relaxation length decreases with increasing vertical tire deflection and increasing inflation pressure.

INTRODUCTION

Existing experimental data on aircraft tire behavior under static, kinematic, and dynamic conditions, most of which are discussed in reference 1, are limited in both scope and quantity particularly for large tires. This lack of scope has hindered those engaged in design problems concerning landings with yaw, ground handling, and wheel shimmy. A program was therefore undertaken to determine values of the essential tire parameters for a range of tire sizes under static, kinematic, and dynamic

conditions. Some static force-deflection tests of the program have been
completed and the results were reported in reference 2. The present
paper presents results from part of the kinematic test program for two
56-inch-diameter, 56 × 16, type VII, extra-high-pressure, 24-ply-rating
tires.

Most of the test consisted of towing the tire specimens in a yawed
condition. The yaw-angle range covered was from about 0° to 18° and the
inflation-pressure range, from about 30 psi to 230 psi. The vertical
loads covered ranged from about 10,000 to 45,000 pounds per tire. The
towing speed was held constant for each run and did not exceed 4 miles
per hour. The quantities measured included vertical tire deflection,
side force, drag force, self-alining torque, pneumatic caster, rolling
radius, and relaxation length. Relaxation-length measurements were also
determined for the case of approximately zero yaw for both a standing
and rolling tire.

Drag tests were conducted with the wheels locked to obtain measure-
ments in the fore-and-aft direction of the sliding coefficient of fric-
tion and the stiffness of the tires. Some supplementary tests were made
which included measurements of footprint area, vertical-load—deflection
characteristics, and the variation of tire radius and width with infla-
tion pressure.

SYMBOLS

A_g	gross footprint area, sq in.
A_n	net footprint area, sq in.
b	overall tire-ground contact width, in.
d	outside diameter of free tire, in.
F	force, lb
F_R	resultant force, $\sqrt{F_x^2 + F_y^2}$, lb
F_x	drag or fore-and-aft force (ground force parallel to direction of motion), lb
F_y	cornering force (steady-state ground force perpendicular to direction of motion), lb

F_{y_i} instantaneous ground force perpendicular to direction of motion, lb

F_z vertical load on tire, lb

F_ψ normal force (ground force perpendicular to wheel plane, $F_y \cos \psi + F_x \sin \psi$), lb

$2h$ overall tire-ground contact length, in.

K_x fore-and-aft spring constant, $\left(\dfrac{dF_x}{dx}\right)_{x \to 0}$, lb/in.

L relaxation length, in.

L_f unyawed-rolling-force relaxation length of tire, in.

L_s static relaxation length of tire, in.

L_y yawed-rolling relaxation length of tire, in.

L_λ unyawed-rolling-deflection relaxation length of tire, in.

ΔM_z measured portion of self-alining torque, lb-in.

M_{z_0} self-alining torque for $\psi = 0.35^o$, lb-in.

M_z self-alining torque, $\Delta M_z + M_{z_0}$, lb-in.

N cornering power (rate of change of cornering force or normal force with yaw angle for small yaw angles, $dF_y/d\psi$ or $dF_\psi/d\psi$ for $\psi \to 0$), lb/deg

p tire inflation pressure, lb/sq in.

p_0 tire inflation pressure at zero vertical load ($F_z = 0$), lb/sq in.

p_g average gross footprint pressure, F_z/A_g, lb/sq in.

p_n average tire-ground bearing pressure, F_z/A_n, lb/sq in.

p_r rated tire inflation pressure, lb/sq in.

q   pneumatic caster, M_Z/F_ψ, in.

r   outside radius of free tire, in.

r_e rolling radius, in.

s   circumferential distance around the tire, ft

v   rolling velocity, ft/sec

w   maximum tire width, in.

x   displacement in direction of motion, in. or ft

δ vertical tire deflection due to combined vertical and yaw
         loads, in.

δ_0 vertical tire deflection due to vertical load only, in.

η interpolation factor, in.^{3}/deg

λ lateral distortion of the tire equator, in.

λ_0 lateral distortion of tire equator at center of
         contact, in.

μ_x sliding drag coefficient of friction, $F_{X_{max}}/F_Z$

μ_ψ yawed-rolling coefficient of friction, $F_{R_{max}}/F_Z$

ψ angle of yaw, deg

ω wheel rotation, radians

Subscript:

max   maximum

    Bars over symbols denote the average value of the quantities
involved for tires A and B.

DEFINITIONS OF CONCEPTS

Inasmuch as some of the quantities used in this paper are not generally very well known, the following definitions are given to aid the reader.

Footprint area.- The tire contacts the ground in a finite area the shape of which is illustrated in figure 1. Because the tires tested had a rib-type tread, this area consists of alternate strips where the tire contacts the ground and where it does not contact the ground (corresponding to the spaces between the treads). The total area, including the spaces between the treads, is designated as the gross footprint area of the tire. The actual ground-contact area, or bearing area, is referred to as the net footprint area.

Yawed-rolling characteristics.- If a pneumatic-tired wheel is towed unbraked in a straight line while yawed by an angle ψ, it develops an elastic side force which, for small yaw angles, is roughly proportional to the yaw angle. The component of this side force perpendicular to the direction of motion is called the cornering force F_y. The initial rate of change of cornering force with yaw angle is called the cornering power N $\left[\text{that is, } N = \left(\dfrac{dF_y}{d\psi}\right)_{\psi \to 0}\right]$. The yawed-rolling condition also produces a ground moment on the tire which is called the self-alining torque M_z. Other yawed-rolling forces are the drag force F_x (parallel to the direction of motion) and the component of the side force perpendicular to the wheel center plane or normal force F_ψ.

Relaxation length.- The relaxation length is a tire property which has been defined by Temple in reference 3. Consider the situation where the base or ground-contact area of an unyawed tire is laterally deflected relative to the wheel and the wheel is then rolled straight ahead in its initial plane. After the tire has rolled forward a distance equal to the footprint length, then, from that point on, according to the experiments of Kantrowitz (ref. 4) and others, the lateral tire deflection λ_0 dies out exponentially with the distance x rolled. The distance that the tire must roll forward in order for the lateral deflection λ_0 to drop to a fraction $1/e$ of its initial value has been defined by Temple as the relaxation length of the tire. In other words, the variation of lateral deflection λ_0 with distance x rolled is governed by an equation of the type

$$\lambda_o = A_1 e^{-x/L} \tag{1}$$

where A_1 is a constant depending on the initial lateral tire deflection and L is the relaxation length.

The preceding definition of relaxation length in terms of the result of an unyawed-rolling experiment is only one of a number of ways in which this quantity might be defined. Four other slightly different methods of defining this quantity which were employed in the present investigation will now be described. From the point of view of the theory of reference 5, these definitions and the corresponding experiments should lead to the same numerical value of relaxation length; however, because this theory is not completely rigorous, it is not unexpected that the different definitions to be given will not lead to precisely the same value of relaxation length. In order to distinguish these different values of relaxation length to be discussed, they are assigned different names and symbol subscripts.

Static relaxation length L_s.- Consider the experiment where the ground-contact area of a stationary tire is deflected laterally with respect to the wheel plane. The different parts of the center band or equator of the tire are then deflected sidewise from the wheel center plane in the manner illustrated in figure 2. From the available experimental data, it is found that, except in and near the edge of the ground-contact area and near the top of the tire, this distortion curve is essentially an exponential curve of the form

$$\lambda = A_2 e^{-s/L_s} \tag{2}$$

where λ is the lateral distortion of the tire equator, A_2 is a constant, and s is the circumferential distance about the tire. The exponential constant L_s is called the static relaxation length of the tire.

Unyawed-rolling-deflection relaxation length L_λ.- The next definition of relaxation length to be considered is a minor modification of the original definition for the unyawed-rolling case (eq. 1) which is designed to take into account the fact that, owing to experimental difficulties, it was not possible to attain exactly the condition of zero yaw angle in the tests of the present paper. Actually, the minimum yaw angle attained was about $0.35°$. In order to take this small yaw angle into account in the definition of relaxation length, the theory of reference 5 indicates that equation (1) should be replaced by the equation

$$\lambda_0 = \lambda_\infty + A_3 e^{-x/L_\lambda} \tag{3}$$

where A_3 is a constant depending on the initial tire deflection, λ_∞ is the measured tire deflection for steady yawed rolling at the small angle of yaw, and L_λ is a constant which will be called the unyawed-rolling-deflection relaxation length.

Unyawed-rolling-force relaxation length L_f.- In view of the fact that tire lateral force is approximately proportional to tire lateral deflection, the relaxation length for the unyawed-rolling-deflection relaxation-length test could also be determined by measuring the rate of decay of the lateral force F_{y_i} with distance x rolled. This decay proceeds in accordance with the equation

$$F_{y_i} = F_y + A_4 e^{-x/L_f} \tag{4}$$

analogous to equation (3) where F_y is the measured side force for steady yawed rolling at the small angle of yaw and A_4 is a constant. The corresponding relaxation length L_f is called the unyawed-rolling-force relaxation length.

Yawed-rolling relaxation length L_y.- Another definition of relaxation length may be obtained in connection with the experiment where a wheel is set up at an angle of yaw and is then rolled straight ahead. If no skidding occurs, then, according to theory (ref. 5) and to the present test results, after the wheel has rolled forward a distance approximately equal to the footprint length $2h$, the tire builds up a side force which exponentially approaches an end-point condition for steady yawed rolling; that is, the side force F_{y_i} builds up with distance x rolled according to a relation of the form

$$F_{y_i} = F_y - A_5 e^{-x/L_y} \tag{5}$$

where the constant A_5 depends on the initial tire distortion and L_y is called the yawed-rolling relaxation length.

Rolling radius.- The rolling radius of a tire is defined as the ratio of the component of the rolling velocity parallel to the plane of the wheel $v \cos \psi$ to the angular velocity of the wheel about the axle ω

or as the ratio of the component of the rolling displacement parallel
to the plane of the wheel to the angular rotation of the wheel.

APPARATUS

Test Vehicle

The basic test vehicle consisted of the fuselage and wing center
section of a surplus cargo airplane; general views of this vehicle are
shown in figures 3 to 5. The airplane was towed tail first by a tractor
truck at an attitude such that the original airplane shock struts were
vertical. This attitude was necessary in order to use the existing
landing-gear structure and still keep the tires in a vertical plane at
varying angles of yaw. The original yokes and torque links of the
landing-gear struts along with the wheel assemblies were replaced by
steel wheel housings which held the tires and wheels tested. A rigid
truss pinned at four points to the two wheel housings held the wheel
housings in a fixed relative position during towing operations. Holes
located in the wheel housings at angular intervals of $3\frac{1}{2}^{\circ}$ permitted the
wheel frames to be rotated through a nominal yaw-angle range of 0° to
$24\frac{1}{2}^{\circ}$. Actual measurements on the completed test rig, however, showed
the yaw-angle range to be from 0.35° to 24.9°.

The towing loads were taken by two steel cables attached between
the wheel housings and the tow truck chassis. At high yaw angles with
the heavy-weight condition, an additional truck was attached to the tow
truck to provide increased power for towing. The maximum towing force
required was approximately 8,000 pounds.

The airplane tail was supported by the original swiveling tail-
wheel-strut assembly which was modified so that the tail-wheel assembly
rotated about a vertical axis. The axle rested in a slot on the top of
the tow-truck support structure. This slot and pin arrangement permitted
the entire towing load, with the exception of a relatively small amount
of friction force, to be carried by the drag cables.

The weight of the test vehicle acting on the tires was approximately
20,000 pounds in the lightest condition. This weight was varied in incre-
ments by the addition of six steel and concrete weight cans (each weighing
about 8,000 pounds) which were mounted on the airplane structure as shown
in figure 3. Additional weights were also added in the fuselage to obtain
the heaviest weight condition of 90,000 pounds.

For the locked-wheel drag-force investigation, the test setup was as shown in figure 5. The drag cables were disconnected from the tow truck and attached to a hydraulic ram which was anchored to several stationary heavy vehicles. The airplane wheels were locked by means of rods passing through the spokes and bearing on the wheel frames. Pressure was supplied to the ram by the electrically driven pump shown in figure 5.

Instrumentation

The test vehicle was equipped with instruments for measuring side force, self-alining torque, drag, vertical tire deflection, horizontal translation, and wheel rotation. An explanation of the method by which each of the quantities was measured is given in the following sections. Measurements of these quantities were recorded simultaneously on a 14-channel oscillograph mounted in the test vehicle. This oscillograph was equipped with a 0.01-second timer. A sample oscillograph record for a yawed-rolling run is shown in figure 6.

Side force.- The side force acting on the two tires was measured by means of a rigid truss structure which was installed between the two wheel housings and which was equipped with four strain-gage dynamometers. (See fig. 7.)

Self-alining torque.- The same dynamometers used for the side-force measurements were used to obtain the self-alining torque (that is, the moment about a vertical axis through the center of the wheel).

Vertical load.- The vertical load on the tires was measured by a portable commercial strain-gage dynamometer kit.

Drag forces.- Two separate strain-gage dynamometers, indicated as 5 and 6 in figure 7, were used for measuring the drag forces.

Vertical tire deflection.- Vertical-tire-deflection measurements were obtained during the test runs by use of the wheel and strut assembly shown in figure 4(a). Vertical motion of the small solid swiveling wheel, which represents the large tire deflection, is recorded by means of a variable-resistance slide-wire potentiometer.

Fore-and-aft translation.- Fore-and-aft translation of the test vehicle from the initial starting point, during the early stages of each run, was recorded by means of the circular slide-wire potentiometer device which is shown in figure 4(a). This device consists of a drum with a string wound around it, one end of the string being tied to a weight resting on the taxi strip. Translation of the test vehicle thus produces rotation of the drum. This rotation produces a sawtooth-type record (see fig. 6), each sawtooth of which corresponds to a single revolution of the drum.

Horizontal translation during later stages of each run was measured
by means of trailing bicycle wheels attached behind the wheel frames.
These bicycle wheels are equipped with an electrical device which gives
a pulse on the oscillograph for each 0.39 foot of distance traveled.

Wheel rotation.- Rotation of the test wheels was obtained from
revolution-counter devices installed on each of the wheels. These
devices furnished indications on the oscillograph for each 10° of wheel
rotation.

Tires

General description.- The tires tested in this investigation were two
56-inch-diameter, 56×16, type VII, extra-high-pressure, 24-ply-rating,
rib tread tires which were made by different manufacturers. One tire was
new and unused. This tire is referred to in this paper as tire A. The
other tire, which will be referred to as tire B, was previously subjected
to the static tests which are reported in reference 2. The specifica-
tions for these tires given in table I were either obtained from refer-
ence 6 or by direct measurement after the conclusion of the tests. Fig-
ure 8 shows the deflated and inflated cross sections of the tires tested.
These cross sections were obtained from plaster casts taken after the
conclusion of the tests and, consequently, they show the tire cross sec-
tion for a worn condition. There appears to be no appreciable difference
in the inflated outer profiles for the two tires. However, there is seen
to be an appreciable difference in cross-sectional thickness of the two
tire treads.

Tire wear.- During the course of the present investigation, there
was an appreciable progressive change in the cross-sectional shape of
the tires due to skidding and working of the tires. Therefore, the
chronological order in which the test data was collected is of some
importance in the interpretation of the data. This chronological order
is indicated in this paper by a series letter which is assigned to all
test data. Specifically, series A represents conditions at the beginning
of the tests; series B represents conditions for a later period of time,
and so forth.

The change in tire-tread pattern due to tire wear throughout the
tests is illustrated in figure 9. At the beginning of the tests both
tires had a rectangular cross-sectional tread pattern (fig. 9(a)) and
this pattern was substantially preserved throughout most of series A
to C. Toward the end of series C, however, the side of the tread in
intimate contact with the ground began to wear away and produced the
tread pattern illustrated in figure 9(b). This wear increased substan-
tially during series D and for series E to G the tire profile remained
approximately as indicated in figure 9(c). The small projecting edges

of the tread were then cut off and for the remainder of the tests
(series H and I) the tread cross section was again essentially rectan-
gular with rounded-off corners, as shown in figure 9(d).

Tire radius.- The variation of the unloaded tire radii with infla-
tion pressure and tire wear is shown in figure 10. Each measurement
shown was taken after the tires had been left at constant pressure for
at least 24 hours. For test series E to H, the radius of the tires is
defined as the maximum radius less the height of the small projecting
edge shown in figure 9(c); thus, the indicated difference in tire radius
for series A to C and E to I is largely due to the wearing off of the
tread. It should also be noted that the tire radii during the later
stages of this investigation (series E to I in fig. 10) differ slightly
from the radii measured after the conclusion of the tests (table I and
fig. 8). The difference, approximately 1 percent, is probably due to
the fact that the earlier measurements were made during a period of
time when the tires were being regularly subjected to severe loadings
whereas the later measurements were made after the tires had been com-
pletely unloaded for a long period of time.

A radius-pressure hysteresis loop for tire B is shown in figure 11.
The elapsed time from start is shown for a few of the measurements pre-
sented. The variation in tire radius for a given pressure is seen to
amount to as much as 1 percent for this relatively slow rate of change
of pressure (roughly, four hours for most of the cycle).

Tire width.- The variation of maximum tire width with inflation
pressure is shown in figure 12 for both tires. These measurements were
all made after the conclusion of testing (tires well worn) and each
measurement was taken after the tires had been kept at constant pressure
for at least 24 hours in order to minimize hysteresis effects.

Test Surface

All yawed-rolling and drag tests were conducted by towing the test
vehicle along the center of a 9-inch-thick reinforced-concrete taxi strip.
This taxi strip had a slight crown such that the tires on the test vehi-
cle were subject to a slight tilt. However, this tilt was less than 1°.
The texture of the taxi strip, a boarded concrete surface, as determined
from plaster casts, is shown in figure 13 for three random positions on
the strip. All other tests were conducted on a much smoother, level,
reinforced-concrete surface.

Precision of Data

The instruments used in these tests and the methods of reducing data are believed to yield results usually accurate within the following limits:

Vertical load on tires, F_z, percent . . . . ± 3

Cornering force, F_y, percent . . . . ± 3

Force perpendicular to wheel plane, F_ψ, percent . . . . ± 3

Drag force per tire, F_x, lb . . . . ± 300

Measured moment, ΔM_z, lb-in. $\pm 3,000$

Tire inflation pressure, p_0 or p, lb/sq in. . . . . ± 3

Free radius, r, in. . . . . ± 0.02

Rolling radius, r_e, in. . . . . ± 0.1

Horizontal translation, x, in. . . . . ± 3

Vertical tire deflection, δ_0 or δ, in. . . . . ± 0.2

Yaw angle, ψ, deg . . . . ± 0.1

TEST PROCEDURE

The present investigation of tire characteristics is divided into the following parts: yawed-rolling tests, relaxation-length tests, locked-wheel drag tests, and supplementary measurements.

Yawed-Rolling Tests

For each run of the yawed-rolling tests, the test vehicle was moved into towing position on the dry, clean, concrete taxi strip and the wheel housings were rotated and locked at the particular yaw angle desired. The tires were adjusted to the test inflation pressure and the vertical tire deflections noted. The vehicle was then towed a distance of approximately 50 feet within a speed range of from 1 to 4 miles per hour. Figure 4 shows one of the tires during a run at 17.9° yaw.

All test runs at yaw angles of 0.35°, 3.9°, 7.4°, 10.9°, 14.4°, and 17.9° were made with both wheels symmetrically yawed with respect to the longitudinal axis of the test vehicle. Because these particular yaw angles were the only angles attainable on the test vehicle, the only way that intermediate yaw angles could be obtained was by unsymmetrically yawing the two wheels with respect to the longitudinal axis of the test vehicle. This was done to obtain intermediate yaw angles of 2.1° and 5.7° (that is, in order to obtain 2.1°, one wheel was yawed by 0.35° and

the other, by 3.9°). When towed ahead in this unsymmetrically yawed condition, the test vehicle first veers off to the side because of the unsymmetrical forces. After a short run, however, the vehicle runs smoothly with the longitudinal axis of the test vehicle yawed with respect to the direction of motion such that both wheels have the same final intermediate yaw angle with respect to the direction of motion.

In general, at the beginning of each run, the tires could not practically be set in an equilibrium condition but were instead subject to a certain amount of distortion (and thus, forces and moments) which appeared as a consequence of residual stresses left over from the previous runs and from moments resulting from the changing of the yaw angles of the wheels.

The following measurements were recorded continuously from the start of the run: side force, self-alining torque, drag force, vertical tire deflection, wheel rotation, and vehicle translation in the direction of motion.

All runs except one (run 185 of table II) were made with the tires toed out in the direction of motion. For this one particular run, the usual direction of motion was reversed in order to give an indication of the effects of unsymmetrical tread wear. In order to investigate this unsymmetrical wear effect more thoroughly, each of the tires was removed from its wheel housing after test series G and was replaced so that the former outboard side of the tire became the inboard side. Tow tests were then continued in the usual toed-out condition throughout test series H and I.

Relaxation-Length Tests

Four types of relaxation length were determined in this investigation (see section entitled "Definitions of Concepts"). The methods used to determine these types of relaxation length were as follows:

Static relaxation length L_s.- The standing tires were given initial lateral deflection by pulling outward, by means of hydraulic rams, plates placed underneath the tire. The lateral distortion of each tire center tread relative to the wheel center plane was then measured for several points around the tire circumference between the footprint edge and a point 180° from the center of contact.

Unyawed-rolling-force relaxation length L_f.- With the wheel housings positioned close to 0° yaw (actually 0.35°), the tires were given initial lateral deflections by pulling out on plates placed underneath (as for

the static relaxation-length tests). The test vehicle was then rolled ahead off the plates for a distance of about 50 feet with the recording oscillograph taking a continuous record of side force and horizontal translation.

Unyawed-rolling-deflection relaxation length L_λ.- This procedure entailed rubbing the center tread of each tire with chalk so that a trace of each center tread would appear on the concrete surface as the tires were rolled ahead. The chalked tires were first given an initial lateral deflection. The test vehicle was then towed forward about 50 feet and the distance between the tire-center-tread traces was measured at intervals from the start up to the point of constant distance between tread traces.

(The rolling procedure for this relaxation length is the same as that for the unyawed-rolling-force relaxation length. Actually, the same test runs were used to obtain test data for determining both of these relaxation lengths.)

Yawed-rolling relaxation length L_y.- The basic data for the yawed-rolling relaxation length were obtained from the initial (force buildup) phase of the 3.9° yawed-rolling tests. This constant was evaluated in this paper for this yaw angle only, since, for larger angles, skidding appeared to be too significant and for smaller angles the accuracy of measurement was usually too poor.

Locked-Wheel Drag Tests

The method used to determine tire stiffness and sliding drag in the fore-and-aft direction was as follows: The setup for the locked-wheel drag tests previously described was used, the test vehicle being pulled forward on the taxi strip with the wheels set at approximately 0° yaw ($\psi = 0.35^\circ$) and locked to prevent wheel rotation. As the test vehicle was pulled forward at a speed less than 10 inches per minute, a continuous record was taken of drag force and horizontal displacement. This procedure was repeated throughout a range of tire inflation pressures for one weight condition. In addition, several runs were made with the concrete surface in a wet condition.

During these tests, the weight of the test vehicle remained constant; however, the vertical load on the tires decreased slightly with increasing drag force as a consequence of the moment produced by the drag force. This change in vertical load was taken into account in the computation of friction coefficients. (It was not taken into account in the other tests since the effect was very small for those conditions.)

Supplementary Tests and Measurements

In addition to the tests just described, several supplementary
tests were made. These tests included vertical-load-deflection measure-
ments and footprint-area determinations. The vertical-load-deflection
characteristics of the two tire specimens were determined for one infla-
tion pressure (about 220 lb/sq in.) with the tires mounted on the test
vehicle. Tire-contact or footprint-area measurements were made for the
tire specimens at several inflation pressures and vertical tire deflec-
tions. These measurements were obtained from the imprint left on a
piece of heavy paper placed between a chalked portion of the tires and
a smooth concrete hangar floor. Several typical imprints are shown in
figure 1.

RESULTS AND DISCUSSION

Most of the experimental data obtained from this investigation are
presented in tables II to VI and figures 8 to 47.

Yawed-Rolling Tests

Table II contains all test data obtained during the final steady-
state stage of each yawed-rolling run. Data are presented for 9 differ-
ent test series (A to I) which represent either different vertical
loadings, different tire wear, or different orientation of the tires.
The variation of normal force $\bar{F}_\psi$, self-alining torque $\bar{M}_\psi$, and pneumatic
caster $\bar{q}$ with yaw angle are shown in figure 14 for all vertical loads
and inflation pressures. Some details pertinent to the interpretation
of these data are discussed in the appendix. Sample rolling-radius data
for two typical test conditions are plotted in figure 15 as functions of
yaw angle and vertical tire deflection.

The buildup of cornering force with horizontal distance rolled
during the initial stages of the yawed-rolling runs is illustrated in
figure 16 for typical runs at several pressures and for three test
series. Inasmuch as for most runs there was an initial residual force
or preload in the tires, the original test curves did not usually pass
through the origin. In order to take this fact into consideration, the
test curves shown in this figure have been horizontally shifted (if neces-
sary) so that the extrapolation of each curve is made to pass through
the origin. For most of these curves, the initial rate of buildup appears
to increase with increasing yaw angle (as is predicted by theory, that is,
ref. 5) and that the force generally approaches close to its maximum value
before the tires have rolled more than 6 feet.

Relaxation-Length Tests

Samples of the test data obtained from the four different methods used to determine the relaxation length of the tire specimens are shown in figure 17 for test series A, B, and E. In parts (a), (b), and (c) of figure 17, these data are plotted in semilogarithmic coordinates in order that the expected exponential curves (according to theory) should appear as straight lines. The relaxation lengths for the conditions shown here and for all other conditions of this investigation were obtained by fitting straight lines to such semilogarithmic plots for each test run and are tabulated together in tables II to IV.

It is seen from figure 17 that usually the test results do appear to give substantially straight lines in these semilogarithmic plots; thus, the theoretical exponential variation of force with distance rolled (for the rolling relaxation lengths) or distance around the tire periphery (for the static relaxation length) is supported. The same data shown for series B in figure 17(b) is replotted in linear coordinates in figure 17(d). The solid lines drawn on these plots (fig. 17(d)) are the same solid faired lines which were fitted through the data in figure 17(b).

It should be noted that, for the static-relaxation-length data, the test data do not agree well with the assumed exponential variation near the two endpoint conditions at the edge of the tire footprint and at the top of the tire (for example, see fig. 17(a)). This discrepancy is due largely to the finite bending stiffness of the tire which requires that the slope of the tire-distortion curve must be zero at the edge of the tire footprint ($s = h$) and also at the top of the tire and both of these factors conflict with an exponential variation.

Locked-Wheel Drag Tests

Most of the experimental data obtained from the locked-wheel drag tests are presented in table V. Also, typical data are shown in figure 18 for the buildup of fore-and-aft force with horizontal distance pulled for several runs.

Supplementary Tests

The vertical-load—vertical-tire-deflection characteristics curves for the two tires are given in figures 19 to 21 and the tire-footprint data are given in table VI.

Discussion of Parameters

Normal force F_ψ.- The variation of the steady-state normal force
with yaw angle, obtained from the data in table II, is shown in fig-
ure 14 for all test series. For each condition of initial vertical tire
deflection $\bar{\delta}_0$ and inflation pressure $\bar{p}$, it is seen that the normal
force increases with increasing yaw angle and reaches a maximum value at
between 14° and 18° yaw. The maximum normal force tends to decrease with
increasing inflation pressure. (This observation is discussed later in
more detail under the subject of yawed-rolling coefficient of friction.)
For the case of constant inflation pressure, shown in figure 22,
increasing the vertical load increases the maximum normal force.

Cornering force F_y.- The cornering force follows substantially
the same trends that were described for the normal force, as is shown
in figure 23, for a typical loading condition.

Cornering power N.- The variation of cornering power with verti-
cal tire deflection and inflation pressure for the different series
tested is shown in figures 24(a) and 24(b), respectively. These data
are derived from the initial slope of the normal-force—yaw-angle curves
given in figure 14. In order to show more clearly the trends of these
data, the effects of inflation pressure and vertical tire deflection,
respectively, on cornering power have been isolated in figures 25 and
26. For the constant vertical tire deflection of 3.2 inches considered
in figure 25, the cornering power increases nonlinearly with increasing
inflation pressure. The data for other constant vertical tire deflec-
tions seem to follow this same trend. For the constant-pressure range
shown in figure 26, the cornering power increases with increasing verti-
cal tire deflection up to a vertical tire deflection of around 3.0 inches
where a maximum is reached. Increasing the vertical tire deflection
beyond this point tends to reduce the cornering power.

Self-alining torque M_z.- The variation of self-alining torque with
yaw angle is shown in figure 14 for all test series. The self-alining
torque generally increases with increasing yaw angle for yaw angles less
than 5° to 8°. Between 5° and 8°, a maximum is reached and increasing
the yaw angle beyond this range usually decreases the self-alining torque
considerably. For constant vertical load, the data indicate that
increasing the tire inflation pressure tends to reduce the magnitude of
the self-alining torque at most yaw angles. In the case of constant
inflation pressure, illustrated in figure 22, increasing the vertical
load tends to increase the self-alining torque.

Effect of tire wear on normal force and self-alining torque.- The
influence of tire wear on normal force and self-alining torque can be
seen in figure 27 which presents data both for the unworn tire condition

(series A) and for a considerably worn condition (series F). For the
most part, this comparison indicates no extremely large changes in either
normal force or self-alining torque; however, reversing the tire tread
(reversing the tires in the wheel housings) decreased the maximum normal
force considerably as is illustrated in figure 28. A likely explanation
for this phenomenon could lie in the fact that the tire-tread beads
resulting from unsymmetrical tread wear (see fig. 9) fold over on top
of the treads under towing conditions with the tires reversed as is shown
schematically in figure 29. Such a folding of the tread bead would tend
to reduce the tread-contact area considerably and thus increase the
bearing pressure between the tire and the ground. This increase in
bearing pressure would result in a reduced friction coefficient (to be
discussed later) and would thus reduce the maximum attainable normal
force.

Maximum self-alining torque $M_{z_{max}}$.- The variation of maximum self-
alining torque with inflation pressure is shown in figure 30(a) and with
vertical tire deflection by figure 30(b) for the test series investigated.
These data are taken from the faired curves drawn through the data pre-
sented in figure 14. In order to show more clearly the trends of the
maximum self-alining-torque data, the effects of vertical tire deflection
and inflation pressure on the maximum self-alining torque have been
isolated in figures 31 and 32. For constant inflation pressure (see
fig. 31), the maximum self-alining torque tends to increase nonlinearly
with increasing vertical tire deflection whereas, for constant vertical
tire deflection (see fig. 32), the maximum self-alining torque increases
more or less linearly with increasing inflation pressure.

Pneumatic caster $\bar{q} = \bar{M}_z/\bar{F}_\psi$.- The variation of pneumatic caster
with yaw angle for all test conditions is shown in figure 14. The vari-
ation of pneumatic caster with vertical tire deflection for the vertical
load and inflation pressure range tested is shown in figure 33 for each
test yaw angle (data obtained from table II). This figure shows that,
for a constant yaw angle, the pneumatic caster increases with increasing
vertical tire deflection. For constant vertical tire deflection, any
systematic pressure effect on the pneumatic caster is obscured by the
scatter of the test data. Faired values of pneumatic caster taken from
figure 33 for several constant vertical tire deflections are plotted
against yaw angle in figure 34. Figure 34 shows that the pneumatic cas-
ter is a maximum at small angles of yaw and generally decreases with
increasing yaw angle for the test range covered.

Drag force $\bar{F}_x$.- The variation of drag force with yaw angle for the
rated-vertical-load condition (test series B) for the three different
inflation pressures tested is shown in figure 35. The data in figure 35
indicate that the drag force, except at small yaw angles, increases more
or less linearly with increasing yaw angle for the yaw-angle range covered.

Essentially the same results were obtained for the other test series and inflation pressures investigated. In order to show trends more clearly, the ratio of drag force to cornering force $\bar{F}_x/\bar{F}_y$ is plotted against yaw angle in figure 36 for the different test series and tire inflation pressures investigated. If the total horizontal ground force under yawed rolling was normal to the wheel plane, then the drag force $\bar{F}_x$ would be equal to the cornering force $\bar{F}_y$ multiplied by the tangent of the yaw angle or $\dfrac{\bar{F}_x}{\bar{F}_y} = \tan \psi$. Tan ψ is represented in this figure by a solid line. In general, the data fall near or above this line and indicate that a small force parallel to the wheel plane usually is present throughout the yaw-angle range investigated.

Yawed-rolling coefficient of friction $\bar{\mu}_\psi = \dfrac{\bar{F}_{R_{max}}}{\bar{F}_z}$.- The variation of the yawed rolling coefficient of friction with average bearing or ground pressure is shown in figure 37. The data shown in this figure are derived from data given in table II and in figures 19 and 41 (to be discussed later). The trend of the data shown indicates that the yawed-rolling friction coefficient decreases with increasing bearing pressure from approximately 0.94 at 60 pounds per square inch down to approximately 0.56 at an average bearing pressure of 320 pounds per square inch.

Sliding drag (fore-and-aft) coefficient of friction $\bar{\mu}_x = \dfrac{\bar{F}_{x_{max}}}{\bar{F}_z}$.- The variation of sliding drag coefficient of friction with average bearing pressure for both dry and wet concrete for the one condition of constant vertical load tested is shown in figure 38. The data shown in this figure was obtained from table V. The sliding drag coefficient of friction for the dry-concrete condition appears to decrease with increasing bearing pressure from approximately 0.85 at a bearing pressure of 50 pounds per square inch down to approximately 0.75 at a bearing pressure of 200 pounds per square inch. The friction coefficients found for the limited number of tests made with the concrete in a wet condition indicate a reduction in the sliding drag coefficient of friction of about 10 to 15 percent over that for the dry-concrete condition.

A comparison of the sliding drag coefficient of friction with the yawed-rolling coefficient of friction is shown in figure 39. Both coefficients seem to show approximately the same trends.

Fore-and-aft spring constant $\bar{K}_x$.- The variation of fore-and-aft spring constant with tire inflation pressure, obtained from data in table V, for the one constant vertical load condition tested is shown

in figure 40. These data are derived from the initial slope of the fore-and-aft (drag) force $\bar{F}_x$ against horizontal displacement $\bar{x}$ curves. Samples of these curves for three test inflation pressures are presented in figure 18. For the one constant-vertical-load condition tested, figure 40 indicates that the fore-and-aft spring constant does not change markedly with inflation pressure for the range of conditions investigated.

Vertical-load—vertical-tire-deflection characteristics.- The average vertical-load—vertical-tire-deflection characteristics of the two tire specimens are shown in figure 19 by means of a family of constant-vertical-load curves where the ordinate is the initial vertical tire deflection $\bar{\delta}_0$ and the abscissa is the tire inflation pressure $\bar{p}$. Each constant-vertical-load curve represents one of the test series or constant-vertical-load conditions tested. These curves are faired curves obtained by averaging the data taken from yaw, relaxation length, and footprint area tests. (Test data for yaw angles greater than 2.1° were omitted because, under such yaw angles, large cornering-force preloads were sometimes encountered which could affect the accuracy of the initial vertical tire deflection considerably.) The scatter of the test data was found to range approximately ± 0.2 inches and is mainly attributed to hysteresis effects, although tire wear and accuracy of measurement also contribute to the scatter to some extent. Figure 20 shows the hysteresis effects on the test data obtained from the locked-wheel drag tests (table V). The difference between the increasing and decreasing pressure curves is considerable and amounts to as much as 0.5 inch vertical tire deflection. Vertical-load—vertical-tire-deflection data for the one condition of constant tire inflation pressure investigated ($p = 219$ lb/sq in., unloaded) is shown in figure 21. These data indicate that tire A is slightly stiffer than tire B.

Footprint area A_g, A_n.- The variation of gross footprint area A_g, net footprint area A_n, and the ratio of net footprint area to gross footprint area A_n/A_g with vertical tire deflection for the test tires, obtained from the data in table VI, is shown in figure 41. Both the gross footprint area and the net footprint area appear to increase linearly with increasing vertical tire deflection for vertical tire deflections greater than 1 inch. The ratio of net footprint area to gross footprint area appears to decrease slightly with increasing vertical tire deflection and averages approximately 70 percent of the gross footprint area. This ratio will, of course, change for tires having tread designs different from the ones tested.

Footprint length $2h$ and width b.- The variation of footprint length and width with vertical tire deflection, obtained from data in table VI, is shown in figure 42. These data indicate that both the footprint length and the width increase nonlinearly with increasing vertical tire deflection. Also shown in this figure as solid lines are the

lengths of chords of circles having diameters equal to the free diam-
eter d and maximum width w, respectively, of the tire at its rated
inflation pressure and located at a distance $r - \delta_0$ from the center
of the circles. A comparison of these quantities indicates that the
experimental values of footprint length and width are smaller than the
corresponding chord lengths over the vertical-tire-deflection range
tested.

Average bearing pressure $\bar{p}_n = \overline{F_z/A_n}$ and average gross footprint
pressure $\bar{p}_g = \overline{F_z/A_g}$.- The variation of average bearing pressure and
average gross footprint pressure with tire inflation pressure is given
in figure 43. The data shown in figure 43 are derived from the faired
vertical-tire-deflection—inflation-pressure curves given in figure 19
and from the faired footprint-area—vertical-tire-deflection curves
given in figure 41. The heavy solid line shown represents $\bar{p}_n$ or $\bar{p}_g = \bar{p}$.
Comparison of this line with the average-bearing-pressure curves indicates
that the average bearing pressure becomes increasingly larger than the
inflation pressure with increasing inflation pressure. The average gross
footprint pressure, on the other hand, decreases as the inflation pres-
sure increases from being slightly larger at low inflation pressures to
being smaller than the inflation pressure at high inflation pressures.
The offset of both the average bearing pressure and the gross footprint
pressure at zero inflation pressure is indicative of the inherent carcass
stiffness of the tire.

Increasing the vertical tire deflection is seen to increase both the
average-bearing-pressure and the average-gross-footprint-pressure curves.

Relaxation length L.- The variation of the four types of relaxation
length with tire inflation pressure is shown in figure 44. The variation
for the static relaxation length with tire inflation pressure is shown in
figure 44(a), for the unyawed-rolling-force and the unyawed-rolling-
deflection relaxation lengths in figure 44(b), and for the yawed-rolling
relaxation length in figure 44(c). In order to show trends more clearly,
the effects of vertical tire deflection on the relaxation length has
been isolated in figure 45 where the relaxation length is plotted against
tire inflation pressure for several constant vertical tire deflections.
For comparative purposes, the same faired lines drawn through the data
in figure 45(a) are reproduced in figures 45(b) and 45(c). The agreement
between the static and the unyawed-rolling relaxation lengths is fairly
good for the vertical-tire-deflection range shown. The yawed-rolling
relaxation lengths appear to average about 25 percent less than the static
relaxation lengths for the vertical-tire-deflection range shown. Some
of this difference is thought to be caused by the twisting moment or
self-alining torque present in the yawed-rolling case. As evidence for
this fact, some previously unpublished data for a 45-inch diameter tire

(tire C of ref. 2) is presented in figure 46 where the variation of static relaxation length with twisting moment or twist is shown for one condition of combined constant vertical force and constant side force. The moment for this data was applied in a direction such as to tend to simulate the yawed-rolling condition. These data indicate that the static relaxation length decreases with increasing twisting moment or twist.

Figure 47 presents a comparison of static relaxation lengths obtained from reference 2 for a 56 × 16, 32-ply-rating tire with the data for the 56 × 16, 24-ply-rating tire specimens used in the present tests. Because the rated inflation pressures differ for these two tire types, a direct comparison of their respective relaxation lengths on the basis of equal inflation pressures would be of dubious significance. Therefore, in order to provide a more significant comparison, the data are shown in figure 47 in terms of the pressure ratio p/p_r where p_r is the rated inflation pressure for the tire specimen. Fairly good agreement is seen to exist between the different tires for the pressure ratios considered.

In general, the test results indicate that the relaxation length decreases with increasing vertical tire deflection and increasing inflation pressure.

Rolling radius r_e.- The variation of rolling radius with yaw angle, obtained from data in table II, for two typical test conditions is shown in figure 15(a). The rolling radii for both test tires appear to be in good agreement and remain more or less constant in magnitude with increasing yaw angle up to at least a yaw angle of 14.4°. The trend of the data at the higher yaw angles is uncertain because one tire, usually tire A, was observed to be slipping more than the other at this condition. The variation of rolling radius with vertical tire deflection for several of the test inflation pressures is shown in figure 15(b). The data presented in figure 15(b) were obtained from table II and are for yaw angles of 0.35° and 2.1°. The trends of these data indicate that, for constant pressure, the rolling radius decreases with increasing vertical tire deflection and that, for constant vertical tire deflection, the rolling radius increases with increasing inflation pressure.

Speed effects.- Within the speed range tested (1 to 4 miles per hour), no apparent effects of speed were found to exist for the quantities measured.

CONCLUSIONS

Tow tests were made at the Langley Aeronautical Laboratory primarily to determine the yawed-rolling characteristics of two 56 × 16, type VII, extra-high-pressure, 24-ply-rating airplane tires. The results of these tests indicated the following conclusions:

1. The normal force reached a maximum at between 14° and 18° yaw for the vertical load range tested, and this maximum tended to decrease with increasing tire inflation pressure.

2. The cornering power under constant tire inflation pressure increased with increasing vertical tire deflection up to about 3.0 inches vertical tire deflection where a maximum was reached. Increasing the vertical tire deflection beyond this point tended to decrease the cornering power. For the case of constant vertical tire deflection, the cornering power increased with increasing tire inflation pressure.

3. The self-alining torque generally increased with increasing yaw angle for yaw angles less than 5° to 8°. Between 5° and 8°, a maximum was reached and increasing the yaw angle beyond this range tended to decrease the self-alining torque considerably.

4. The maximum self-alining torque for the case of constant vertical tire deflection increased more or less linearly with increasing tire inflation pressure whereas for the case of constant inflation pressure the maximum self-alining torque increased nonlinearly with increasing vertical tire deflection.

5. The pneumatic caster was a maximum at small angles of yaw and generally decreased with increasing yaw angle for the test range covered.

6. The yawed-rolling friction coefficient decreased with increasing bearing pressure from approximately 0.94 at a bearing pressure of 60 pounds per square inch down to approximately 0.56 at a bearing pressure of 320 pounds per square inch.

7. The sliding drag coefficient of friction for the dry concrete condition also decreased with increasing bearing pressure from approximately 0.85 at a bearing pressure of 50 pounds per square inch down to 0.75 at a bearing pressure of 200 pounds per square inch. The limited number of tests made with the concrete in the wet condition indicated a 10 to 15 percent reduction in the sliding drag friction coefficient over the dry-concrete condition.

8. In general, the test results indicate that the relaxation length decreases with increasing vertical tire deflection and increasing inflation pressure.

Langley Aeronautical Laboratory,
    National Advisory Committee for Aeronautics,
        Langley Field, Va., June 11, 1954.

APPENDIX

DETAILS OF CORNERING-FORCE AND SELF-ALINING-TORQUE MEASUREMENTS

In conducting the yawed-rolling tests a certain amount of difficulty was encountered as a consequence of the fact that it was impractical to set the wheels on the test vehicle exactly to a zero yaw condition; the minimum attainable angle was about 0.35°. This fact is important because, in order to obtain cornering-force and self-alining-torque data for any yaw angle, it is necessary to subtract the dynamometer-record deflections for the yawed-rolling case from those for the reference zero yaw case. In the case of cornering force, this difficulty was resolved by rolling the test vehicle both forward and backward at the minimum yaw angle (0.35°) and by taking the average record deflection for the two cases as corresponding to the zero yaw condition. The cornering force for this 0.35° yaw angle was taken as half the difference in force for the rolled-forward and rolled-backward conditions.

For the self-alining torque, the record deflections for the zero yaw condition could not be accurately determined; consequently, it was not possible to obtain direct measurements of the self-alining torque. Instead all moment measurements were made with reference to the 0.35° minimum yaw condition; that is, the measured moment (designated as ΔM_z) represents the difference in self-alining torque for the yaw angle considered and for the 0.35° condition. In order to obtain the actual self-alining torque M_z, it is necessary to add to the measured quantity ΔM_z the self-alining torque for 0.35° yaw (designated as M_{z_O}) or $M_z = M_{z_O} + \Delta M_z$. The quantity M_{z_O} was estimated from the static-torsional-elasticity-test data for one of the test tires which is given in reference 2. This procedure for correcting the measured moment ΔM_z to M_z is believed to be fairly satisfactory both because the torsional elastic properties of static and slowly rolling tires are at least approximately similar (for example, see experimental data in ref. 5) and because the correction term M_{z_O} is usually relatively small in comparison with the measured term ΔM_z.

REFERENCES

1. Hadekel, R.:   The Mechanical Characteristics of Pneumatic Tyres.
      S & T Memo. No. 5/50, British Ministry of Supply, TPA 3/TIB,
      Mar. 1950.

2. Horne, Walter B.:   Static Force-Deflection Characteristics of Six
      Aircraft Tires Under Combined Loading.   NACA TN 2926, 1953.

3. Temple, G.:   Note on American Work on Kinematic and Dynamic Shimmy.
      Rep. No. A.D. 3158, British R.A.E., Nov. 1940.

4. Kantrowitz, Arthur: Stability of Castering Wheels for Aircraft
      Landing Gears.   NACA Rep. 686, 1940.

5. Von Schlippe, B., and Dietrich, R.:   Zur Mechanik des Luftreifens.
      Junkers Flugzeug- und Motorenwerke, A.G., Dessau. (Available from
      CADO as ATI 105296.)

6. Anon.:   Military Specification Casings; Aircraft Pneumatic Tire.
      Military Specification, MIL-C-5041, Sept. 16, 1949; Amendment-2,
      Feb. 8, 1951.

TABLE I.- TIRE SPECIFICATIONS

Specifications	Military specification (ref. 6)	End of test, tires in worn condition	
		Tire A	Tire B
Tire: Type[a]	VII	-----	-----
Ply rating	24	-----	-----
Static load, lb	45,000	-----	-----
Inflation pressure, lb/sq in.	178	-----	-----
Burst pressure, lb/sq in.	712 (minimum)	-----	-----
Moment of static unbalance, oz-in. . .	90	-----	-----
Diameter, deflated, in.	----------------	54.40	53.70
Diameter, inflated, in.	55.26 (minimum) 56.40 (maximum)	56.16	56.24
Maximum width, deflated, in.	-----------------	15.36	15.87
Maximum width, inflated, in.	16.00 (maximum)	16.00	16.06
Bead width, in.	3.88 (maximum)	2.80	3.00
Minimum wall thickness, in.	-----------------	1.1	0.9
Wall thickness at tread center line (including tread), in.	-----------------	1.3	1.0
Depth of tread (at tread center line), in.	0.35 (maximum)	0.15	0.15
Casing weight, lb	268 (maximum)	253	247
Tread pattern	Rib or nonskid	Rib	Rib
Innertube: Thickness, in.		0.2	
Weight, lb		26.7	
Wheel: Rim diameter, in.		32.5	
Weight, lb		217	

[a]Type VII is an extra high pressure tire.

TABLE II.- YAW TEST DATA

(a) SERIES A: $\bar{F}_z$ = 17,000 lb; $(F_z)_{tire\ A}$ = 17,000 lb; $(F_z)_{tire\ B}$ = 16,900 lb.

Run	Average Values											Tire A				Tire B			
	$\bar{p}$, lb/sq in.	$\bar{\delta}_o$, in.	$\bar{\delta}$, in.	$\bar{\psi}$, deg	$\bar{F}_y$, lb	$\bar{F}_x$, lb	$\bar{F}_\psi$, lb	$\Delta\bar{M}_z$, lb-in.	$\bar{M}_z$, lb-in.	$\bar{q}$, in.	$\bar{L}_y$, in.	p, lb/sq in.	δ_o, in.	δ, in.	r_e, in.	p, lb/sq in.	δ_o, in.	δ, in.	r_e, in.
1	61	3.5	3.3	0.35	620	*	620	0	4,300	6.94	**	58	3.5	3.5	-----	63	3.5	3.5	-----
2	62	3.7	3.7	.35	580	*	580	0	4,700	8.10	**	63	3.7	3.7	-----	61	3.7	3.7	-----
3	62	3.7	3.7	.35	530	*	530	0	4,700	8.87	**	63	3.7	3.7	-----	61	3.7	3.7	-----
4	61	---	---	.35	620	*	620	0	------	----	**	61	---	---	-----	60	---	---	-----
5	56	3.8	3.8	.35	690	*	690	0	4,700	6.81	**	56	3.8	3.8	25.5	55	3.9	3.9	25.3
6	57	3.9	3.9	.35	530	*	530	0	4,900	9.25	**	55	4.0	4.0	25.4	58	3.8	3.8	25.4
7	60	3.6	3.6	.35	640	*	640	0	4,500	7.03	**	60	3.7	3.7	25.5	60	3.5	3.5	25.5
8	60	3.6	3.4	2.1	2,980	400	2,990	17,500	21,600	7.22	**	60	3.7	3.4	25.5	60	3.5	3.4	25.5
9	59	3.6	----	3.9	5,030	600	5,060	37,600	------	----	----	57	3.6	---	25.5	61	3.6	---	25.6
10	57	3.7	3.8	3.9	4,950	600	4,980	33,400	38,100	7.65	**	55	3.9	4.0	25.5	58	3.6	3.5	25.5
11	61	3.5	3.8	7.4	8,920	1,200	9,000	37,900	42,700	4.74	**	58	3.5	3.8	25.7	63	3.5	3.8	25.8
12	54	3.7	3.9	7.4	8,760	1,800	8,920	39,500	44,400	4.98	**	54	3.7	3.8	25.6	54	3.7	4.1	25.6
13	62	3.7	----	10.9	11,900	2,400	12,140	21,600	------	----	**	63	3.7	---	-----	61	3.7	---	-----
14	59	3.7	4.2	10.9	11,680	2,500	11,940	29,100	34,600	2.90	**	60	3.6	4.1	25.7	57	3.7	4.2	25.8
15	60	3.6	4.3	14.4	12,610	3,200	13,010	13,800	19,500	1.50	**	61	3.6	4.3	-----	60	3.6	4.2	-----
16	60	3.6	4.2	14.4	12,680	3,300	13,100	12,500	18,100	1.38	**	61	3.6	4.3	25.9	60	3.6	4.1	25.5
17	59	3.6	4.3	14.4	12,340	3,100	12,720	18,400	24,100	1.89	**	59	3.6	4.6	25.7	59	3.6	4.0	25.7
18	89	2.7	2.7	.35	760	*	760	0	3,300	4.34	**	94	2.7	2.7	-----	84	2.7	2.7	-----
19	87	2.9	2.7	2.1	3,840	400	3,850	17,200	20,500	5.32	**	87	3.1	2.7	26.1	87	2.8	2.6	26.1
20	85	2.8	3.0	3.9	6,780	700	6,810	28,500	32,300	4.74	12.8	84	2.9	2.9	26.1	86	2.8	3.1	26.1
21	82	2.8	3.2	7.4	10,380	1,500	10,490	27,900	32,100	3.06	**	80	2.8	3.4	26.2	83	2.8	2.9	26.2
22	84	2.8	3.2	10.9	12,210	2,000	12,370	19,700	23,900	1.93	**	85	2.8	3.1	26.2	83	2.8	3.3	26.2
23	89	2.7	3.2	14.4	12,580	3,100	12,960	11,000	15,300	1.18	**	94	2.7	3.1	26.7	84	2.7	3.2	26.0
24	174	1.9	1.9	.35	730	*	730	0	2,400	3.29	**	173	2.0	2.0	-----	173	1.9	1.9	-----
25	169	1.9	1.9	.35	800	*	800	0	2,400	3.00	**	169	1.9	1.9	27.0	169	1.9	1.9	27.0
26	169	1.9	1.9	.35	790	*	790	0	2,400	3.04	**	169	2.0	2.0	27.0	169	1.9	1.9	27.0
27	168	1.9	1.9	.35	890	*	890	0	2,400	2.70	**	167	2.0	2.0	27.0	168	1.9	1.9	27.0
28	164	1.9	1.9	2.1	4,540	300	4,550	8,200	10,600	2.33	**	165	2.0	1.9	26.9	162	1.9	1.9	27.0
29	168	1.8	1.8	3.9	7,640	400	7,650	19,700	21,900	2.86	11.9	168	1.9	1.8	26.9	168	1.7	1.7	27.0
30	168	1.9	2.0	7.4	11,030	1,500	11,130	20,700	23,300	2.09	**	169	2.0	2.1	27.1	166	1.8	1.8	27.1
31	170	1.9	2.0	10.9	12,550	2,000	12,700	18,700	21,300	1.68	**	173	----	---	26.7	168	1.9	2.0	27.0
32	164	1.9	1.7	14.4	12,010	2,900	12,350	7,400	9,300	.75	**	168	1.9	1.8	27.3	159	1.8	1.6	26.7

*Force too small to be measured accurately.

**Relaxation length not determined.

TABLE II.- YAW TEST DATA - Continued

(b) SERIES B: $\bar{F}_z$ = 23,700 lb; $(F_z)_{\text{tire A}}$ = 23,700 lb; $(F_z)_{\text{tire B}}$ = 23,800 lb.

Run	Average values											Tire A				Tire B			
	$\bar{p}$, lb/sq in.	$\bar{\delta}_0$, in.	$\bar{\delta}$, in.	$\bar{\psi}$, deg	$\bar{F}_y$, lb	$\bar{F}_x$, lb	$\bar{F}_\psi$, lb	$\Delta\bar{M}_x$, lb-in.	$\bar{M}_z$, lb-in.	$\bar{q}$, in.	$\bar{L}_y$, in.	p, lb/sq in.	δ_0, in.	δ, in.	r_e, in.	p, lb/sq in.	δ_0, in.	δ, in.	r_e, in.
33	79	3.8	3.8	0.35	------	*	------	0	5,300	-----	**	79	3.8	3.8	25.7	79	3.8	3.8	25.5
34	79	3.9	3.9	.35	780	*	780	0	5,500	7.05	**	79	3.8	3.8	25.6	78	3.9	3.9	25.5
35	80	3.8	3.8	.35	830	*	830	0	5,400	6.51	**	82	3.8	3.8	25.6	79	3.8	3.8	25.5
36	79	3.9	3.9	.35	870	*	870	0	5,500	6.32	**	80	3.8	3.8	25.6	79	3.9	3.9	25.4
37	83	3.9	3.9	.35	950	*	950	0	5,600	6.02	**	83	3.8	3.8	25.7	83	3.9	3.9	25.7
38	82	3.8	3.8	.35	720	*	720	0	5,400	7.50	**	82	3.8	3.8	25.6	82	3.8	3.8	25.6
39	79	3.9	---	2.1	3,280	600	3,300	23,600			**	79	4.0	---	----	79	3.9	---	----
40	79	3.9	3.9	2.1	3,060	300	3,070	30,400	35,900	11.69	**	80	3.9	4.0	25.7	79	3.9	3.7	25.6
41	79	4.1	4.0	3.9	5,850	1,000	5,880	31,000	36,700	6.24	----	79	4.1	3.9	25.5	79	4.1	4.0	25.5
42	79	3.9	4.3	7.4	10,880	1,900	11,030	54,000	60,300	5.47	**	79	3.9	4.4	25.7	78	4.0	4.2	25.8
43	80	4.0	4.5	10.9	14,390	3,100	14,720	36,400	43,200	2.93	**	81	4.0	4.6	25.7	79	4.0	4.5	25.9
44	79	3.9	4.6	10.9	13,880	2,900	14,180	37,200	44,100	3.11	**	79	3.9	4.6	25.7	79	3.8	4.6	26.0
45	79	3.9	4.7	14.4	16,400	4,200	16,930	27,300	34,400	2.03	**	80	3.8	4.6	25.7	79	4.0	4.7	25.8
46	79	---	---	14.4	------	------	------	------	------	-----	**	80	---	---	25.7	79	---	---	25.7
47	81	3.9	4.9	17.9	16,200	4,900	16,920	31,000	38,600	2.28	**	81	3.8	4.9	26.2	81	4.0	4.9	25.3
48	127	2.8	2.8	.35	1,010	*	1,010	0	4,100	4.06	**	127	2.8	2.8	26.5	126	2.8	2.8	26.5
49	126	2.8	2.7	2.1	5,240	400	5,250	27,500	31,300	5.96	**	126	2.9	2.7	26.5	126	2.8	2.6	26.5
50	128	2.8	2.8	2.1	4,860	400	4,870	25,300	29,400	6.04	**	128	2.9	2.8	26.6	128	2.7	2.7	26.6
51	128	2.8	2.6	3.9	8,800	900	8,840	30,600	34,200	3.87	17.9	128	2.8	2.7	26.6	128	2.8	2.4	26.5
52	126	2.8	2.9	7.4	13,600	2,200	13,770	39,000	43,300	3.14	**	126	2.8	3.0	26.5	126	2.7	2.8	26.7
53	126	2.8	2.9	10.9	13,350	2,900	15,620	23,900	28,200	1.81	**	126	2.8	2.9	26.1	126	2.8	2.9	26.5
54	127	2.8	2.9	10.9	15,490	3,000	15,780	22,200	26,500	1.68	**	128	2.8	3.0	26.4	127	2.8	2.9	26.5
55	127	2.7	3.0	14.4	16,330	3,800	16,760	23,400	27,900	1.66	**	126	2.7	3.0	26.6	127	2.7	3.1	26.3
56	128	2.7	2.9	17.9	15,690	4,300	16,250	21,400	25,700	1.58	**	130	2.7	2.9	27.5	127	2.7	2.8	25.7
57	202	2.1	2.1	.35	1,050	*	1,050	0	3,200	3.05	**	202	2.3	2.3	27.1	202	2.0	2.0	27.1
58	203	2.1	2.1	.35	1,050	*	1,050	0	3,200	3.05	**	203	2.2	2.2	27.1	203	2.1	2.1	27.3
59	202	2.1	2.1	.35	1,210	*	1,210	0	3,200	2.64	**	202	2.1	2.1	27.3	202	2.0	2.0	27.2
60	203	2.0	2.0	.35	1,070	*	1,070	0	2,900	2.71	**	206	2.1	2.1	27.1	204	1.9	1.9	27.2
61	203	2.1	2.1	.35	950	*	950	0	3,200	3.37	**	203	2.1	2.1	27.2	203	2.1	2.1	27.2
62	202	2.1	2.1	.35	990	*	990	0	3,200	3.23	**	202	2.1	2.1	27.2	202	2.1	2.1	27.1
63	203	2.1	2.1	.35	980	*	980	0	3,200	3.27	**	203	2.1	2.1	27.2	203	2.1	2.1	27.3
64	200	2.1	2.2	2.1	5,070	300	5,080	20,300	23,700	4.67	**	200	2.1	2.2	27.2	203	2.0	2.0	27.3
65	203	2.1	2.0	2.1	5,210	300	5,220	22,000	24,900	4.77	**	203	2.1	1.8	27.2	200	2.1	2.3	27.2
66	202	2.1	2.1	3.9	9,400	700	9,430	20,400	23,600	2.50	----	202	2.2	2.0	27.1	203	2.1	2.1	27.3
67	202	2.0	2.1	7.4	13,700	1,500	13,780	25,100	28,300	2.05	**	202	---	2.1	27.1	202	2.1	2.2	27.2
68	202	2.0	2.1	10.9	14,980	2,500	15,180	17,900	21,100	1.39	**	202	2.0	2.1	27.2	202	2.0	2.1	27.1
69	202	2.1	2.2	10.9	14,790	2,500	15,000	16,300	19,700	1.31	**	202	2.1	2.1	27.3	202	2.0	2.0	27.0
70	202	2.0	1.9	14.4	15,510	3,500	15,890	14,100	16,800	1.06	**	202	2.0	2.0	27.2	203	2.0	2.3	27.2
71	202	2.1	2.1	17.9	14,960	4,100	15,500	18,100	21,300	1.37	**	202	2.1	2.1	28.0	202	---	2.1	26.4

*Force too small to be measured accurately.
**Relaxation length not determined.

TABLE II.- YAW TEST DATA - Continued

(c) SERIES C: $\bar{F}_z$ = 32,700 lb; $(F_z)_{tire\ A}$ = 32,900 lb; $(F_z)_{tire\ B}$ = 32,500 lb.

Run	Average values											Tire A				Tire B			
	p, lb/sq in.	δ_0, in.	δ, in.	$\bar{\psi}$, deg	$\bar{F}_y$, lb	$\bar{F}_x$, lb	$\bar{F}_\psi$, lb	$\Delta\bar{M}_z$, lb-in.	$\bar{M}_z$, lb-in.	$\bar{q}$, in.	l_y, in.	p, lb/sq in.	δ_0, in.	δ, in.	r_e, in.	p, lb/sq in.	δ_0, in.	δ, in.	r_e, in.
72	130	3.7	3.4	2.1	4,650	500	4,670	25,100	30,600	6.55	**	130	3.8	3.4	26.3	130	3.7	3.4	26.3
73	130	3.7	3.6	2.1	4,520	300	4,530	24,400	30,400	6.71	**	130	3.7	3.5	26.3	131	3.7	3.6	26.2
74	130	3.6	3.7	3.9	8,410	500	8,420	56,200	62,500	7.42	----	131	3.7	3.7	26.2	130	3.5	3.7	26.2
75	131	3.5	3.6	7.4	14,380	2,300	14,560	59,500	65,500	4.50	**	131	3.4	3.4	26.3	131	3.5	3.7	26.4
76	135	3.6	3.9	10.9	18,360	3,800	18,750	52,800	59,700	3.18	**	135	3.5	3.9	----	135	3.6	3.9	----
77	155	3.1	3.1	.35	1,190	*	1,190	0	5,300	4.45	**	155	3.1	3.1	----	155	3.1	3.1	----
78	147	3.2	3.2	.35	1,140	*	1,140	0	5,400	4.74	**	148	3.1	3.1	26.6	146	3.3	3.3	26.4
79	148	3.2	3.2	.35	1,230	*	1,230	0	5,400	4.39	**	148	3.1	3.1	26.5	148	3.3	3.3	26.4
80	147	---	---	.35	1,080	*	1,080	0			**	149	---	---	26.5	145	---	---	26.4
81	155	3.1	3.5	14.4	20,810	5,000	21,400	35,200	41,500	1.94	**	155	3.1	3.6	26.7	155	3.1	3.5	26.4
82	144	3.2	3.6	17.9	21,760	6,200	22,610	32,000	38,400	1.70	**	144	3.2	3.5	----	144	3.3	3.6	26.4
83	147	3.3	3.6	17.9	20,870	6,000	21,700	30,600	37,000	1.71	**	148	3.3	3.5	27.2	146	3.3	3.6	25.8
84	174	2.9	2.7	2.1	6,070	600	6,090	25,100	29,600	4.86	**	174	3.0	2.6	26.9	174	2.8	2.7	26.9
85	173	3.1	2.9	3.9	9,770	700	9,800	42,500	47,600	4.86	----	173	3.2	2.9	26.6	173	3.1	2.9	26.6
86	174	2.9	3.0	3.9	10,390	700	10,410	38,800	44,100	4.24	17.8	174	3.0	3.1	26.8	174	2.9	2.9	26.7
87	174	2.9	3.0	7.4	15,690	2,100	15,830	48,200	53,500	3.38	**	174	2.8	3.1	27.0	174	2.9	3.0	----
88	173	2.9	3.0	10.9	19,050	3,500	19,370	43,000	48,300	2.49	**	173	2.9	3.0	26.9	173	2.9	3.0	26.6
89	178	2.9	3.1	14.4	20,150	4,800	20,710	32,700	38,400	1.85	**	178	2.8	3.1	26.9	178	2.9	3.1	26.6
90	175	2.9	3.1	17.9	21,160	5,900	21,950	28,700	34,400	1.57	**	175	3.0	2.9	26.8	175	2.9	3.3	26.4
91	232	2.2	2.2	.35	1,220	*	1,220	0	3,700	3.03	**	232	2.2	2.2	27.2	232	2.2	2.2	27.2
92	232	2.3	2.3	.35	1,320	*	1,320	0	4,000	3.03	**	232	2.4	2.4	27.1	232	2.3	2.3	27.3
93	232	2.3	2.3	.35	1,270	*	1,270	0	4,000	3.15	**	232	2.3	2.3	27.3	232	2.3	2.3	27.3
94	232	---	---	.35	1,170	*	1,170	0			**	232	---	---	27.3	232	---	---	27.2
95	227	2.3	2.3	.35	1,300	*	1,300	0	4,000	3.08	**	226	2.3	2.3	26.8	228	2.3	2.3	27.2
96	232	2.4	2.4	.35	1,040	*	1,040	0	4,300	4.13	**	232	2.5	2.5	27.2	232	2.3	2.3	27.3
97	233	2.3	2.4	2.1	5,840	500	5,850	13,900	18,300	3.13	**	233	2.3	2.5	27.1	233	2.4	2.3	27.3
98	232	2.3	2.1	2.1	5,790	400	5,800	12,500	16,200	2.79	**	232	2.3	2.1	27.3	232	2.3	2.3	27.3
99	233	2.4	2.4	3.9	10,460	700	10,480	41,700	46,100	4.40	----	233	2.4	2.3	27.2	233	2.4	2.5	27.2
100	229	2.4	2.3	3.9	10,890	600	10,910	32,600	36,600	3.35	11.5	228	2.4	2.2	27.2	229	2.4	2.4	27.2
101	231	2.3	2.3	7.4	16,350	2,000	16,470	41,300	45,300	2.73	**	230	2.3	2.3	27.3	231	2.3	2.4	27.2
102	232	2.4	2.5	10.9	19,030	3,100	19,270	30,900	35,600	1.85	**	232	2.4	2.6	27.4	232	2.5	2.5	27.0
103	231	2.5	2.5	14.4	19,900	4,500	20,390	31,700	36,400	1.79	**	231	2.5	2.5	27.2	231	2.5	2.4	27.2
104	230	2.4	2.5	17.9	19,570	5,300	20,250	27,200	31,900	1.58	**	230	2.4	2.6	28.6	230	2.5	2.4	25.9

*Force too small to be measured accurately.
**Relaxation length not determined.

TABLE II.- YAW TEST DATA - Continued

(d) SERIES D: $\bar{F}_z = 39,800$ lb; $(F_z)_{tire A} = 39,900$ lb; $(F_z)_{tire B} = 39,700$ lb.

Run	Average values											Tire A				Tire B			
	$\bar{p}$, lb/sq in.	$\bar{\delta}_o$, in.	$\bar{\delta}$, in.	$\bar{\psi}$, deg	$\bar{F}_y$, lb	$\bar{F}_x$, lb	$\bar{F}_\psi$, lb	$\Delta\bar{M}_z$, lb-in.	$\bar{M}_z$, lb-in.	$\bar{q}$, in.	$\bar{L}_y$, in.	p, lb/sq in.	δ_o, in.	δ, in.	r_e, in.	p, lb/sq in.	δ_o, in.	δ, in.	r_e, in.
105	128	4.0	3.8	2.1	3,780	600	3,800	38,700	45,100	11.87	**	128	4.0	3.6	26.1	128	4.1	4.0	26.0
106	130	4.0	3.8	2.1	3,580	700	3,600	38,100	44,600	12.39	**	131	4.0	3.9	26.1	129	4.1	3.7	26.0
107	127	4.1	4.2	3.9	6,980	800	7,020	70,200	77,500	11.04	--	127	4.1	4.2	26.1	127	4.2	4.2	25.9
108	128	4.2	4.1	3.9	6,800	1,200	6,870	65,100	72,200	10.51	--	128	4.3	4.3	26.0	128	4.1	3.9	25.9
109	126	4.2	4.3	7.4	13,510	2,900	13,770	78,000	85,500	6.21	**	126	4.3	4.3	26.1	126	4.2	4.4	26.0
110	126	4.1	4.5	10.9	17,910	5,100	18,550	67,000	75,000	4.04	**	126	4.0	4.5	26.1	127	4.2	4.5	26.1
111	151	3.5	3.3	2.1	4,790	600	4,810	32,100	37,800	7.86	**	151	3.5	3.4	26.4	150	3.5	3.2	26.4
112	153	3.5	3.3	2.1	4,810	600	4,830	34,200	39,900	8.26	**	153	3.5	3.4	26.4	153	3.5	3.2	26.4
113	150	3.7	3.5	3.9	8,310	1,100	8,370	60,600	66,800	7.98	--	150	3.7	3.6	26.2	150	3.7	3.5	26.2
114	150	3.7	3.8	7.4	15,350	2,900	15,600	70,800	77,800	4.99	**	150	3.8	3.8	26.5	150	3.7	3.7	26.4
115	152	3.6	4.1	10.9	20,220	4,900	20,780	63,800	71,600	3.45	**	152	3.6	4.2	26.5	151	3.7	4.0	26.5
116	232	2.7	2.7	.35	1,190	*	1,190	0	5,300	4.45	**	232	2.7	2.7	27.2	231	2.6	2.6	27.1
117	230	2.7	2.7	.35	1,320	*	1,320	0	5,300	4.02	**	229	2.8	2.8	27.1	230	2.7	2.7	27.0
118	232	2.7	2.7	.35	1,220	*	1,220	0	5,300	4.34	**	232	2.6	2.6	----	232	2.7	2.7	----
119	230	2.7	2.7	.35	1,210	*	1,210	0	5,300	4.38	**	229	2.7	2.7	27.1	230	2.8	2.8	27.0
120	232	2.6	2.6	.35	1,220	*	1,220	0	5,000	4.10	**	232	2.6	2.6	27.2	232	2.6	2.6	27.0
121	231	2.6	2.6	.35	1,280	*	1,280	0	5,000	3.91	**	231	2.6	2.6	27.0	231	2.6	2.6	27.0
122	231	2.7	2.6	2.1	6,830	300	6,840	24,200	29,200	4.27	**	231	2.7	2.6	27.1	231	2.7	2.5	27.0
123	230	2.6	2.6	2.1	6,790	500	6,800	24,400	29,400	4.32	**	230	2.5	2.4	27.2	230	2.7	2.8	27.1
124	231	2.8	2.6	3.9	11,100	700	11,120	52,300	57,300	5.15	--	232	2.9	2.5	26.9	231	2.8	2.6	27.0
125	230	2.7	2.6	3.9	10,990	700	11,010	50,100	55,100	5.00	--	229	2.6	2.6	27.0	230	2.8	2.6	27.0
126	231	2.7	2.7	7.4	18,570	2,800	18,780	50,400	55,700	2.97	**	231	2.7	2.6	27.2	231	2.7	2.9	27.0
127	231	2.7	2.8	10.9	22,020	4,800	22,550	43,900	49,600	2.20	**	231	2.6	2.7	27.1	231	2.7	2.9	27.0
128	232	2.7	2.8	14.4	22,810	6,400	23,680	26,500	32,200	1.36	**	232	2.8	2.8	27.3	232	2.7	2.8	27.6
129	231	2.7	2.7	17.9	21,930	7,600	23,200	24,700	30,000	1.29	**	231	2.7	2.7	28.2	231	2.8	2.7	26.2

*Force too small to be measured accurately.
**Relaxation length not determined.

TABLE II.- YAW TEST DATA - Continued

(e) SERIES E: $\bar{F}_z$ = 45,200 lb; $(F_z)_{\text{tire A}}$ = 45,400 lb; $(F_z)_{\text{tire B}}$ = 45,000 lb.

Run	Average values											Tire A				Tire B			
	$\bar{p}$, lb/sq in.	δ_o, in.	$\bar{\delta}$, in.	$\bar{\psi}$, deg	$\bar{F}_y$, lb	$\bar{F}_x$, lb	$\bar{F}_\psi$, lb	$\Delta\bar{M}_z$, lb-in.	$\bar{M}_z$, lb-in.	$\bar{q}$, in.	L_y, in.	p, lb/sq in.	δ_o, in.	δ, in.	r_e, in.	p, lb/sq in.	δ_o, in.	δ, in.	r_e, in.
130	151	4.0	3.8	2.1	4,900	900	4,930	40,400	47,400	9.61	**	151	3.9	3.7	26.1	151	4.0	3.9	26.1
131	152	4.0	3.8	2.1	4,730	800	4,760	40,900	47,900	10.06	**	150	3.9	3.7	26.2	154	4.0	3.9	26.1
132	152	4.1	4.0	3.9	8,460	1,000	8,510	74,700	82,200	9.66	20.0	153	4.1	4.0	26.1	150	4.2	4.0	26.1
133	151	4.1	3.9	3.9	8,420	1,400	8,500	74,400	81,700	9.61	----	151	4.0	3.8	26.1	151	4.1	4.0	26.2
134	150	---	4.0	7.4	14,860	3,100	15,140	86,300	93,700	6.19	**	150	---	3.9	26.3	150	---	4.1	----
135	152	4.2	4.7	10.9	19,990	4,900	20,560	84,100	93,400	4.54	**	152	4.2	4.5	26.3	152	---	4.9	26.2
136	183	3.6	3.6	.35	1,090	*	1,090	0	7,200	6.61	**	183	3.6	3.6	26.7	183	3.6	3.6	26.6
137	180	3.7	3.5	2.1	5,510	800	5,540	39,300	46,100	8.32	**	180	3.7	3.5	26.6	180	3.7	3.5	26.5
138	183	3.4	3.2	2.1	5,850	700	5,850	41,100	47,100	8.05	**	183	3.4	3.1	26.5	183	3.4	3.2	26.4
139	181	3.6	3.4	3.9	9,880	600	9,900	57,600	64,200	6.48	----	181	3.6	3.4	26.6	180	---	---	26.5
140	182	3.6	3.4	3.9	9,850	1,000	9,900	60,900	67,900	6.82	----	180	3.6	3.4	26.6	184	3.5	3.3	26.5
141	181	3.5	3.4	3.9	9,510	1,000	9,560	49,900	56,500	5.91	----	181	3.4	3.3	26.6	181	3.5	3.5	25.9
142	180	3.6	3.7	7.4	17,280	3,700	17,610	79,800	87,200	4.95	**	180	3.6	3.8	26.6	179	---	3.7	----
143	180	3.5	3.6	10.9	22,290	5,400	22,910	65,600	72,700	3.17	**	180	3.5	3.8	26.7	180	3.4	3.8	26.5
144	233	2.9	2.9	.35	1,260	*	1,260	0	6,000	4.76	**	232	2.9	2.9	----	235	2.9	2.9	----
145	232	3.0	3.0	.35	1,310	*	1,310	0	6,300	4.81	**	232	3.0	3.0	----	232	3.1	3.1	----
146	232	2.9	2.9	.35	1,350	*	1,350	0	6,000	4.44	**	232	2.8	2.8	27.0	232	2.9	2.9	27.0
147	232	3.0	3.0	.35	1,210	*	1,210	0	6,300	5.21	**	231	3.0	3.0	----	232	3.0	3.0	----
148	232	2.9	2.9	.35	1,410	*	1,410	0	6,000	4.26	**	232	2.9	2.9	27.0	232	2.9	2.9	27.0
149	232	2.9	2.9	.35	------	*	------	0	6,000	----	**	232	2.9	2.9	27.0	232	3.0	3.0	26.9
150	232	2.9	2.9	.35	1,210	*	1,210	0	6,000	4.96	**	232	2.9	2.9	27.0	233	2.9	2.9	26.9
151	230	3.0	3.0	.35	1,120	*	1,120	0	6,200	5.54	**	230	3.0	3.0	27.0	230	3.0	3.0	----
152	232	2.8	2.8	.35	1,320	*	1,320	0	5,700	4.32	**	232	2.8	2.8	27.1	232	2.8	2.8	27.0
153	232	3.0	2.7	2.1	6,490	600	6,510	32,000	37,300	5.73	**	232	3.0	2.5	27.1	232	3.1	2.8	27.0
154	233	2.9	2.8	2.1	6,160	400	6,170	28,700	34,400	5.58	**	233	2.8	2.9	27.1	234	2.9	2.7	27.0
155	232	3.2	3.0	3.9	11,350	1,000	11,390	49,200	55,500	4.87	----	232	3.3	2.9	26.8	232	3.1	3.1	27.0
156	232	2.8	3.1	3.9	11,540	1,200	11,590	48,200	54,800	4.73	16.5	232	2.8	3.1	27.0	232	---	2.9	----
157	232	2.9	2.8	7.4	19,860	3,200	20,110	65,300	71,000	3.53	**	232	2.8	2.7	----	232	3.0	2.9	----
158	232	2.9	3.0	7.4	19,570	3,300	19,830	61,800	68,100	3.43	**	232	2.9	2.9	27.2	232	2.8	3.0	----
159	233	3.0	3.0	10.9	23,340	5,000	23,860	53,900	60,200	2.52	**	233	2.9	2.9	----	232	3.0	3.1	----
160	232	2.9	3.0	10.9	22,710	5,000	23,250	53,100	59,400	2.55	**	232	2.9	3.0	----	232	2.9	3.1	----
161	232	---	3.2	14.4	24,660	6,600	25,550	37,900	44,900	1.76	**	231	---	3.2	27.2	232	---	---	26.7
162	232	2.9	3.2	17.9	24,250	8,300	25,630	32,300	39,300	1.53	**	232	2.9	2.9	27.8	232	---	3.3	26.3

*Force too small to be measured accurately.
**Relaxation length not determined.

TABLE II.- YAW TEST DATA -- Continued

(f) SERIES F: $\bar{F}_z$ = 17,400 lb; $(F_z)_{tire\ A}$ = 17,300 lb; $(F_z)_{tire\ B}$ = 17,400 lb.

Run	Average values											Tire A				Tire B			
	$\bar{p}$, lb/sq in.	$\bar{\delta}_o$, in.	$\bar{\delta}$, in.	$\bar{\psi}$, deg	$\bar{F}_y$, lb	$\bar{F}_x$, lb	$\bar{F}_\psi$, lb	$\Delta\bar{R}_z$, lb-in.	$\bar{R}_z$, lb-in.	$\bar{q}$, in.	$\bar{l}_y$, in.	p, lb/sq in.	δ_o, in.	δ, in.	r_e, in.	p, lb/sq in.	δ_o, in.	δ, in.	r_e, in.
163	61	3.4	3.4	0.35	530	*	530	0	4,100	7.74	**	61	3.3	3.3	25.8	62	3.4	3.4	25.8
164	60	3.5	3.3	2.1	2,680	300	2,690	18,000	22,000	8.18	**	60	3.5	3.3	25.9	60	3.5	3.3	25.8
165	59	3.6	3.5	3.9	4,690	800	4,730	32,900	37,200	7.86	----	59	3.6	3.6	25.7	59	3.6	3.4	25.8
166	60	3.4	3.6	7.4	8,760	1,700	8,910	34,300	38,800	4.35	**	60	3.5	3.8	26.1	60	3.5	3.4	25.9
167	59	3.5	3.9	10.9	11,070	2,700	11,380	32,700	37,700	3.31	**	59	3.5	3.8	25.9	59	---	4.0	25.8
168	60	3.4	4.1	14.4	12,850	4,000	13,440	29,000	34,400	2.56	**	59	3.4	4.2	25.9	60	3.4	4.1	25.9
169	60	3.4	4.3	17.9	13,060	4,800	13,900	23,500	29,200	2.10	**	60	---	4.5	26.2	60	3.4	4.2	25.4
170	84	2.6	2.5	2.1	3,470	300	3,480	17,100	19,900	5.72	**	84	2.6	2.6	26.5	84	2.6	2.4	26.4
171	84	2.7	2.7	3.9	6,070	600	6,100	29,500	32,700	5.36	----	84	2.7	2.7	26.4	84	2.8	2.7	26.3
172	85	2.6	2.8	7.4	9,980	1,700	10,120	28,000	31,500	3.11	**	85	2.4	2.5	26.6	85	2.7	3.0	26.4
173	84	2.7	3.0	10.9	11,740	2,800	12,060	24,100	27,900	2.31	**	84	---	3.1	26.4	84	2.7	2.8	26.2
174	84	2.8	3.1	14.4	13,010	3,300	13,420	22,300	26,300	1.96	**	84	---	3.1	26.6	85	2.8	3.1	26.2
175	84	2.8	3.2	17.9	13,310	4,200	13,960	18,400	26,600	1.62	**	84	---	3.2	26.9	84	2.8	3.2	25.8
176	170	1.7	1.7	.35	830	*	830	0	2,000	2.41	**	170	1.6	1.6	27.3	170	1.7	1.7	27.4
177	167	1.8	1.8	.35	760	*	760	0	2,200	2.89	**	167	1.9	1.9	27.3	166	1.7	1.7	27.4
178	169	1.7	1.7	.35	880	*	880	0	2,000	2.27	**	169	1.6	1.6	----	169	1.8	1.8	----
179	168	1.8	1.8	.35	740	*	740	0	2,200	2.97	**	168	1.8	1.8	27.3	168	1.8	1.8	27.1
180	169	1.8	1.8	.35	810	*	810	0	2,200	2.72	**	169	1.9	1.9	27.3	168	1.7	1.7	27.3
181	169	1.7	1.7	.35	850	*	850	0	2,000	2.35	**	169	---	---	27.2	169	1.7	1.7	27.3
182	169	1.7	1.6	2.1	4,050	100	4,050	8,700	10,500	2.59	**	169	1.7	1.5	27.4	169	1.8	1.6	27.5
183	168	1.8	1.8	3.9	6,810	500	6,830	12,200	14,400	2.11	11.7	168	1.9	1.9	27.2	167	1.7	1.8	27.4
184	169	1.7	1.6	3.9	7,350	500	7,370	16,700	18,500	2.51	11.4	169	1.8	1.5	27.4	169	1.6	1.7	27.3
185	169	1.7	1.5	3.9	6,150	----	----	20,800	22,400	----	**	169	1.7	1.4	----	169	1.6	1.5	----
186	168	1.7	1.5	7.4	10,450	1,500	10,560	19,200	20,800	1.97	**	169	1.7	1.5	27.3	168	1.8	1.4	27.3
187	168	1.7	1.7	10.9	11,520	2,300	11,730	15,200	17,200	1.46	**	169	1.8	1.6	27.4	168	1.7	1.7	27.1
188	169	1.8	1.7	14.4	12,120	3,100	12,510	11,300	13,300	1.06	**	169	1.8	1.5	27.7	169	1.8	1.8	26.9
189	167	1.9	1.8	17.9	12,170	3,700	12,720	10,100	12,300	.97	**	168	---	1.7	27.0	166	1.9	1.8	26.7

*Force too small to be measured accurately.
**Relaxation length not determined.

TABLE II.- YAW TEST DATA - Continued

(g) SERIES G: F_z = 9,600 lb; $(F_z)_{tire\ A}$ = 9,700 lb; $(F_z)_{tire\ B}$ = 9,600 lb.

Run	Average values											Tire A				Tire B			
	p, lb/sq in.	δ_0, in.	δ, in.	$\bar\psi$, deg	$\bar F_y$, lb	$\bar F_x$, lb	$\bar F_\psi$, lb	$\Delta \bar N_z$, lb-in.	$\bar R_z$, lb-in.	$\bar q$, in.	L_y, in.	p, lb/sq in.	δ_0, in.	δ, in.	r_e, in.	p, lb/sq in.	δ_0, in.	δ, in.	r_e, in.
190	29	3.6	3.6	0.35	450	*	450	0	3,800	8.44	**	29	3.6	3.6	25.6	29	3.7	3.7	25.3
191	29	3.4	3.2	2.1	1,710	200	1,720	6,500	9,700	5.64	**	29	3.3	3.1	25.7	29	3.4	3.2	25.5
192	29	3.5	3.3	3.9	3,100	300	3,110	20,100	23,500	7.56	--	29	3.4	3.3	25.5	29	3.6	3.3	25.4
193	29	3.5	3.6	7.4	6,310	1,000	6,390	25,700	29,500	4.62	**	29	3.5	3.7	25.7	29	3.6	3.5	25.7
194	29	3.5	3.7	10.9	7,590	1,400	7,720	21,700	25,700	3.33	**	29	3.5	3.5	25.5	29	3.5	3.8	25.7
195	29	3.2	3.9	14.4	8,690	2,100	8,940	6,900	11,200	1.25	**	29	3.1	4.0	26.0	29	3.2	3.7	25.7
196	29	3.4	3.9	17.9	8,560	2,600	8,940	7,400	11,700	1.31	**	29	3.4	3.9	26.2	29	3.5	4.0	24.9
197	39	2.6	2.6	.35	480	*	480	0	2,400	5.00	**	39	2.6	2.6	26.0	39	2.7	2.7	25.9
198	39	2.6	2.5	2.1	1,860	200	1,870	8,500	10,800	5.78	**	39	2.6	2.3	26.2	39	2.7	2.6	26.0
199	39	3.0	2.9	3.9	3,640	400	3,660	17,500	20,400	5.57	--	39	3.1	3.0	25.9	39	3.0	2.9	25.9
200	39	2.6	2.8	7.4	6,670	900	6,730	19,100	21,900	3.25	**	39	2.6	2.7	26.2	39	2.7	2.8	26.1
201	39	---	3.3	10.9	8,100	1,400	8,220	18,400	22,000	2.68	**	39	---	3.3	25.9	39	---	3.3	25.9
202	39	2.5	3.0	14.4	8,860	1,900	9,050	9,400	12,500	1.38	**	39	2.5	3.0	26.3	39	2.6	3.0	25.9
203	39	2.8	3.2	17.9	8,530	2,500	8,890	8,600	12,000	1.35	**	39	2.8	3.2	26.7	39	2.8	3.2	25.3
204	59	2.0	2.0	.35	630	*	630	0	1,700	2.70	**	59	2.0	2.0	26.3	58	2.1	2.1	26.4
205	59	1.9	1.8	2.1	2,480	200	2,490	5,300	6,700	2.69	**	59	1.9	1.8	26.6	59	1.9	1.7	26.7
206	59	2.4	2.2	3.9	4,690	400	4,710	14,600	16,600	3.52	--	59	2.3	2.1	26.3	59	2.3	2.2	26.4
207	59	1.9	2.1	7.4	7,270	1,000	7,340	16,000	17,800	2.43	**	59	1.8	2.3	26.7	59	1.9	1.8	26.6
208	59	2.1	2.3	10.9	8,110	1,500	8,250	15,100	17,300	2.10	**	58	---	2.4	26.6	59	2.1	2.1	26.3
209	84	1.7	1.7	.35	630	*	630	0	1,400	2.22	**	84	1.7	1.7	26.7	84	1.6	1.6	26.8
210	84	1.6	1.6	.35	640	*	640	0	1,300	2.03	**	84	1.7	1.7	26.9	84	1.6	1.6	26.9
211	84	1.6	1.6	.35	640	*	640	0	1,300	2.03	**	84	1.6	1.6	----	83	1.6	1.6	----
212	84	1.6	1.4	2.1	2,700	200	2,710	------	------	----	**	84	1.6	1.3	27.1	83	1.7	1.4	27.0
213	84	1.7	1.7	3.9	4,890	300	4,900	14,300	15,700	3.20	--	84	1.8	1.6	26.7	84	1.6	1.7	26.8
214	84	1.6	1.5	7.4	7,540	800	7,580	13,700	14,800	1.95	**	84	1.7	1.4	27.0	84	1.6	1.6	27.0
215	127	1.3	1.3	.35	550	*	550	0	1,100	2.00	**	127	1.3	1.3	27.0	127	1.3	1.3	27.2
216	126	1.2	1.2	2.1	2,460	200	2,470	------	------	----	**	127	1.2	1.1	27.5	125	1.3	1.3	27.3
217	126	1.5	1.4	3.9	4,910	300	4,920	16,100	17,300	3.52	--	126	1.5	1.3	27.1	126	1.5	1.5	27.2
218	126	1.3	1.3	7.4	6,700	700	6,730	11,800	12,900	1.92	**	126	1.4	1.4	27.2	126	1.3	1.2	27.4
219	168	1.0	1.0	.35	500	*	500	0	800	1.60	**	168	1.0	1.0	27.5	168	1.0	1.0	27.0
220	168	1.0	1.0	2.1	2,440	100	2,440	------	------	----	**	168	1.0	.9	27.6	168	1.0	1.0	27.3
221	166	1.2	1.2	3.9	4,250	300	4,260	9,700	10,800	2.54	--	166	1.3	1.5	27.3	165	1.2	1.0	27.5
222	168	1.1	1.0	7.4	6,310	600	6,330	11,000	11,800	1.86	**	167	---	---	27.4	168	1.1	1.0	27.6

*Force too small to be measured accurately.

**Relaxation length not determined.

TABLE II.- YAW TEST DATA - Continued

(h) SERIES H: $F_z = 9,600$ lb; $(F_z)_{\text{tire A}} = 9,700$ lb; $(F_z)_{\text{tire B}} = 9,600$ lb.

Run	$\bar{p}$, lb/sq in.	$\bar{\delta}_0$, in.	$\bar{\delta}$, in.	$\bar{\psi}$, deg	$\bar{F}_y$, lb	$\bar{F}_x$, lb	$\bar{F}_\psi$, lb	$\Delta\bar{M}_z$, lb-in.	$\bar{M}_z$, lb-in.	$\bar{q}$, in.
223	30	3.4	3.4	0.35	480	*	480	0	3,500	7.29
224	29	3.4	3.4	.35	450	*	450	0	3,500	7.78
225	29	3.6	3.6	.35	450	*	450	0	3,800	8.44
226	29	3.4	3.3	2.1	1,660	200	1,670	11,300	14,700	8.80
227	29	3.6	3.4	2.1	1,550	200	1,560	12,800	16,300	10.45
228	29	3.5	3.4	3.9	3,050	300	3,060	9,800	13,300	4.35
229	29	3.5	3.3	3.9	2,960	400	2,980	13,000	16,400	5.50
230	29	3.6	3.5	5.7	3,710	500	3,740	17,900	21,600	5.78
231	29	3.6	3.6	7.4	4,830	800	4,890	14,000	17,800	3.64
232	29	3.5	3.5	10.9	4,910	1,200	5,050	13,800	17,500	3.47
233	29	3.6	3.5	14.4	4,870	1,700	5,140	12,100	15,800	3.07
234	29	3.3	3.6	17.9	4,560	1,600	4,830	9,700	13,500	2.80
235	39	2.7	2.7	.35	540	*	540	0	2,600	4.81
236	39	2.9	2.9	.35	530	*	530	0	2,900	5.47
237	39	2.9	2.9	.35	470	*	470	0	2,900	6.17
238	39	2.9	2.9	.35	590	*	590	0	2,900	4.92
239	39	2.9	2.9	.35	580	*	580	0	2,900	5.00
240	39	2.9	2.9	.35	540	*	540	0	2,900	5.37
241	39	2.7	2.5	2.1	2,080	100	2,080	9,500	11,800	5.67
242	39	2.8	2.6	2.1	2,130	300	2,140	10,100	12,500	5.84
243	39	3.1	3.0	2.1	2,260	200	2,270	9,600	12,700	5.59
244	39	2.9	2.7	3.9	3,360	400	3,380	10,300	12,900	3.82
245	39	3.1	2.9	3.9	3,220	300	3,230	14,500	17,400	5.39
246	39	3.0	3.0	5.7	3,870	400	3,890	18,200	21,300	5.48
247	39	3.0	3.1	7.4	4,730	600	4,770	13,400	16,600	3.48
248	39	3.0	2.9	10.9	5,040	1,300	5,190	10,200	13,100	2.52
249	39	3.0	3.3	14.4	4,980	1,600	5,220	9,300	12,900	2.47
250	39	3.0	3.0	14.4	5,640	1,800	5,910	------	------	----
251	39	2.9	3.1	14.4	5,700	1,700	5,940	7,200	10,400	1.75
252	39	3.0	3.2	17.9	4,550	1,900	4,910	7,400	10,800	2.20

*Force too small to be measured accurately.

TABLE II.- YAW TEST DATA - Concluded

(i) SERIES I: $\bar{F}_z = 9,600$ lb.

Run	Average values									
	$\bar{p}$, lb/sq in.	$\bar{\delta}_0$, in.	$\bar{\delta}$, in.	$\bar{\psi}$, deg	$\bar{F}_y$, lb	$\bar{F}_x$, lb	$\bar{F}_\psi$, lb	$\Delta\bar{M}_z$, lb-in.	$\bar{M}_z$, lb-in.	$\bar{q}$, in.
253	39	2.9	2.9	0.35	570	*	570	0	2,900	5.09
254	39	---	---	.35	510	*	510	0	-------	----
255	39	2.8	2.8	.35	620	*	620	0	2,800	4.52
256	39	2.8	2.8	.35	590	*	590	0	2,800	4.75
257	39	3.1	2.7	2.1	-----	300	-----	17,000	19,600	----
258	39	2.8	2.6	2.1	2,490	400	2,500	16,300	18,700	7.48
259	39	3.1	3.1	3.9	4,440	500	4,460	19,100	22,300	5.00
260	39	3.0	2.8	3.9	4,170	600	4,200	16,900	19,700	4.69
261	39	3.0	3.3	7.4	7,120	1,100	7,200	17,500	21,100	2.93
262	39	2.9	3.0	7.4	6,710	1,200	6,810	16,900	20,000	2.94
263	39	3.1	3.4	10.9	8,220	1,800	8,410	11,000	14,700	1.75
264	39	3.0	3.2	10.9	7,970	1,800	8,170	13,200	16,600	2.03
265	39	3.1	3.3	14.4	8,380	2,400	8,710	7,500	11,100	1.27
266	39	3.0	3.3	14.4	8,260	2,500	8,620	6,500	10,100	1.17
267	39	2.9	3.2	17.9	8,130	2,600	8,540	4,700	8,100	.95

*Force too small to be measured accurately.

TABLE III.- STATIC-RELAXATION-LENGTH DATA

Run	Test series	Tire A						Tire B					
		p_o, lb/sq in.	p, lb/sq in.	F_z, lb	r, in.	δ_o, in.	L_s in.	p_o, lb/sq in.	p, lb/sq in.	F_z, lb	r, in.	δ_o, in.	L_s in.
268	A	28	29	17,000	27.5	5.1	20.9	29	31	16,900	27.5	5.2	20.5
269	A	56	58	17,000	27.6	3.8	26.5	59	63	16,900	27.7	3.7	25.3
270	A	---	---	17,000	----	---	----	95	---	16,900	27.8	2.7	31.1
271	A	146	148	17,000	27.8	2.2	26.9	146	148	16,900	27.9	2.2	28.2
272	B	78	79	23,700	27.6	3.8	25.3	78	79	23,800	27.7	3.8	19.8
273	B	122	124	23,700	27.7	2.9	26.1	122	124	23,800	27.8	2.9	24.3
274	B	202	203	23,700	27.9	2.1	22.5	202	203	23,800	27.9	2.0	25.6
275	C	128	---	32,900	27.9	3.5	20.3	128	---	32,500	28.0	3.7	22.1
276	C	171	173	32,900	28.0	2.9	23.0	171	173	32,500	28.1	3.1	23.7
277	C	229	---	32,900	28.1	2.5	28.0	230	---	32,500	28.2	2.5	20.7
278	D	126	---	39,900	27.9	4.1	18.7	125	---	39,700	27.9	4.1	15.8
279	D	147	---	39,900	28.0	3.8	22.8	148	---	39,700	28.0	3.8	22.2
280	D	231	---	39,900	28.1	2.7	20.9	231	---	39,700	28.2	2.8	19.8
281	E	143	148	45,400	28.0	4.5	18.9	143	148	45,000	28.0	4.3	18.9
282	E	177	184	45,400	28.1	3.7	20.2	177	183	45,000	28.1	3.8	19.3
283	E	228	231	45,400	28.2	3.3	22.5	228	234	45,000	28.2	3.3	19.0
284	F	57	59	17,300	27.7	3.6	20.8	58	60	17,400	27.7	3.6	20.6
285	F	162	164	17,300	27.9	1.9	24.5	161	162	17,400	27.9	1.9	26.7
286	H	29	29	9,700	27.2	3.5	25.6	28	29	9,600	27.3	3.3	23.6
287	H	38	39	9,700	27.2	2.8	29.7	36	37	9,600	27.3	2.8	23.7

TABLE IV.- UNYAWED-ROLLING RELAXATION-LENGTH DATA

Run	Test series	Average values				
		$\bar{p}$, lb/sq in.	$\bar{F}_z$, lb	$\bar{\delta}_0$, in.	$\bar{L}_f$, in.	$\bar{L}_\lambda$, in.
288	A	58	17,000	3.5	31.6	23.8
289	A	60	17,000	3.7	27.0	----
290	A	60	17,000	3.7	23.3	24.8
291	A	62	17,000	3.7	24.4	20.3
292	A	62	17,000	3.7	23.3	----
293	A	104	17,000	2.4	----	----
294	A	150	17,000	2.0	----	----
295	A	150	17,000	2.1	----	----
296	B	79	23,700	3.8	----	----
297	B	126	23,700	2.7	16.4	21.3
298	B	203	23,700	2.3	20.4	----
299	C	130	32,700	3.7	25.2	----
300	C	131	32,700	3.7	22.9	----
301	C	173	32,700	3.1	23.4	----
302	C	172	32,700	3.1	21.9	----
303	C	231	32,700	2.6	25.3	----
304	C	229	32,700	2.6	21.0	----
305	D	126	39,800	4.2	14.0	----
306	D	126	39,800	4.2	19.5	----
307	D	150	39,800	3.6	19.7	----
308	D	150	39,800	3.7	19.5	----
309	D	232	39,800	2.8	22.6	----
310	D	232	39,800	2.8	28.3	----
311	D	232	39,800	2.8	24.8	----
312	E	150	45,200	4.2	18.8	----
313	E	150	45,200	4.2	18.8	----
314	E	180	45,200	3.7	18.3	----
315	E	180	45,200	3.8	17.1	----
316	E	232	45,200	3.1	23.2	----
317	E	232	45,200	3.1	18.5	----

TABLE V.- LOCKED-WHEEL DRAG TEST DATA

$$\left[\bar{F}_z = 9,730 \text{ lb for } \bar{F}_x = 0\right]$$

Run	Average values				$(F_z)_{\text{tire A}} + (F_z)_{\text{tire B}},$ lb	$(F_x)_{\text{tire A}} + (F_x)_{\text{tire B}},$ lb	Tire A		Tire B		Remarks
	$\bar{p},$ lb/sq in.	$\delta_0,$ in.	$\bar{\mu}_x$	$\bar{E}_x,$ lb/in.			$p,$ lb/sq in.	$\delta_0,$ in.	$p,$ lb/sq in.	$\delta_0,$ in.	
318	19	4.6	0.81	7,800	18,450	14,870	19	4.6	19	4.6	
319	19	4.9	.84	7,160	18,410	15,460	19	4.7	19	5.0	
320	29	3.9	.88	8,640	18,360	16,190	29	3.8	29	4.0	
321	29	3.6	.82	7,700	18,430	15,070	29	3.5	29	3.7	
322	30	3.4	.88	6,750	18,360	16,200	30	3.4	30	3.5	
323	29	3.7	.88	7,700	18,360	16,220	29	3.6	29	3.8	Wet concrete
324	29	3.6	.74	6,900	18,530	13,700	29	3.6	29	3.6	Wet concrete
325	29	3.7	.73	8,100	18,540	13,500	29	3.6	28	3.8	
326	39	2.8	.81	8,300	18,440	14,950	39	2.8	39	2.7	
327	39	3.4	.90	8,130	18,340	16,510	39	3.3	39	3.4	
328	59	2.2	.79	8,900	18,470	14,590	59	2.2	59	2.2	
329	59	2.6	.86	9,590	18,390	15,730	59	2.6	59	2.6	
330	84	1.7	.80	8,310	18,460	14,700	84	1.7	84	1.6	
331	84	2.1	.85	8,450	18,400	15,560	84	2.1	84	2.0	
332	85	1.6	.74	7,600	18,530	13,680	85	1.6	85	1.6	Wet concrete
333	84	1.6	.73	7,770	18,540	13,570	84	1.6	84	1.7	Wet concrete
334	84	1.6	.84	6,510	18,410	15,420	84	1.6	84	1.7	
335	84	1.7	.89	8,340	18,350	16,250	84	1.7	84	1.7	
336	126	1.3	.74	9,400	18,530	13,720	126	1.3	126	1.3	
337	126	1.3	.69	10,250	18,580	12,900	126	1.3	126	1.3	
338	126	1.4	.79	8,250	18,470	14,600	125	1.4	126	1.4	
339	125	1.6	.80	8,300	18,460	14,700	126	1.7	126	1.6	
340	150	1.2	.71	9,780	18,570	13,160	150	1.2	150	1.1	
341	150	1.4	.75	9,100	18,520	13,840	150	1.4	150	1.4	
342	168	1.1	.72	9,370	18,550	13,590	168	1.1	168	1.1	
343	168	1.3	.73	7,790	18,540	13,490	168	1.3	168	1.3	
344	180	1.0	.81	8,030	18,450	14,880	180	1.0	180	1.0	
345	180	1.3	.71	7,770	18,560	13,260	180	1.3	180	1.3	
346	180	1.1	.76	7,320	18,500	14,140	180	1.1	180	1.1	
347	180	1.1	.64	7,260	18,650	11,950	180	1.1	180	1.0	Wet concrete
348	180	1.1	.69	6,990	18,590	12,800	180	1.1	180	1.0	Wet concrete
349	202	1.0	.76	------	18,500	14,070	201	1.1	202	1.1	
350	202	1.2	.71	7,450	18,570	13,160	202	1.2	201	1.1	

TABLE VI.- TIRE FOOTPRINT DATA

Run	Test series	p_o, lb/sq in.	p, lb/sq in.	F_z, lb	δ_o, in.	A_g, in.^{2}	A_n, in.^{2}	b, in.	$2h$, in.
Tire A									
351	C	152	152	------	0.7	47	33	5.4	10.5
352	C	152	153	------	1.7	106	85	8.9	16.3
353	C	152	156	32,900	3.4	240	173	12.9	22.3
354	After I	199	200	8,620	1.0	59	47	6.7	11.3
355	After I	179	180	8,620	1.1	64	50	6.9	11.8
356	After I	168	170	8,620	1.2	66	51	7.0	11.7
357	After I	150	151	8,620	1.3	74	61	7.8	12.4
358	After I	59	59	8,620	2.0	127	94	9.6	15.3
359	After I	18	19	8,620	3.7	274	190	13.2	23.4
Tire B									
360	C	180	180	------	1.1	81	53	7.2	13.0
361	C	180	180	------	1.8	130	84	9.2	16.5
362	C	180	182	32,500	2.8	207	135	11.9	20.4
363	C	135	135	------	1.0	50	29	5.6	10.1
364	C	135	136	------	1.9	116	73	8.7	15.5
365	C	135	137	------	2.8	186	120	11.6	19.1
366	C	135	138	32,500	3.8	248	166	12.8	22.2
367	After I	200	200	8,560	1.0	60	43	6.7	11.3
368	After I	200	200	8,560	1.0	58	42	6.6	11.4
369	After I	180	181	8,560	1.2	61	44	6.8	11.5
370	After I	166	167	8,560	1.1	65	48	6.9	12.0
371	After I	150	151	8,560	1.3	69	49	7.0	11.9
372	After I	150	151	8,560	1.3	69	48	6.9	12.1
373	After I	126	127	8,560	1.3	77	55	7.2	12.7
374	After I	83	84	8,560	1.6	104	70	8.9	14.4
375	After I	83	85	8,560	1.7	108	68	9.0	14.4
376	After I	83	85	8,560	1.7	111	75	9.1	14.9
377	After I	57	58	8,560	1.9	139	94	10.0	16.5
378	After I	37	39	8,560	2.6	190	119	11.6	18.7
379	After I	28	29	8,560	3.1	221	137	11.8	20.6
380	After I	17	19	8,560	4.0	304	193	13.7	24.3
381	After I	---	19	8,560	----	319	221	13.9	24.7
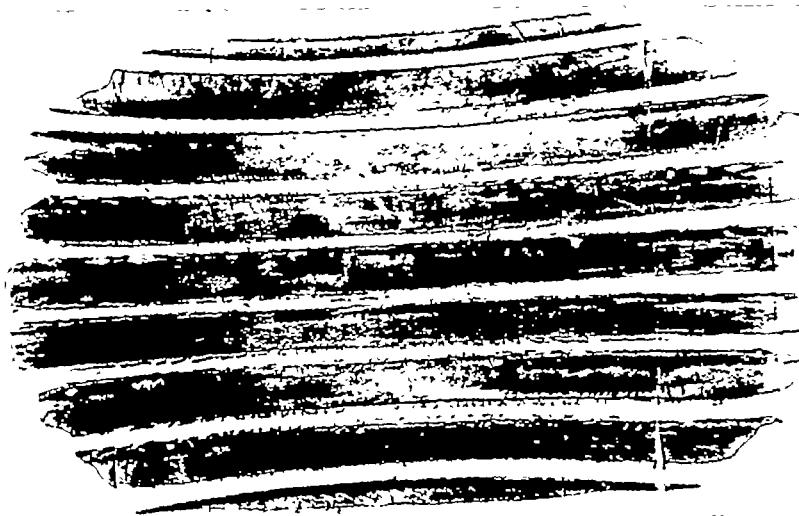
(a) Run 359; $\delta_O = 3.7$ inches; $p = 19$ pounds per square inch.

(b) Run 358; $\delta_O = 2.0$ inches; $p = 59$ pounds per square inch.
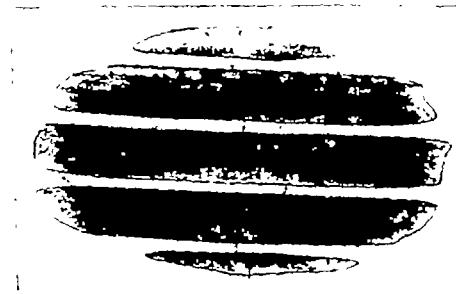
L-84904

(c) Run 356; $\delta_O = 1.2$ inches; $p = 170$ pounds per square inch.

Figure 1.- Typical tire footprints for tire A at $F_z = 8,620$ pounds.
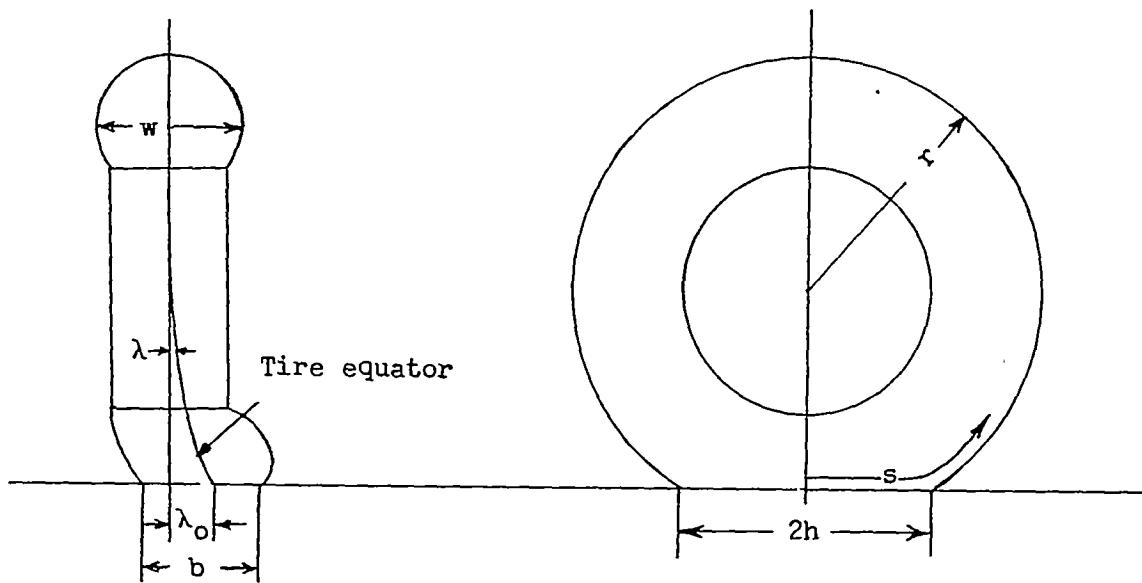
(a) Tire dimensions.
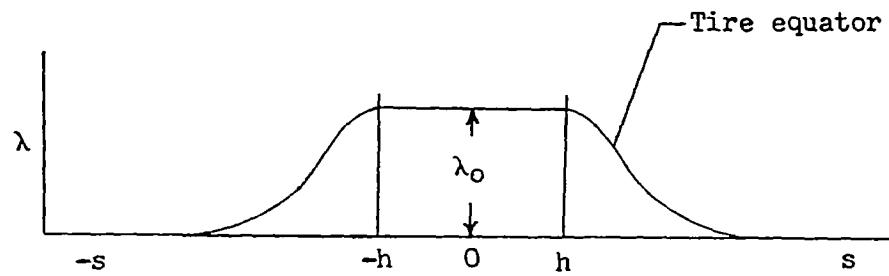
(b) Shape of distortion curve.

Figure 2.- Tire dimensions and tire distortion.

Concrete weight cans
Weight per can = 8,400 lb
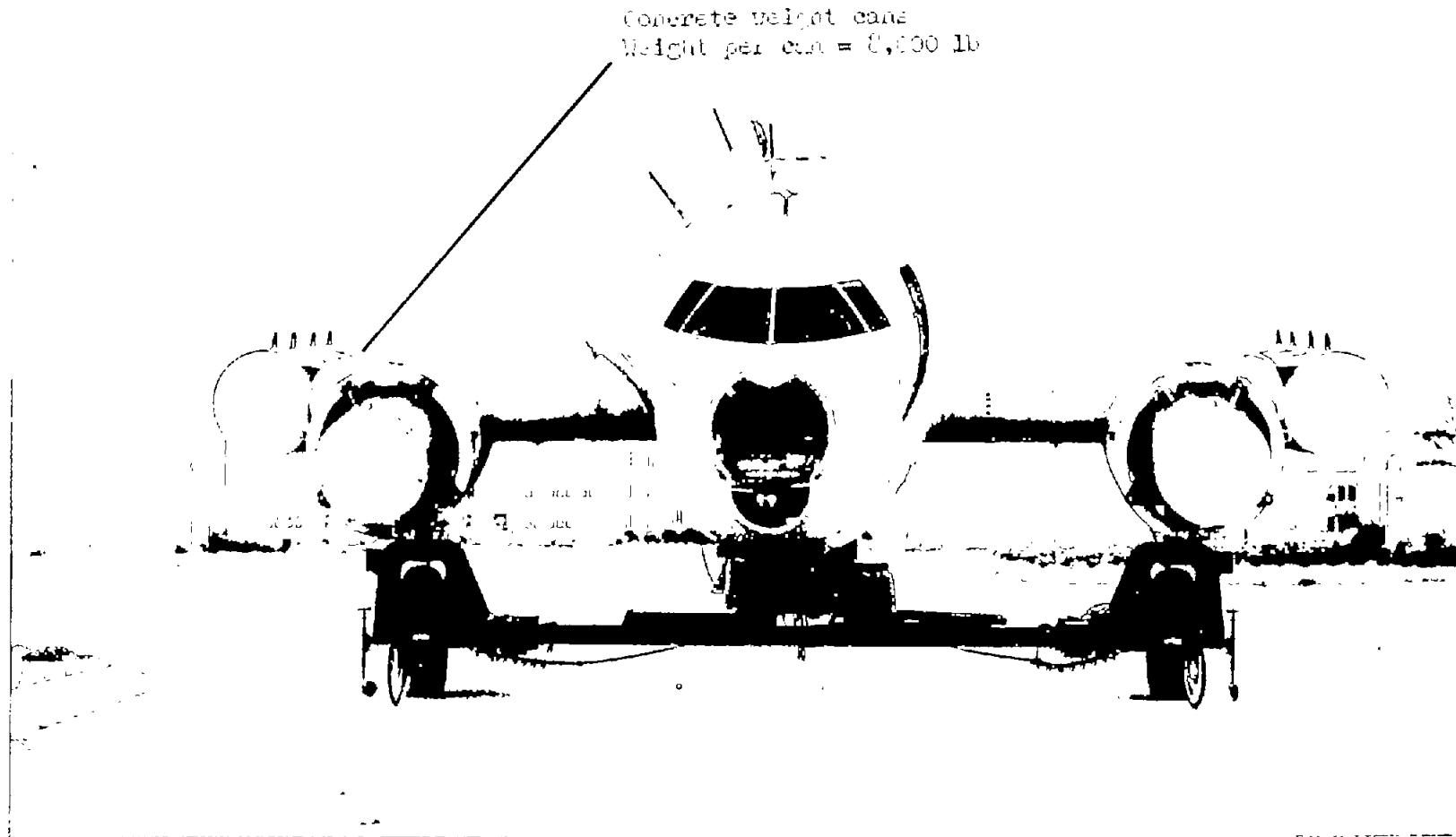
L-79570.1

(a) End view.

Figure 3.- Test vehicle.

L-79571

(b) Side view.

Figure 3.- Concluded.

Slide wire

Wheel and strut assembly

Circular slide wire

Starting point
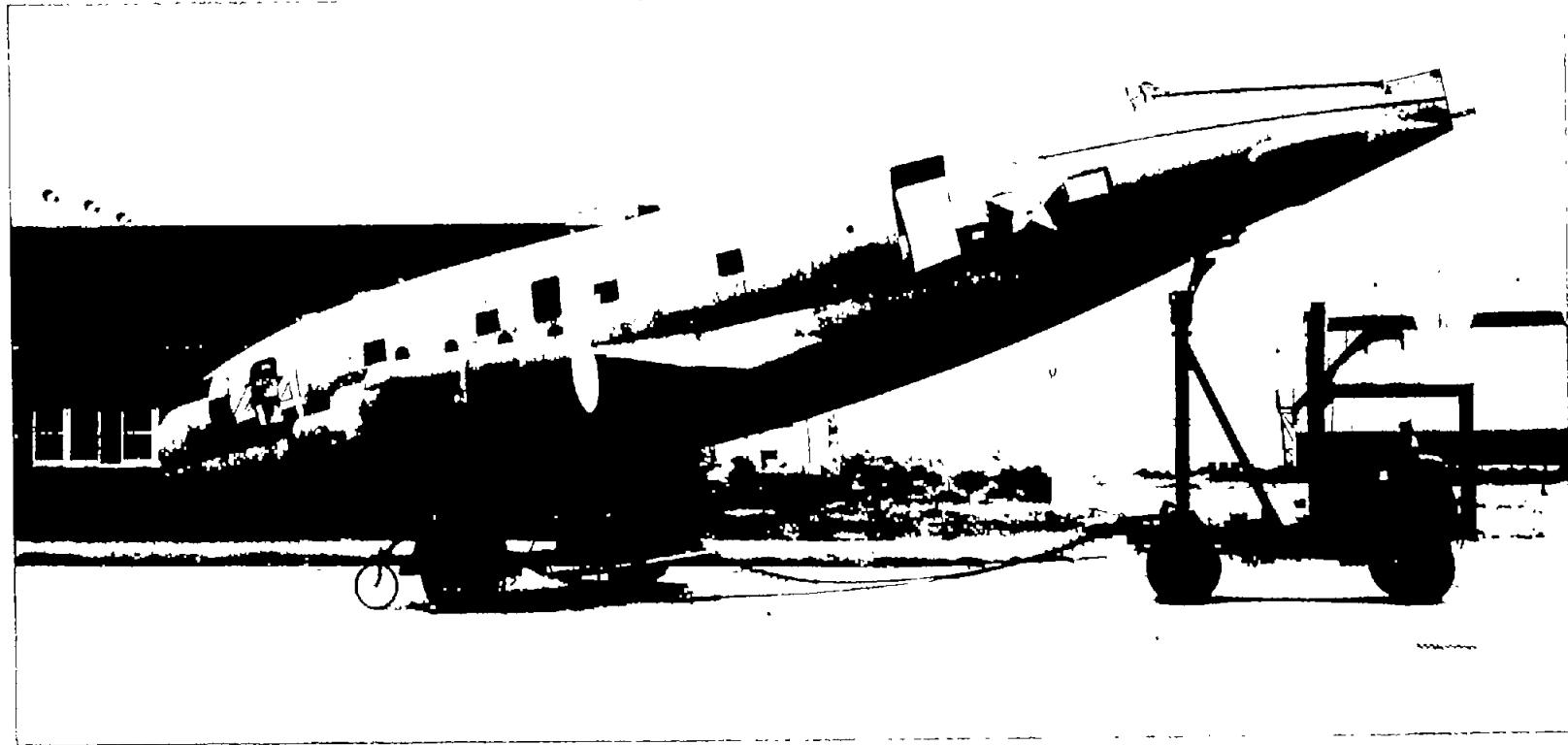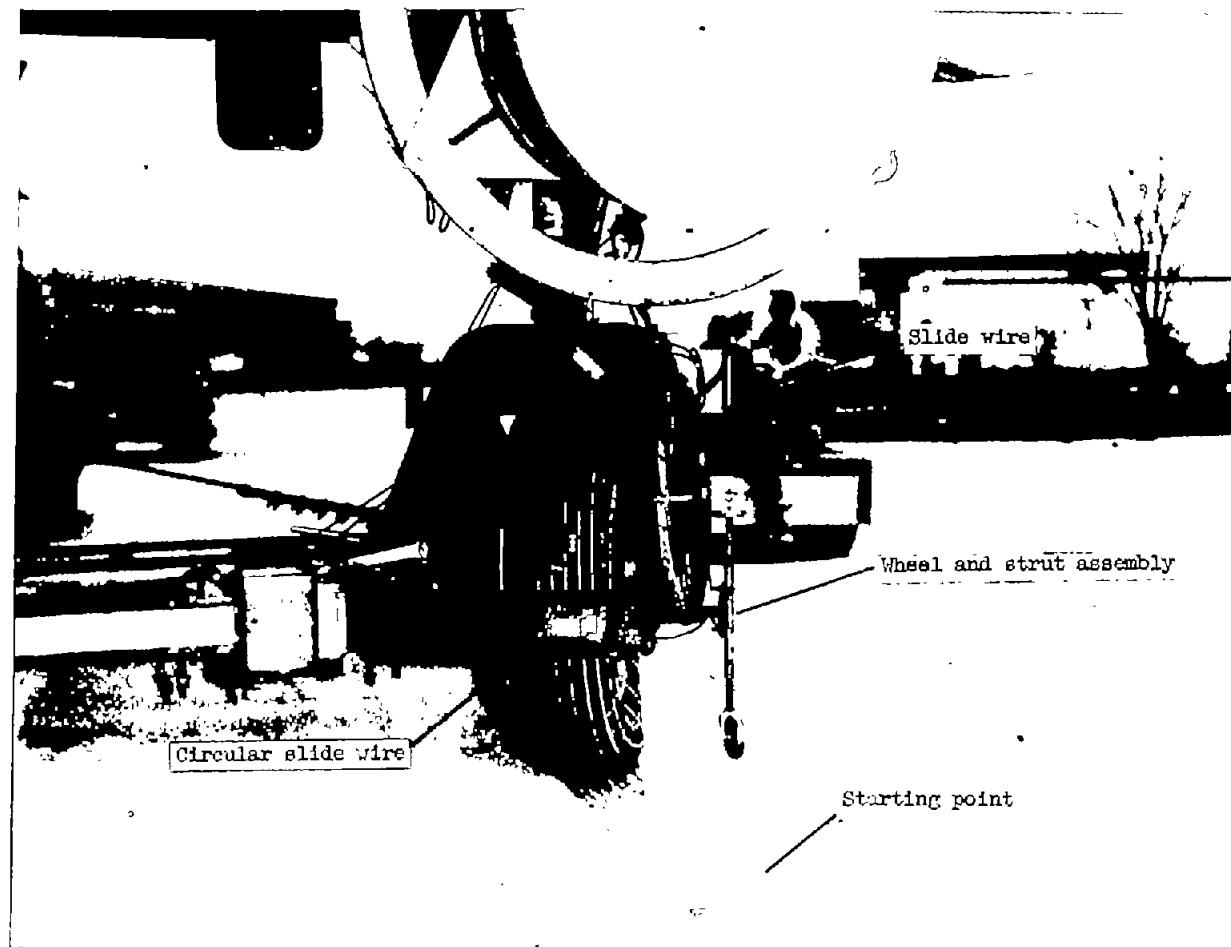
L-79491.1

(a) Rear view.

Figure 4.- Tire A under yawed rolling at $\psi = 17.9^\circ$.

Bicycle wheel

Starting point
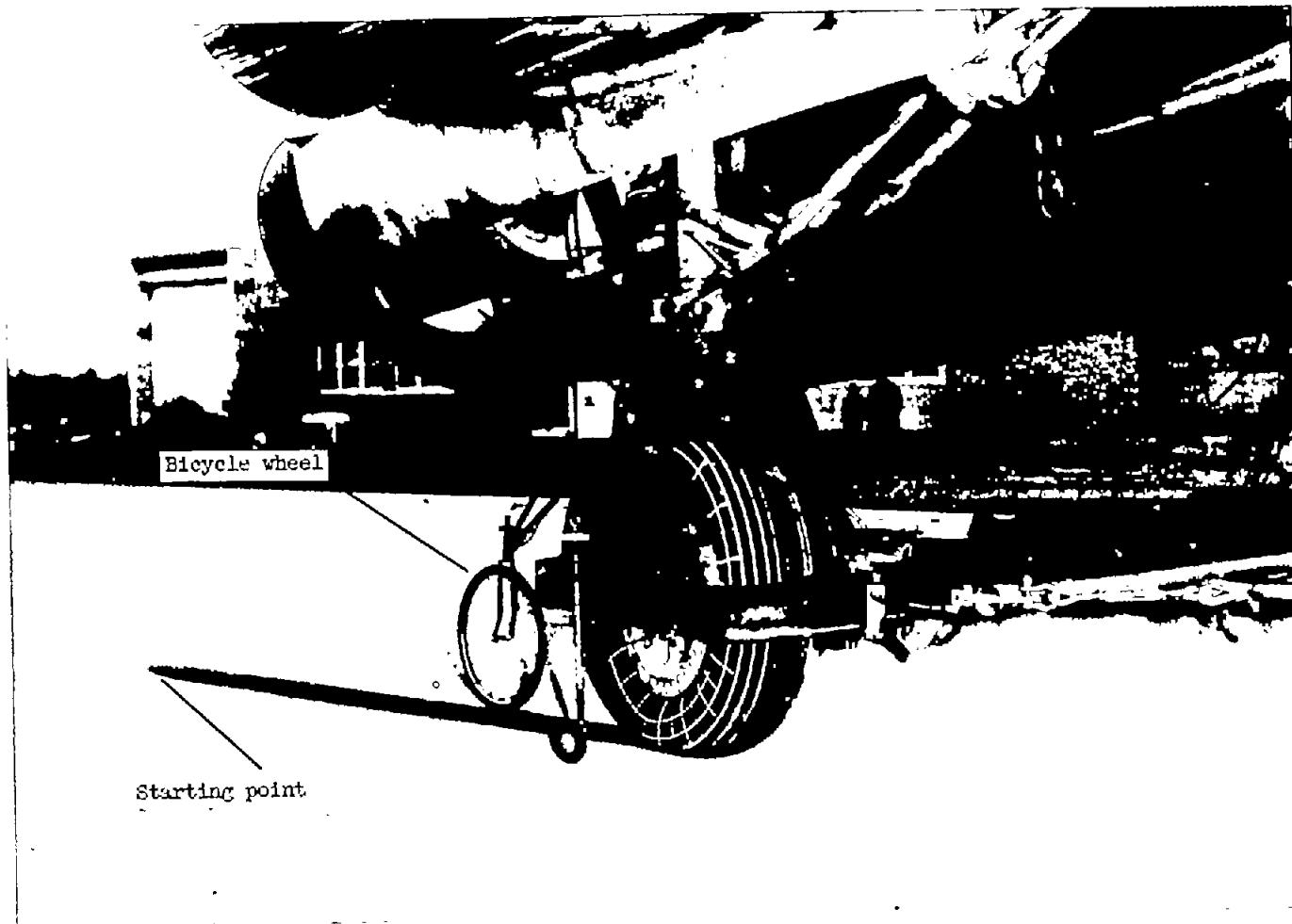
(b) Side view.

L-79492.1

Figure 4.- Continued.

Starting point
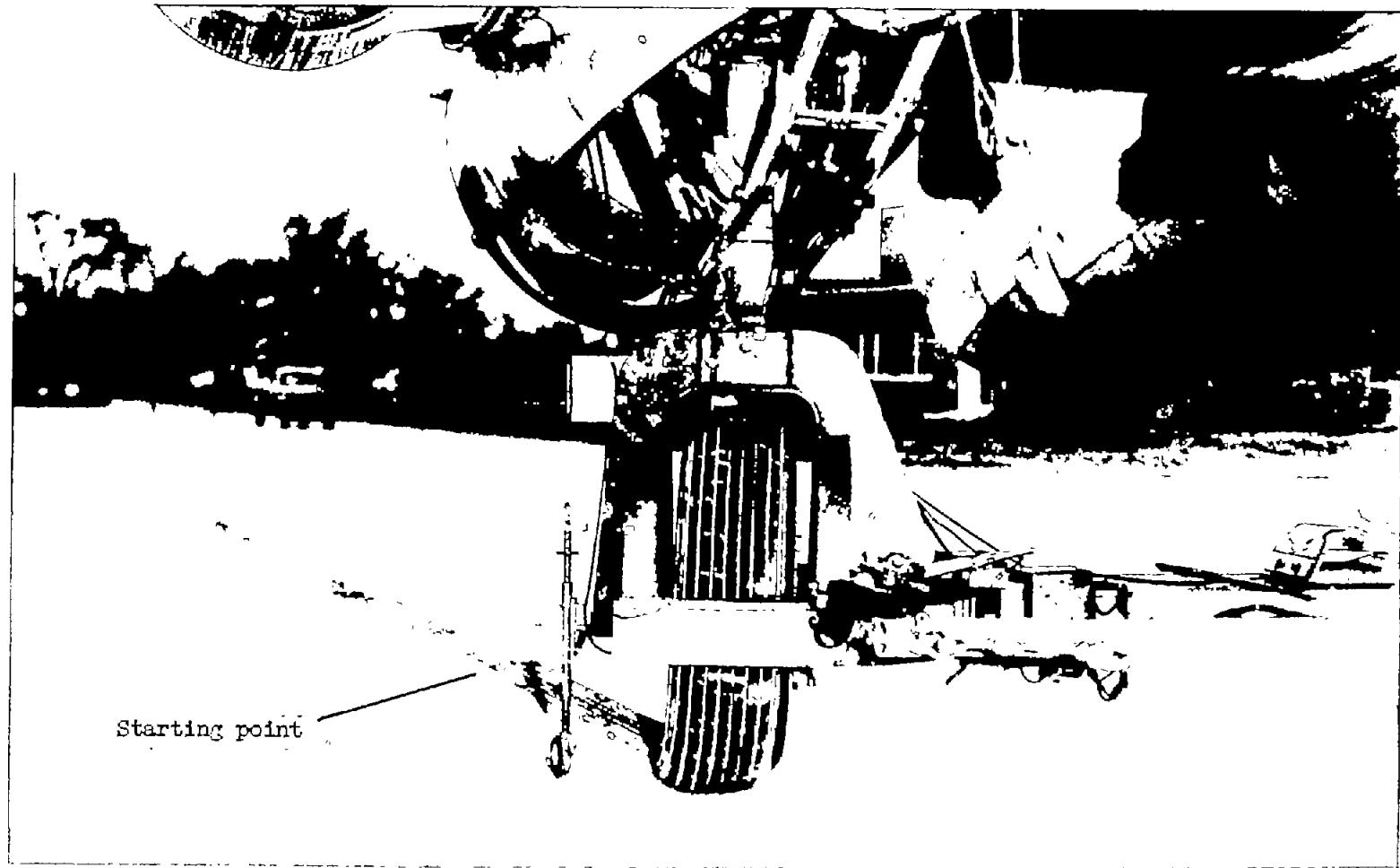
(c) Front view.

L-79493.1

Figure 4.- Concluded.
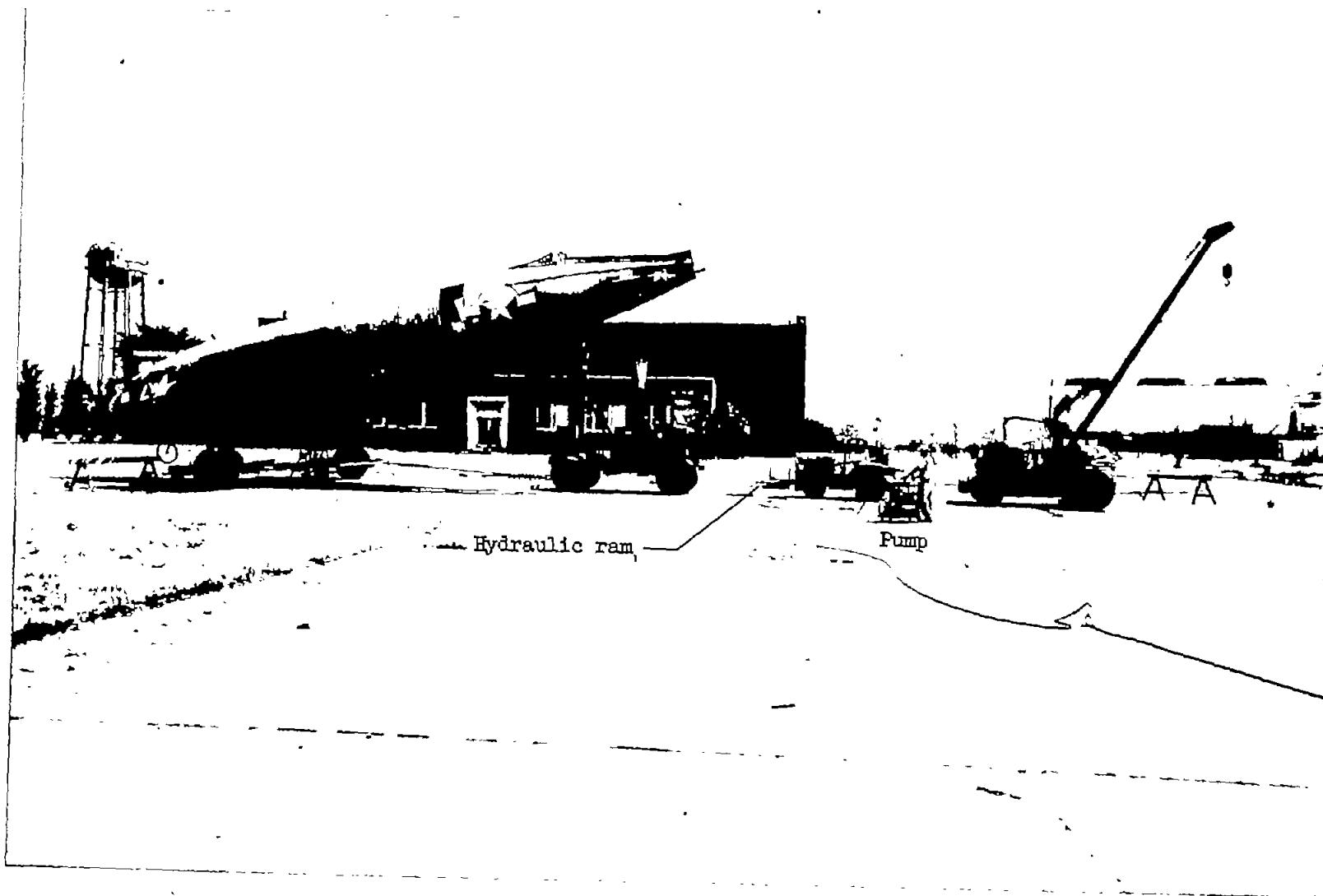
Figure 5.- Locked-wheel drag-test setup.

L-80727.1

(a) Initial-force-buildup stage of run.

(b) Steady-state stage of run.
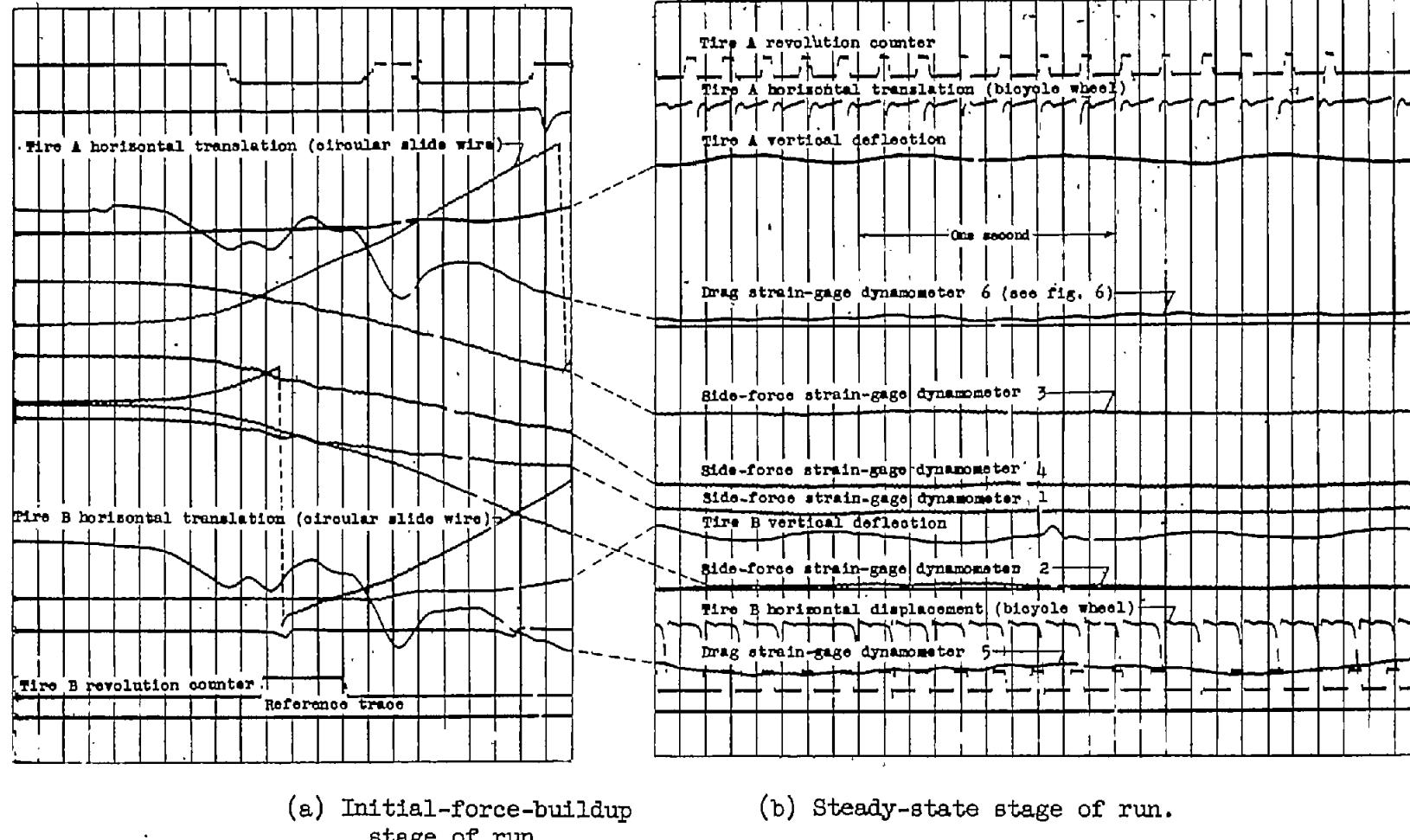
Figure 6.- Typical oscillograph record. Run 47; p = 81 pounds per square inch; δ_0 = 3.9 inches; ψ = 17.9°.
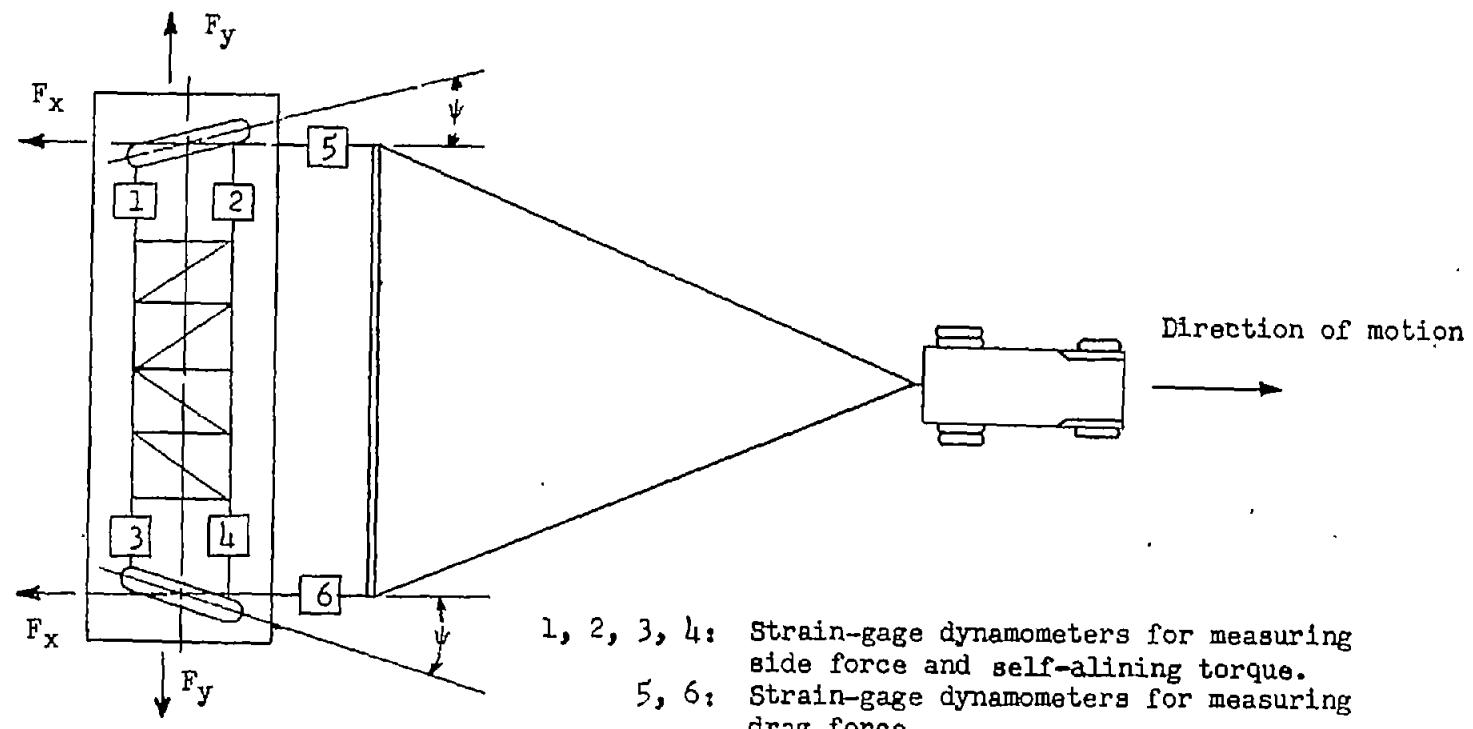
Figure 7.- Strain-gage dynamometer location.

1, 2, 3, 4: Strain-gage dynamometers for measuring
side force and self-alining torque.
5, 6: Strain-gage dynamometers for measuring
drag force.
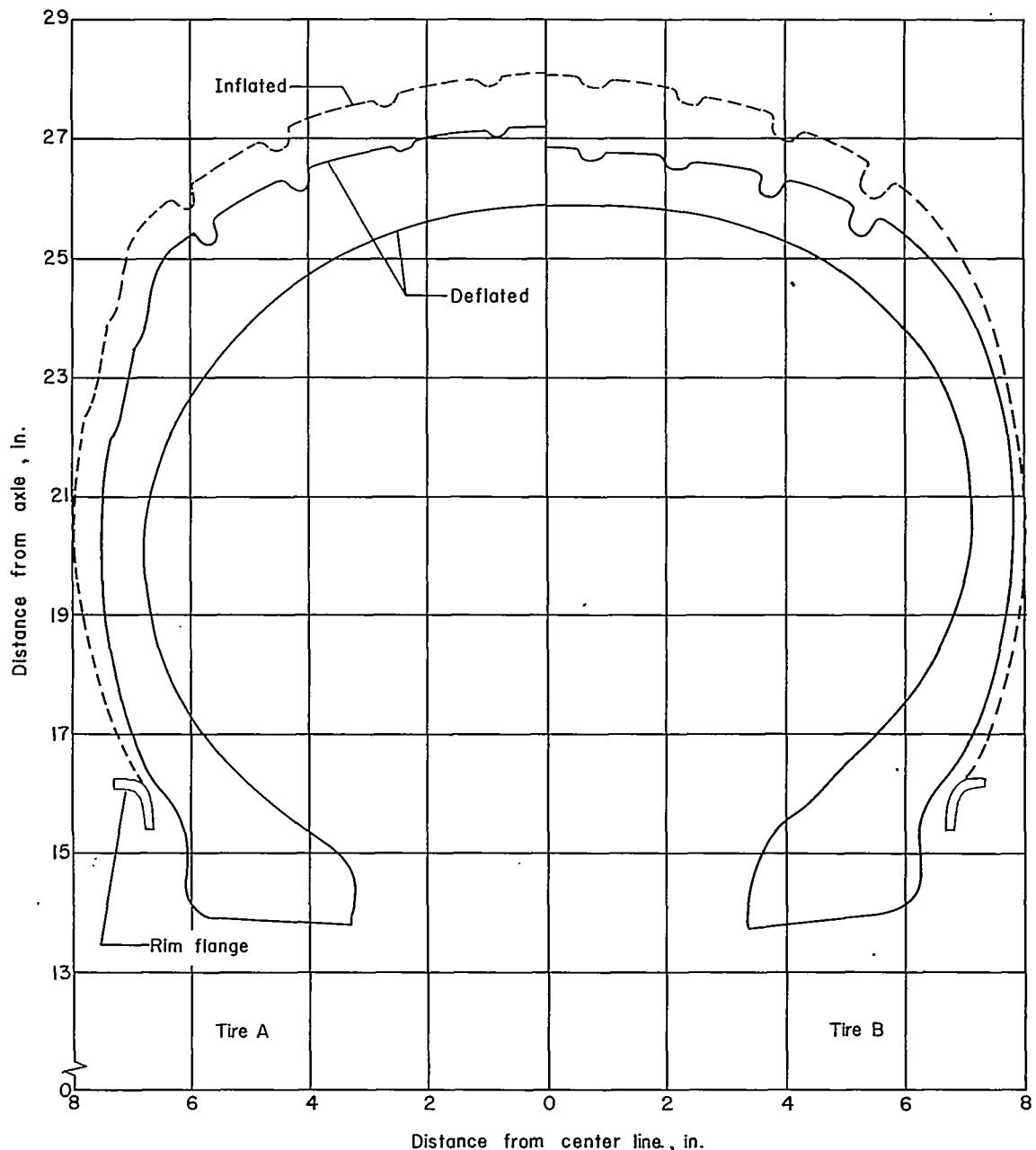
Figure 8.- Tire profiles.
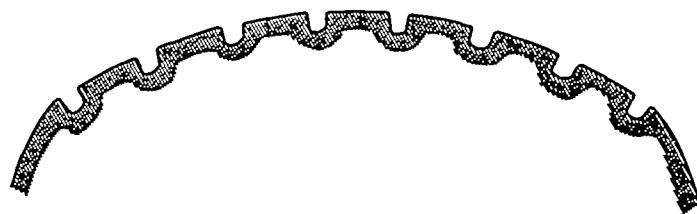
(a) Approximate tread shape of tires A and B
at beginning of test.
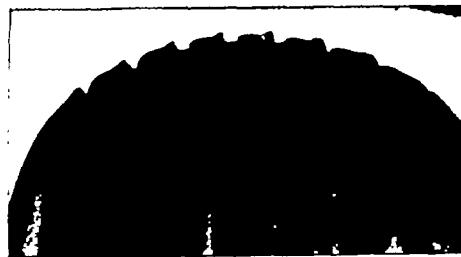
(b) At conclusion of test series C.

(c) At conclusion of test series F.
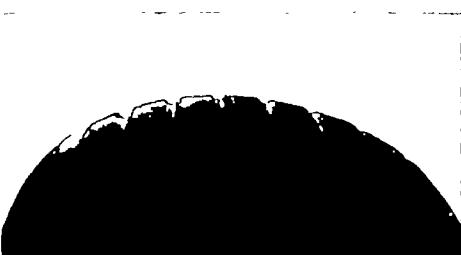
(d) At conclusion of test series I.

Tire A   Tire B

L-84905

Figure 9.- Tire wear.
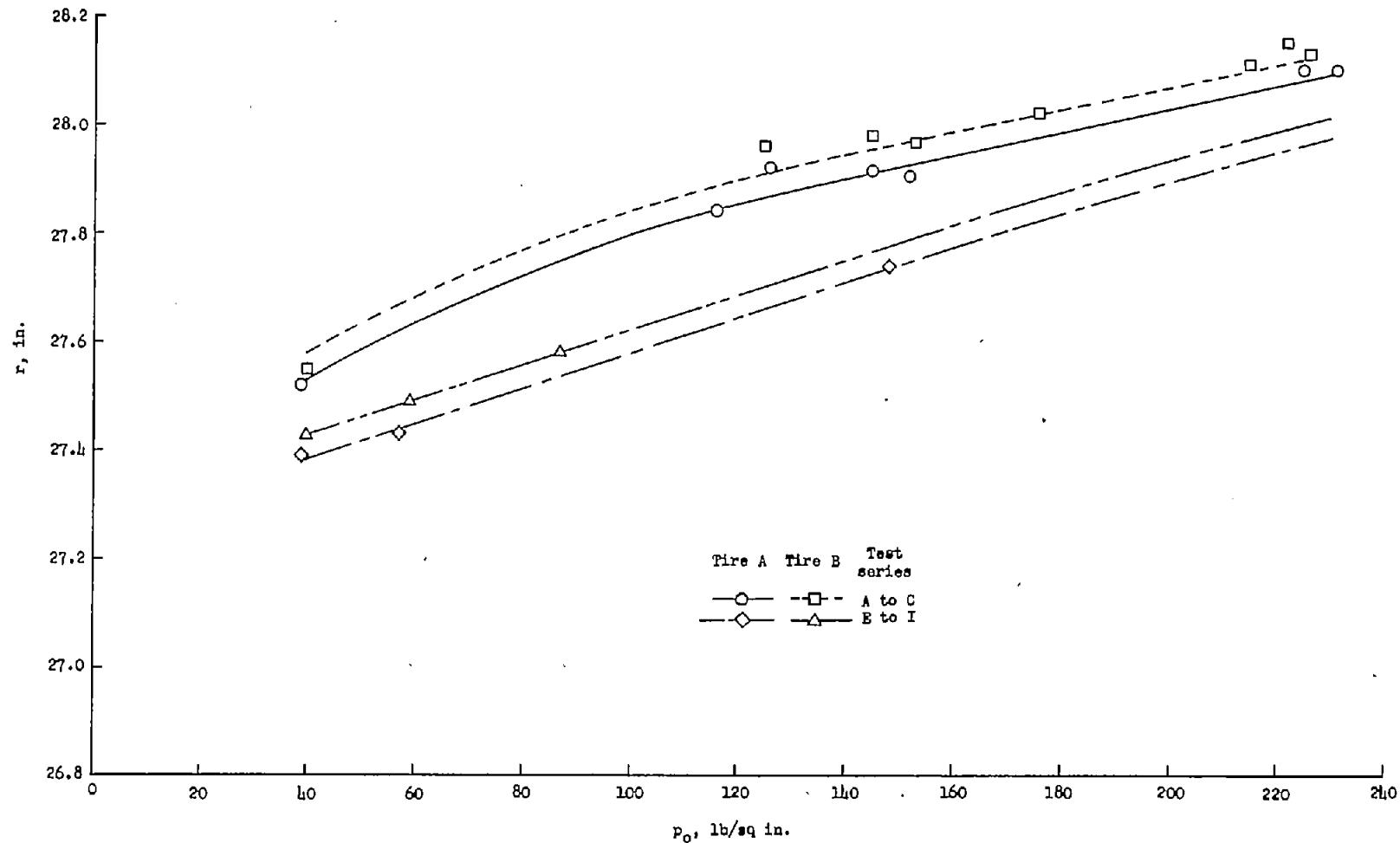
Figure 10.- Variation of unloaded tire radius with inflation pressure
and tire wear. Data shown are at equilibrium and were measured
after 24 hours at constant pressure.
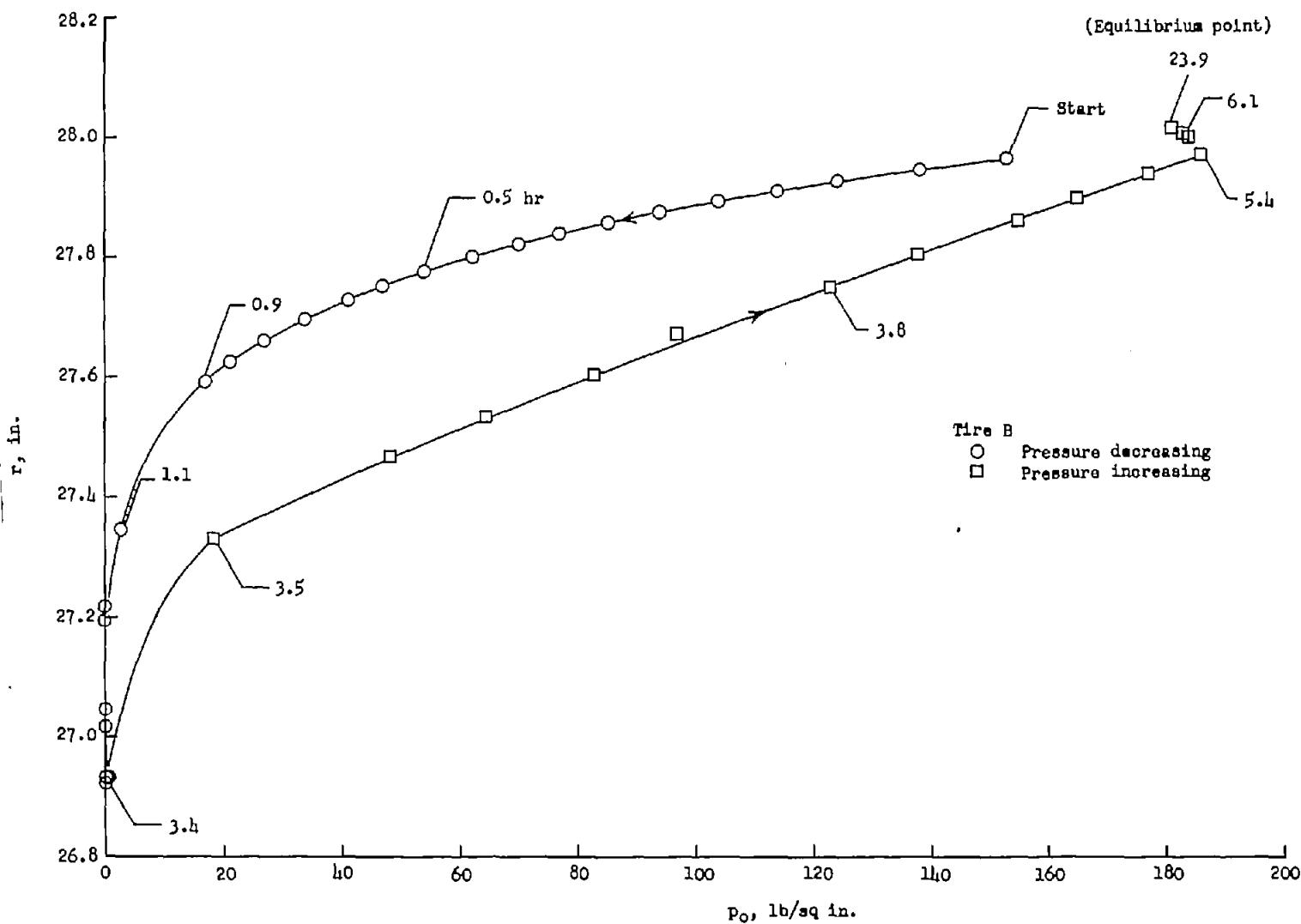
Figure 11.- Radius-pressure hysteresis loop for tire B (unloaded).
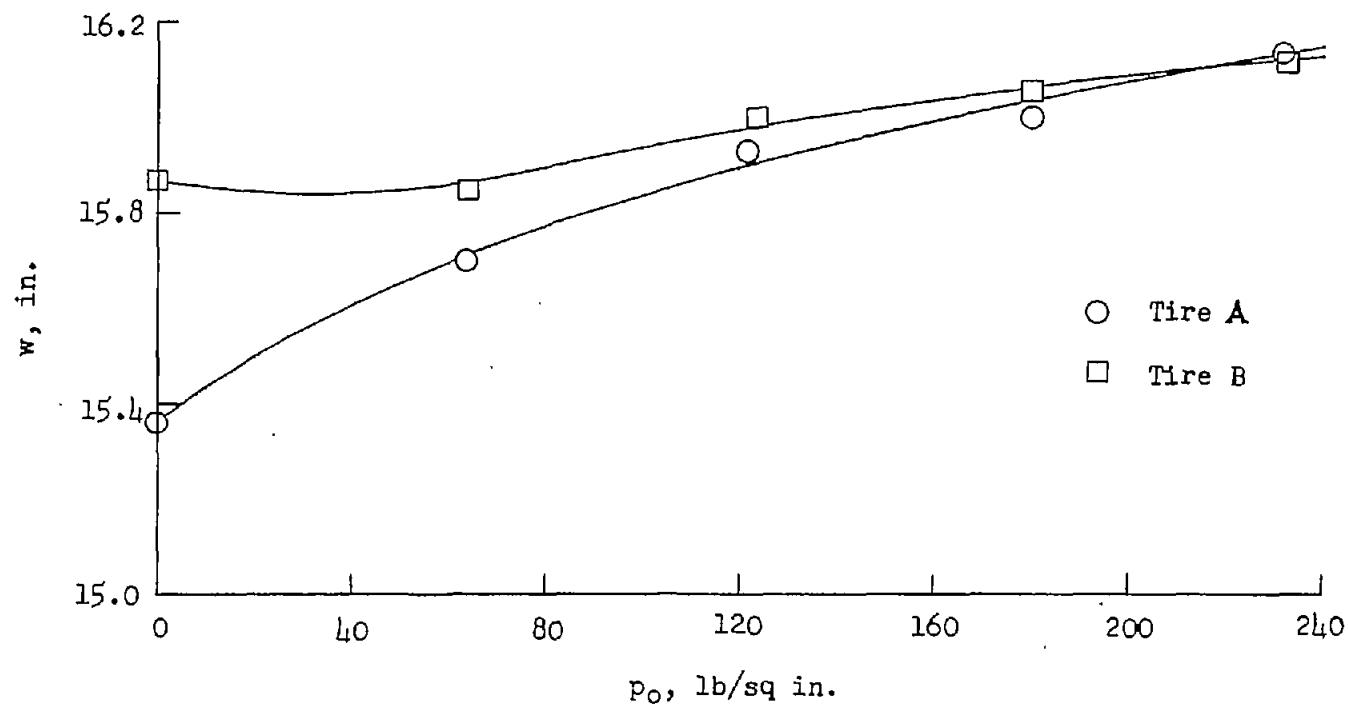
Figure 12.- Variation of maximum tire width with inflation pressure.
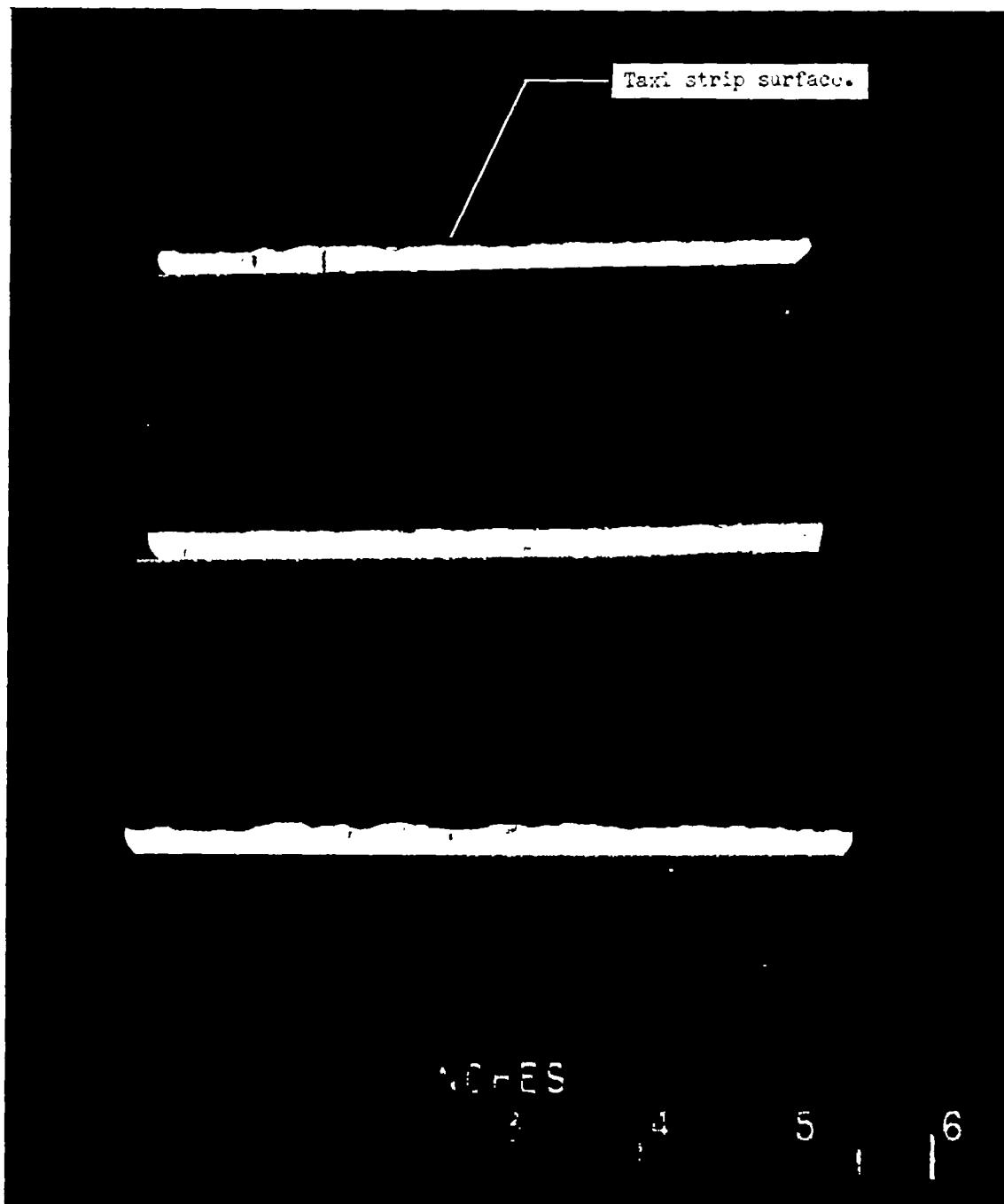
L-84422.1

Figure 13.- Representative samples of concrete-taxi-strip surface roughness.
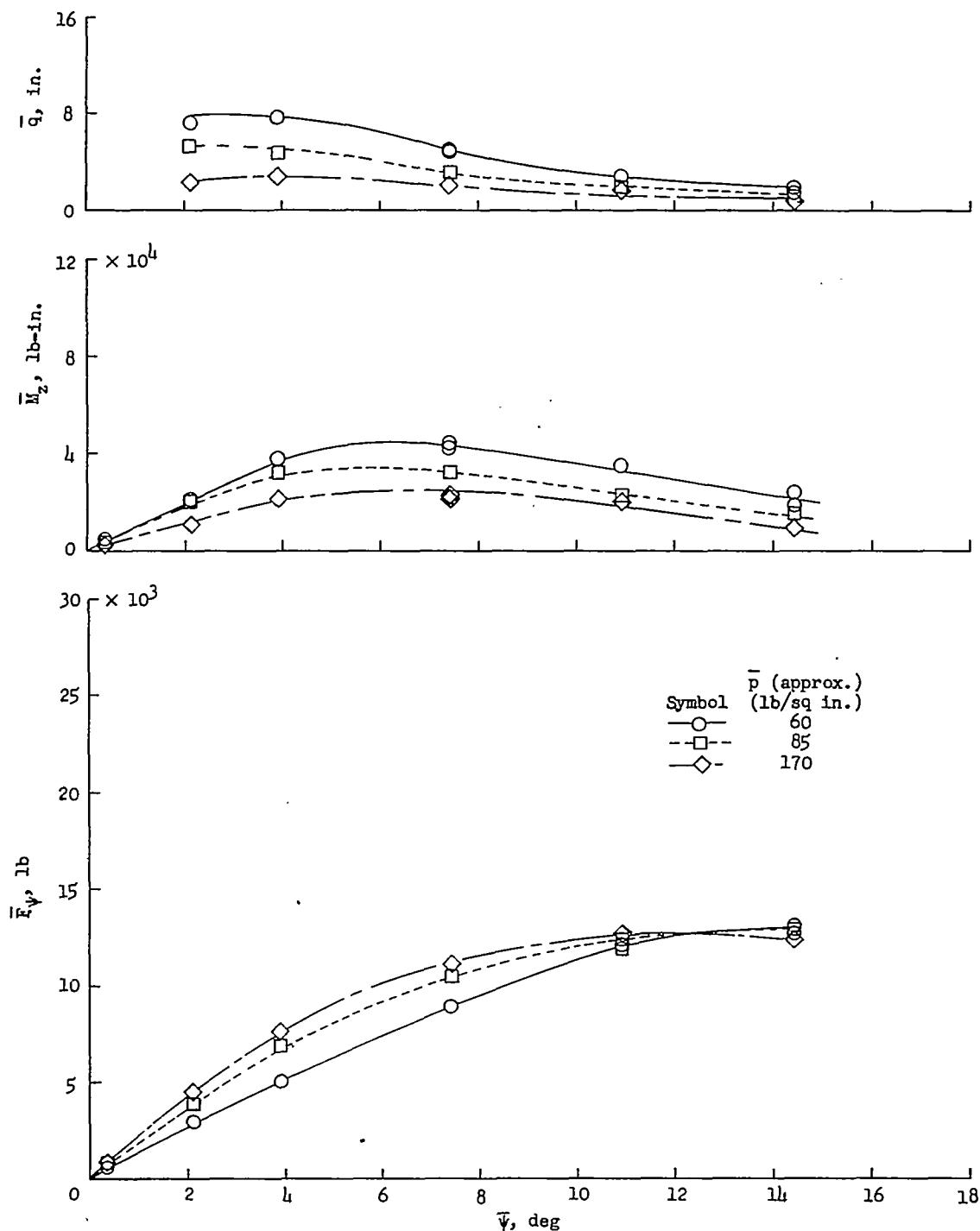
(a) Test series A; $\bar{F}_z$ = 17,000 pounds.

Figure 14.- Variation of normal force, self-alining torque, and pneumatic caster with yaw angle for the different vertical loads and inflation pressures investigated.
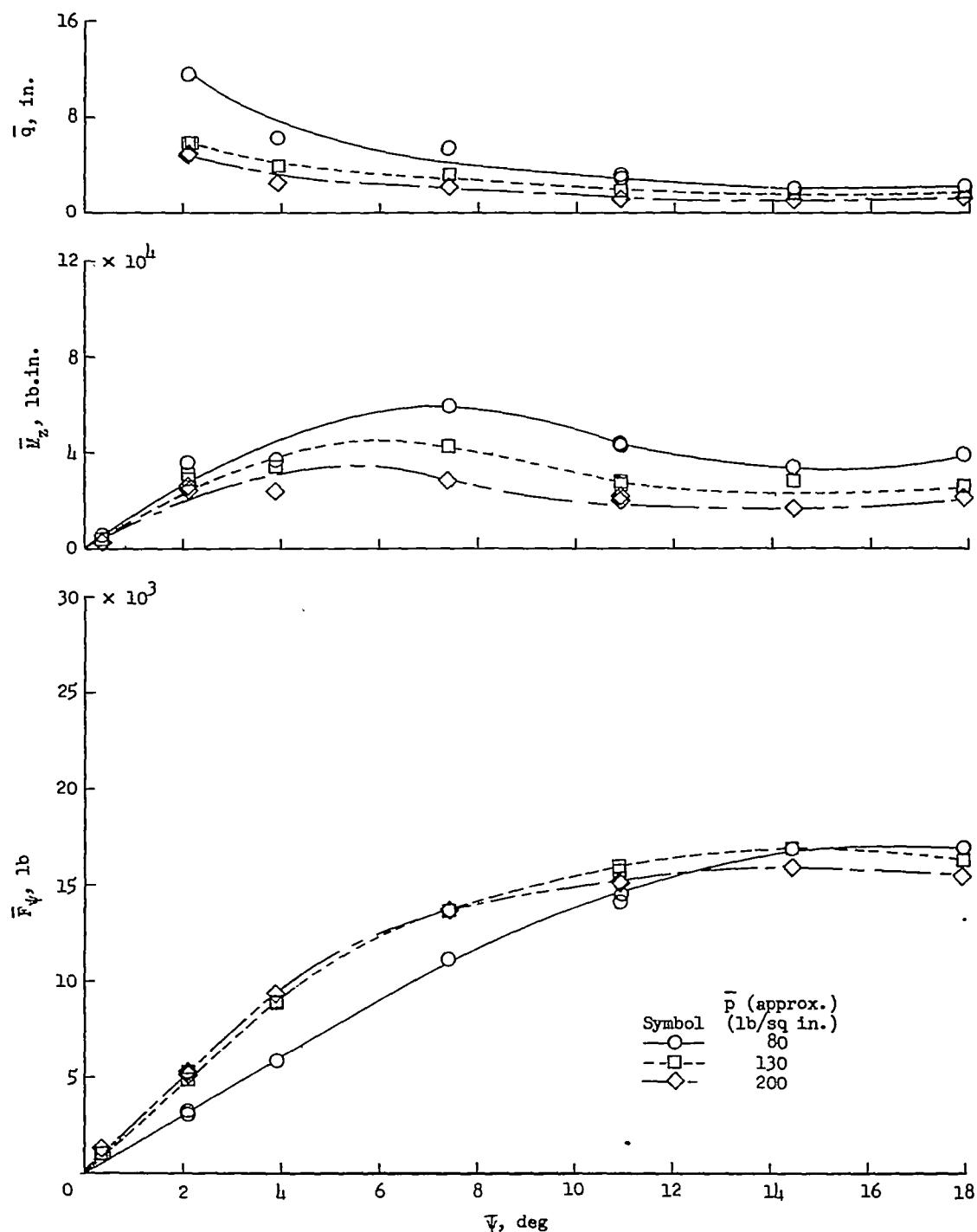
(b) Test series B; $\bar{F}_z$ = 23,700 pounds.

Figure 14.- Continued.
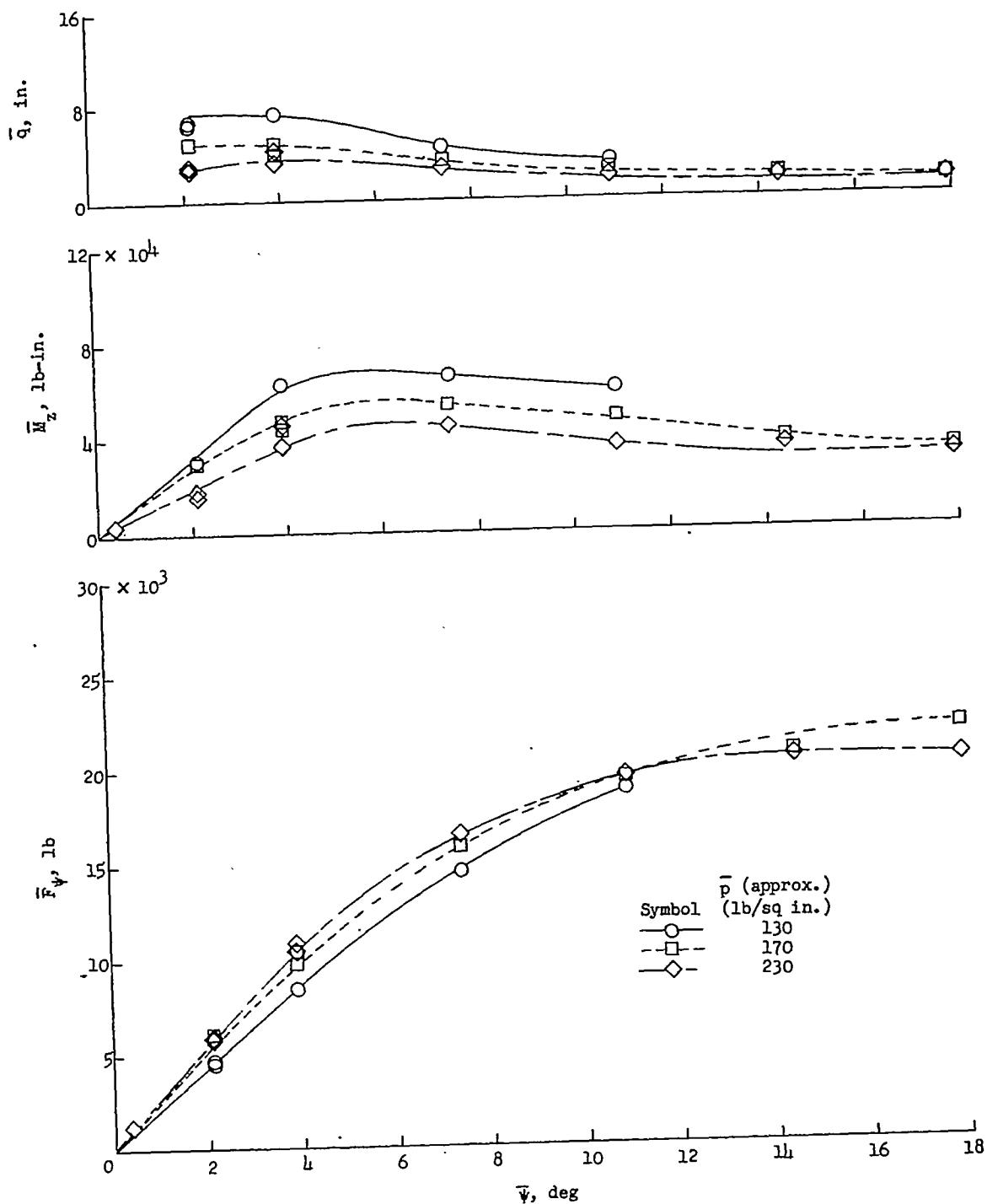
(c) Test series C; $\bar{F}_z$ = 32,700 pounds.

Figure 14.- Continued.
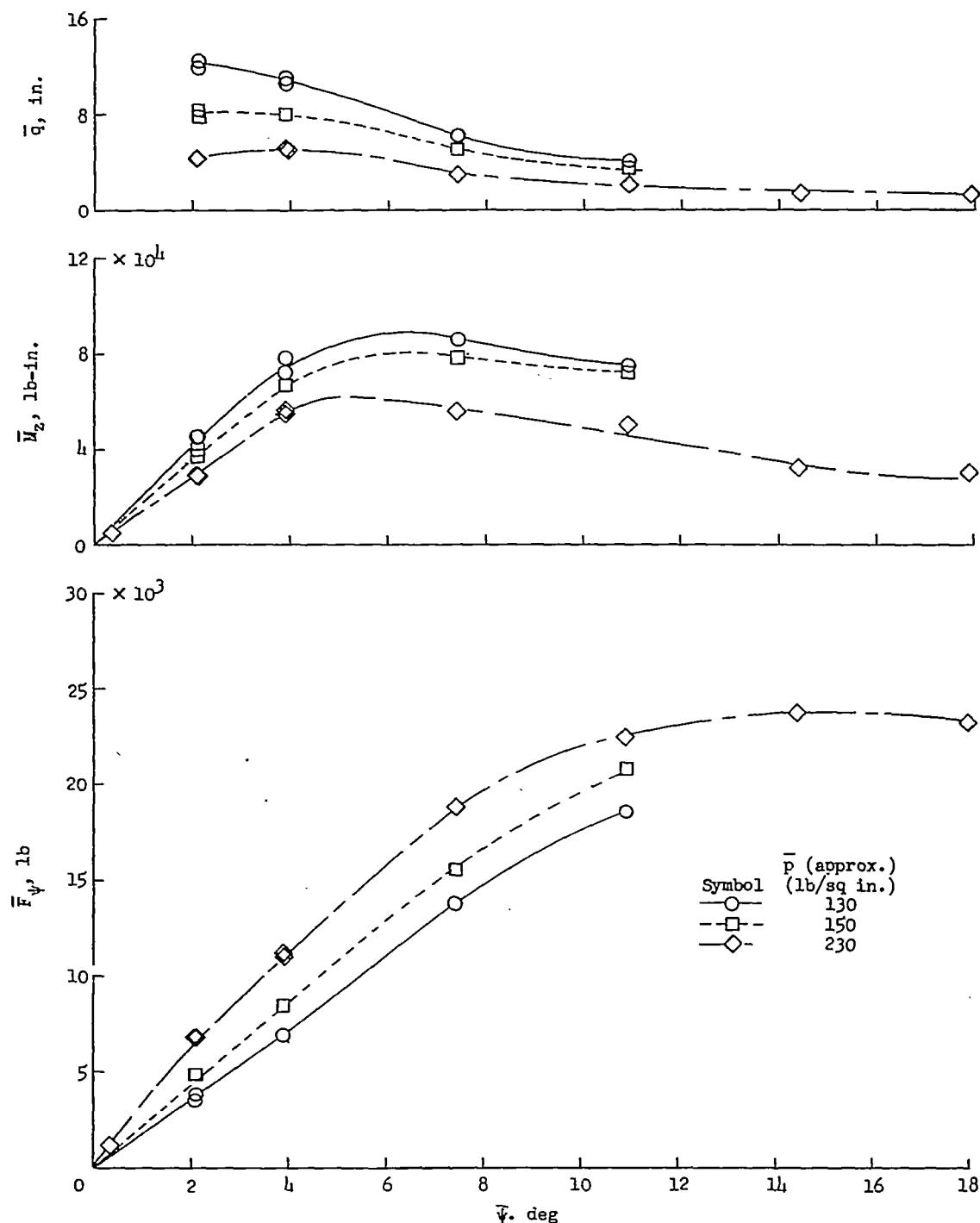
(d) Test series D; $\bar{F}_z = 39,800$ pounds.

Figure 14.- Continued.
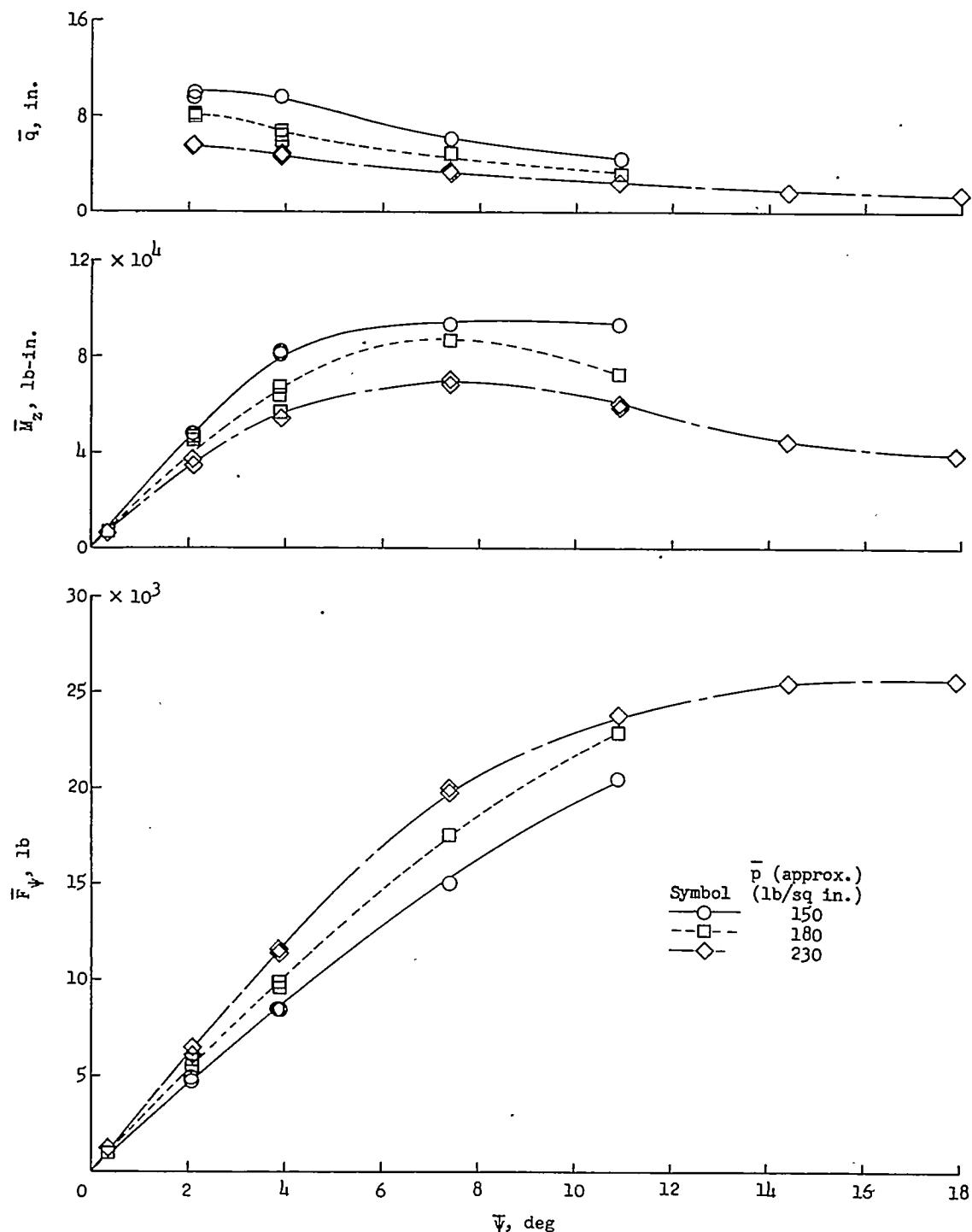
(e) Test series E; $\bar{F}_Z = 45,200$ pounds.

Figure 14.- Continued.
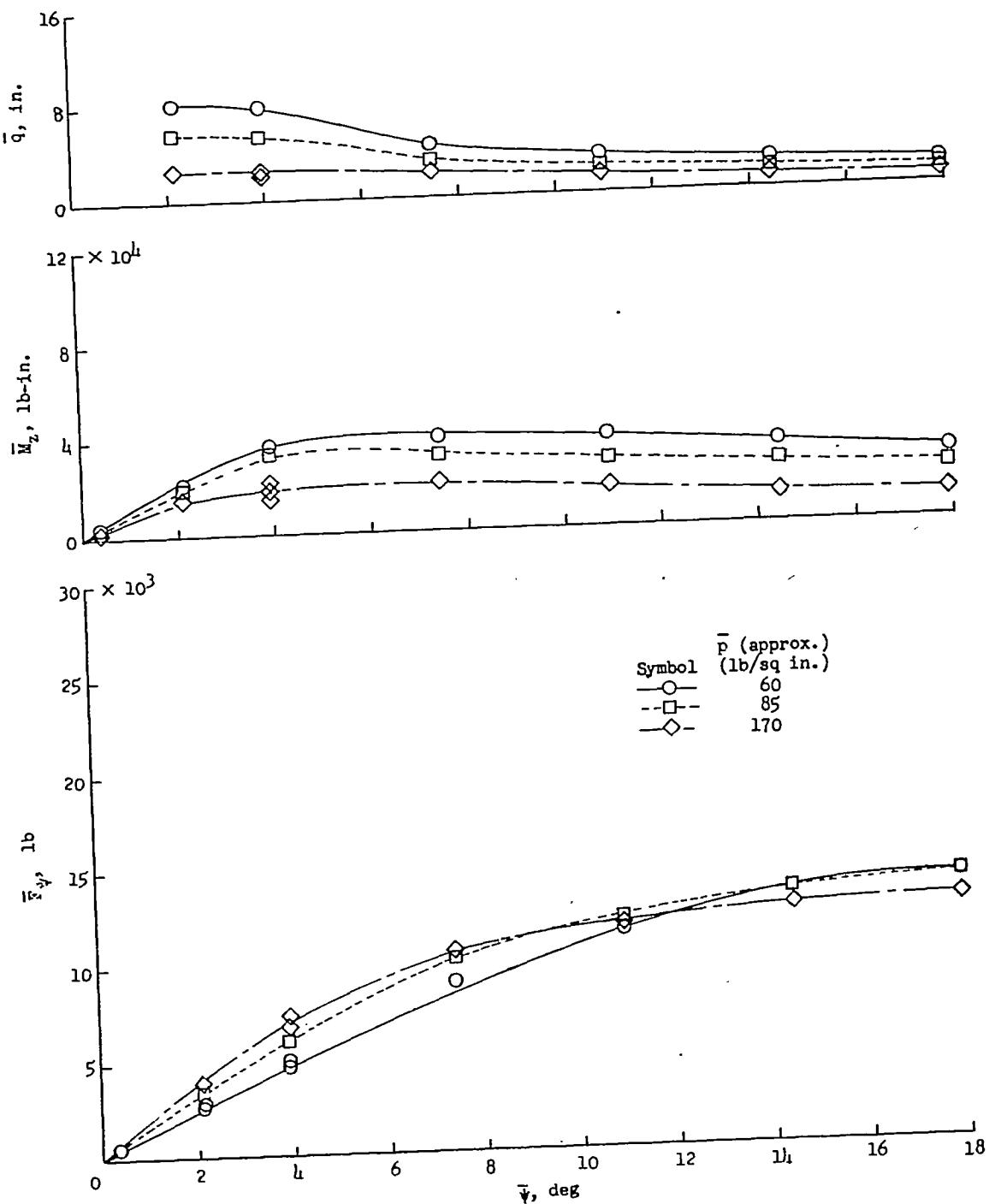
(f) Test series F; $\bar{F}_z = 17,400$ pounds.

Figure 14.- Continued.
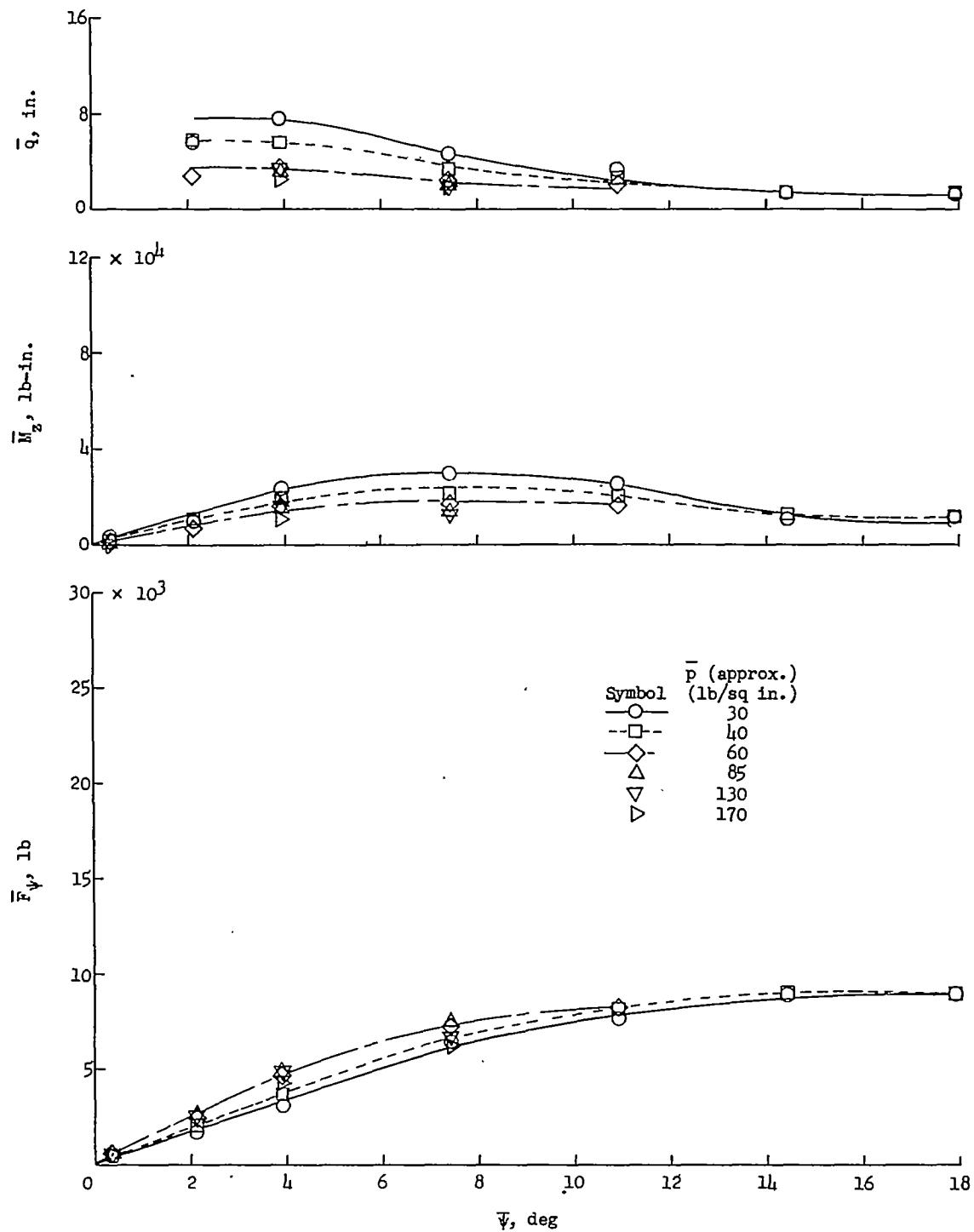
(g) Test series G; $\bar{F}_z = 9,600$ pounds.

Figure 14.- Continued.
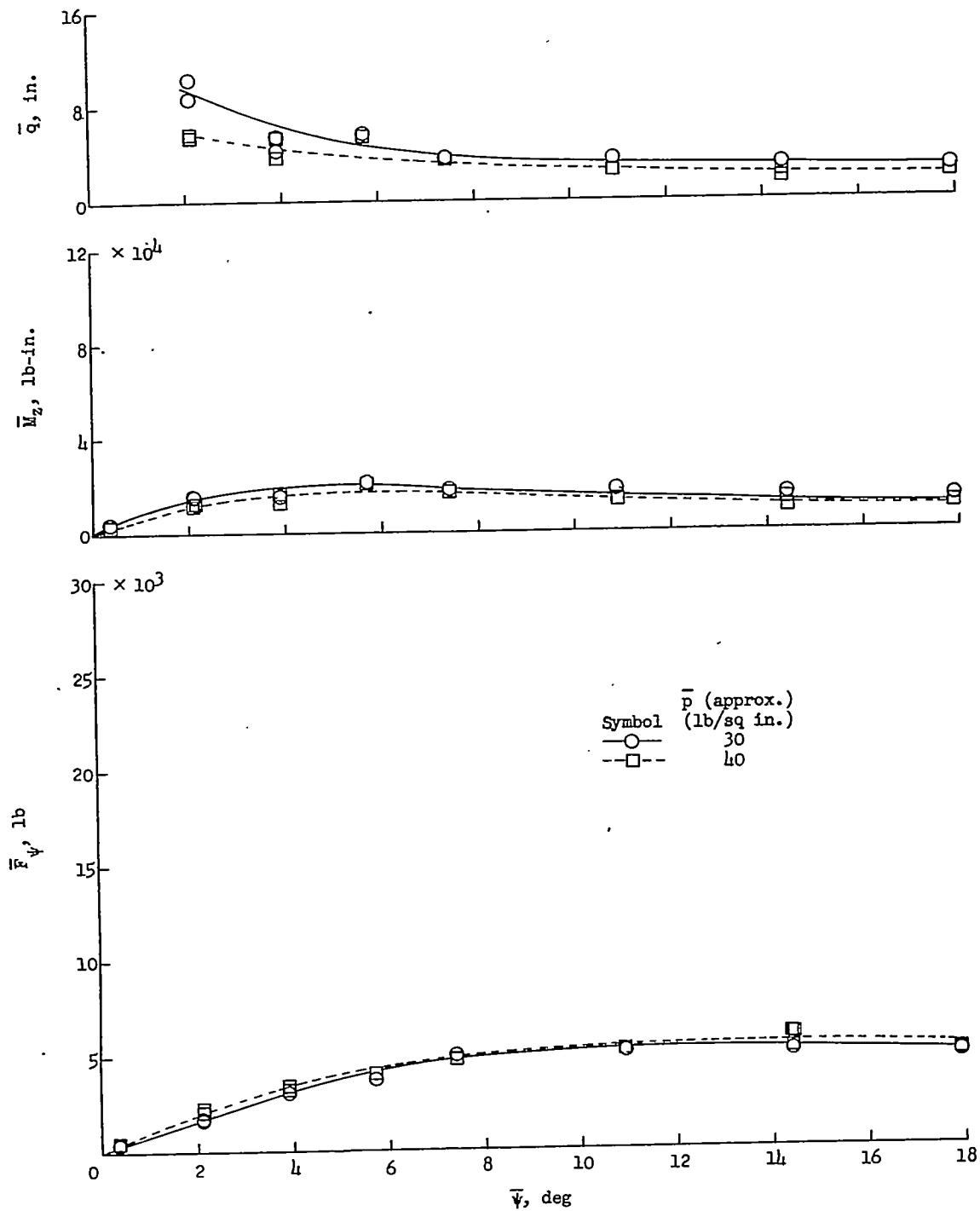
(h) Test series H; $\bar{F}_Z \doteq 9,600$ pounds.

Figure 14.- Continued.
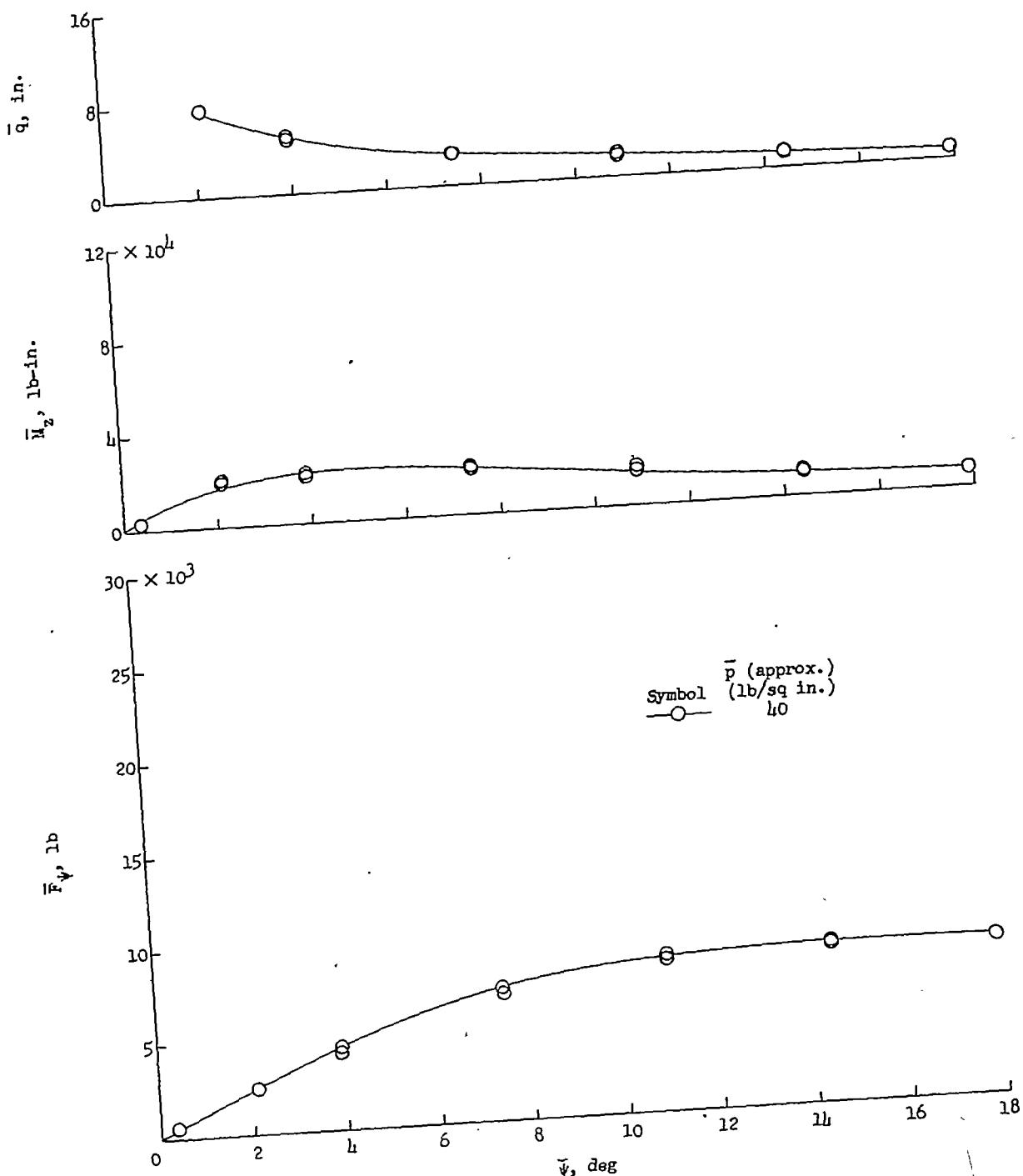
(i) Test series I; $\bar{F}_z$ = 9,600 pounds.

Figure 14.- Concluded.

Tire A	Tire B	p (approx.) (lb/sq in.)	δ_0 (approx.) (in.)	Test series
◯	☐	230	2.4	C
◇	△	60	3.4	F

(a) Variation of rolling radius with yaw angle.

Tire A	Tire B	p (approx.) (lb/sq in.)
◯	☐	230
◇	△	130
▽	▷	60
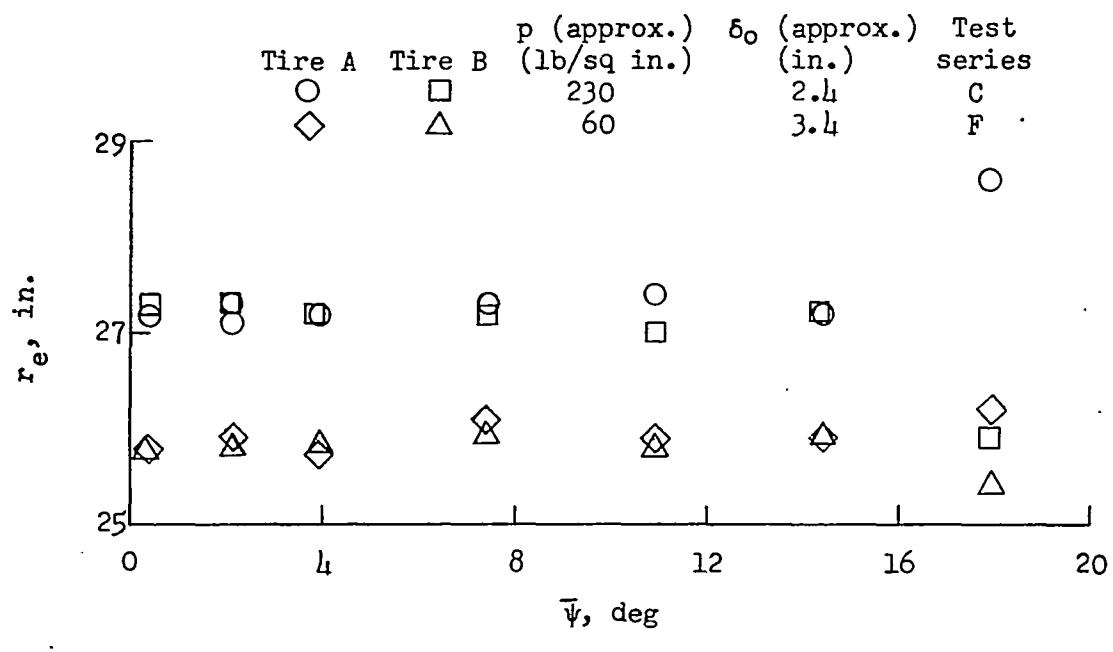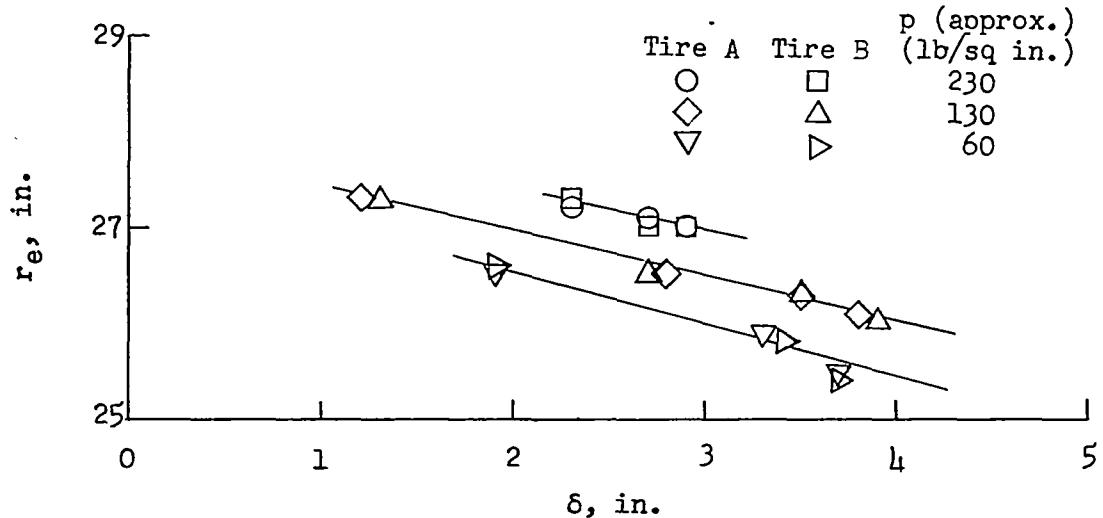
(b) Variation of rolling radius with vertical tire deflection
($\psi = 0.35°$ and $2.1°$).

Figure 15.- Variation of rolling radius with yaw angle and vertical
tire deflection.
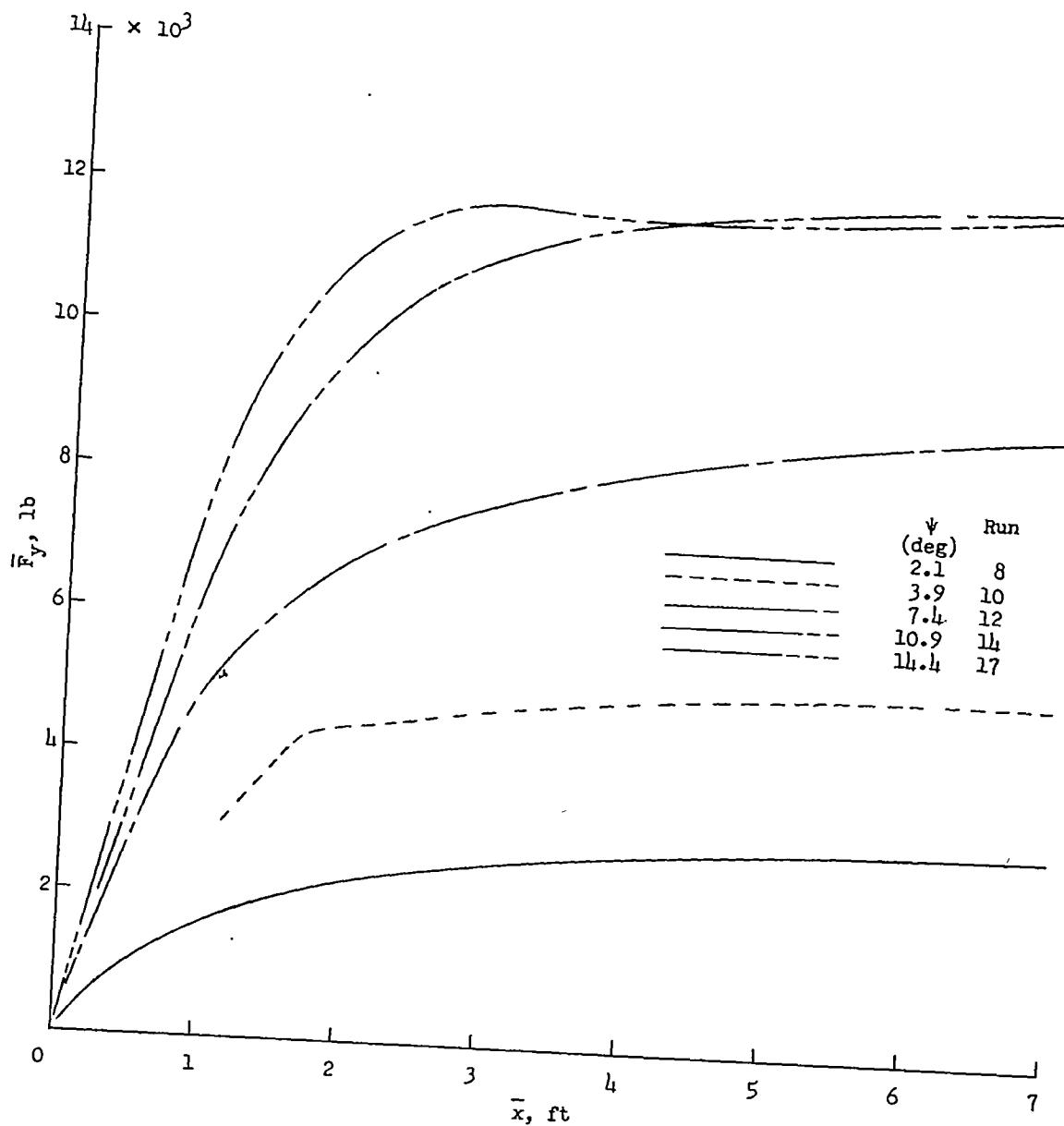
(a) Test series A: $\bar{F}_z = 17,000$ pounds; $\bar{p} \approx 60$ pounds per square inch; $\delta_o \approx 3.7$ inches.

Figure 16.- Buildup of cornering force with distance rolled for some typical runs at several pressures and for three test series.
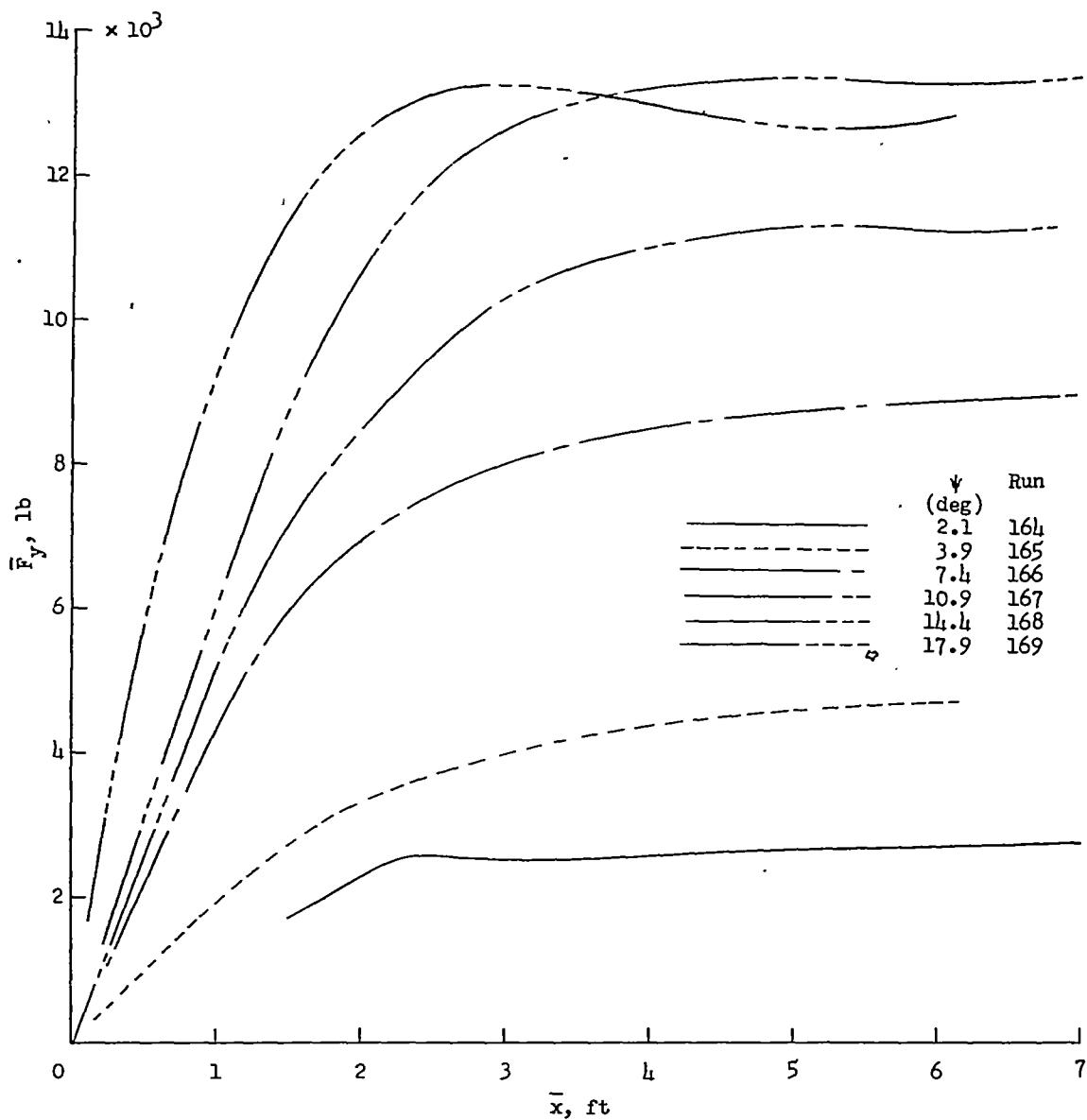
(b) Test series F: $\bar{F}_z = 17,400$ pounds; $\bar{p} \approx 60$ pounds per square inch;
$\bar{\delta}_o \approx 3.5$ inches.

Figure 16.- Continued.
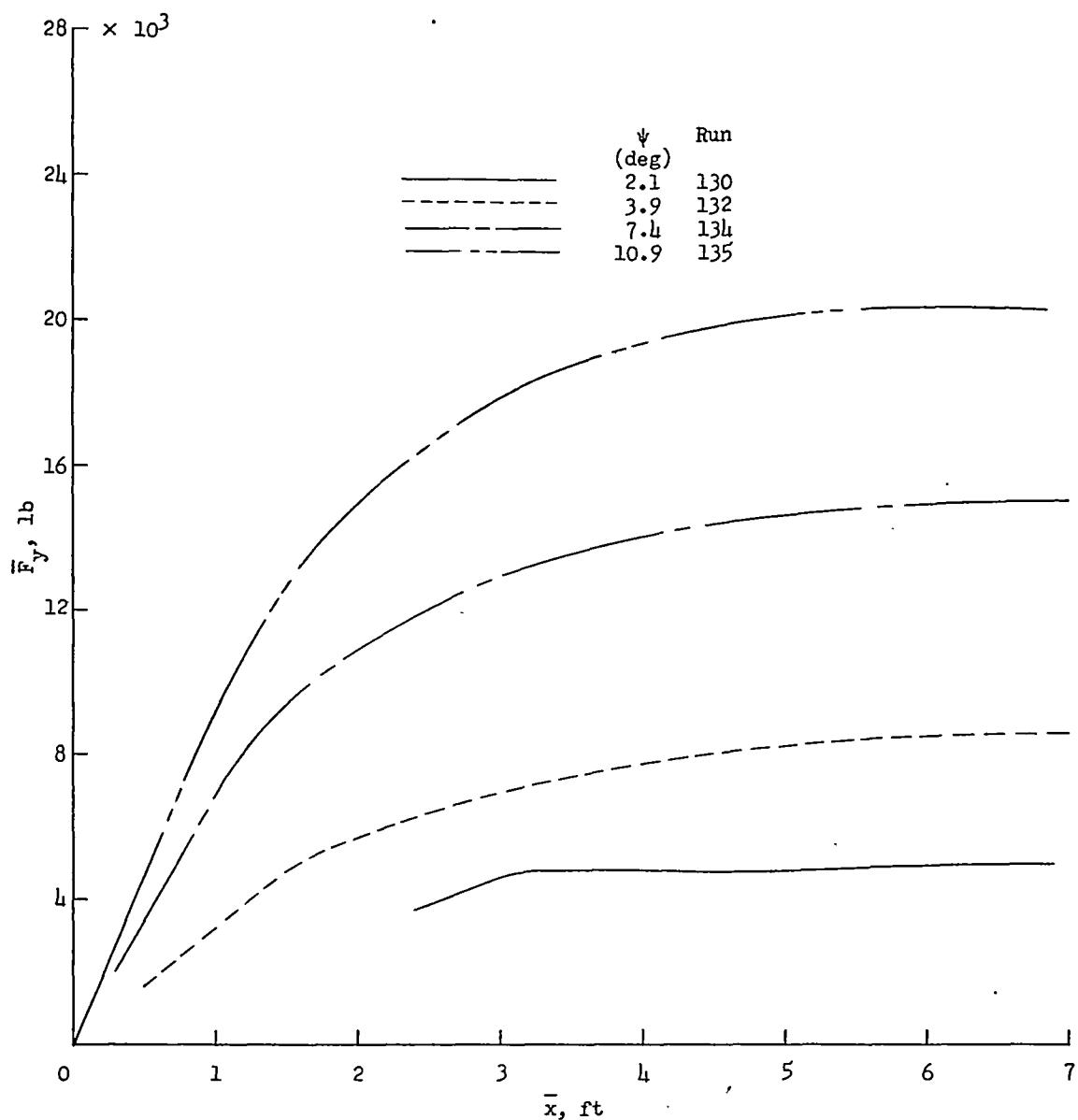
(c) Test series E: $\bar{F}_z = 45,200$ pounds; $\bar{p} \approx 150$ pounds per square inch; $\bar{\delta}_o \approx 4.1$ inches.

Figure 16.- Continued.
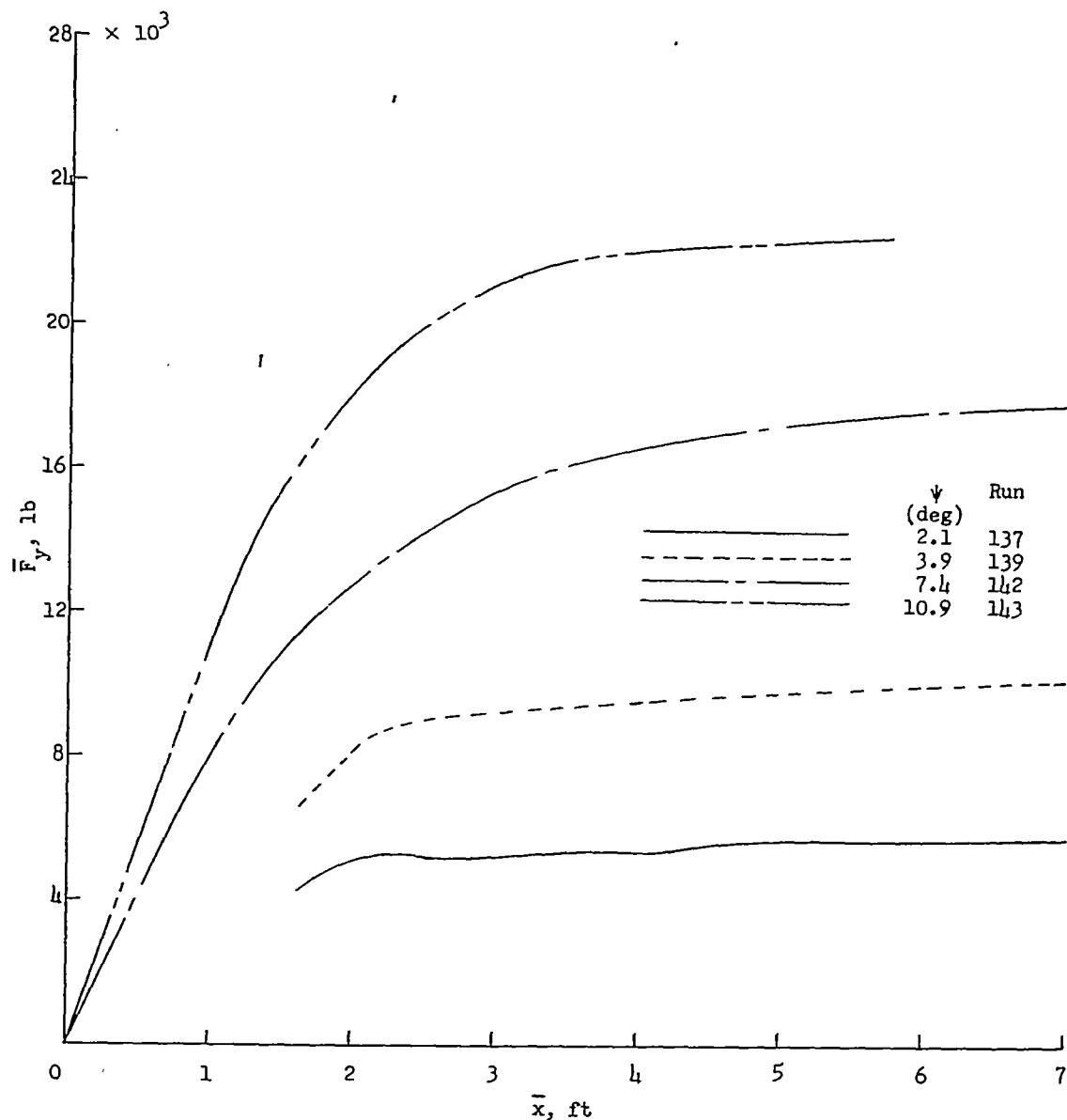
(d) Test series E: $\bar{F}_z = 45,200$ pounds; $\bar{p} \approx 180$ pounds per square inch; $\bar{\delta}_0 \approx 3.6$ inches.

Figure 16.- Continued.

	ψ (deg)	Run
— — — —	3.9	155
——————	7.4	157
— · — · —	10.9	159
——————	14.4	161
— — — —	17.9	162
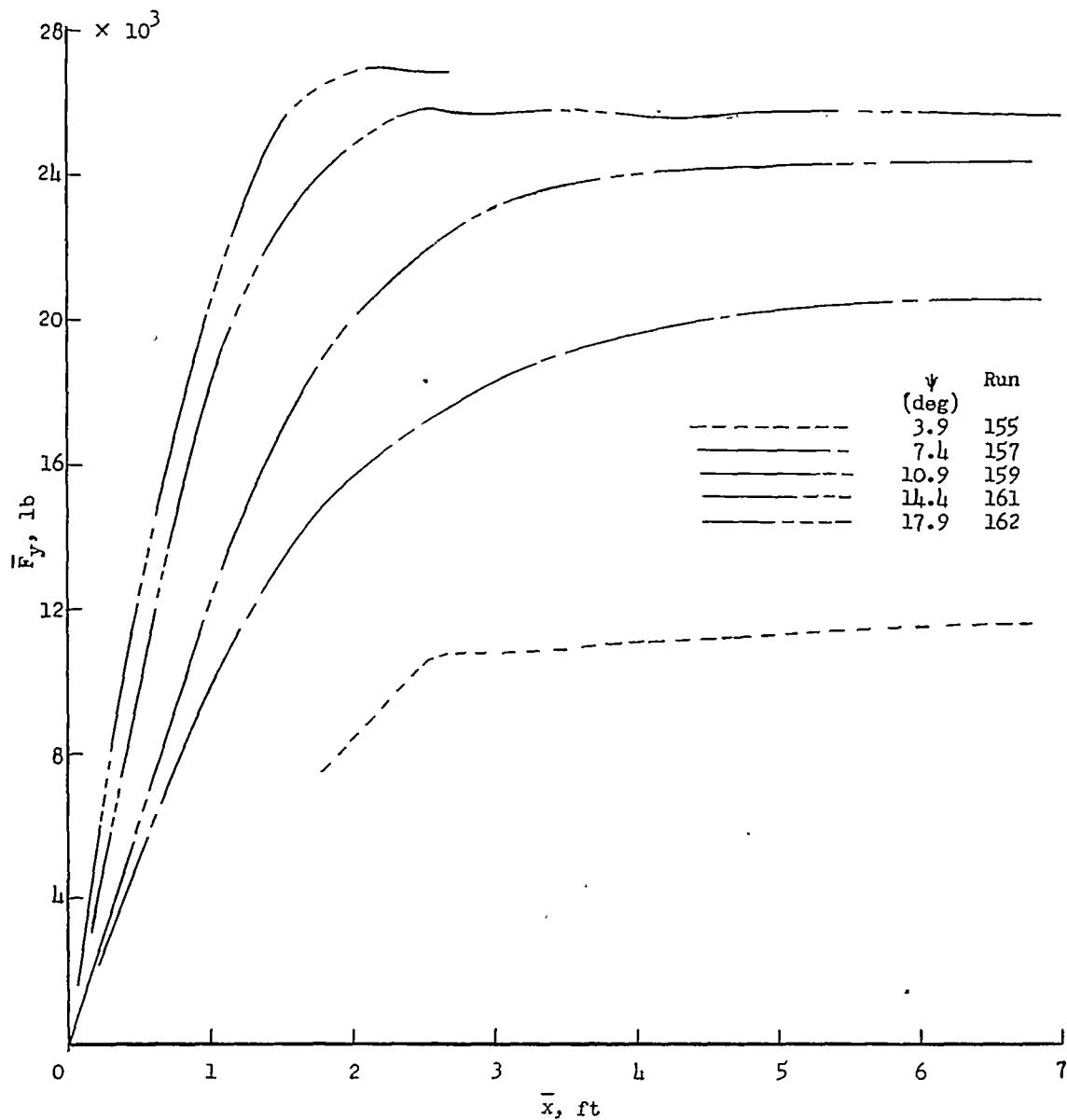
(e) Test series E: $\bar{F}_z$ = 45,200 pounds; $\bar{p} \approx$ 230 pounds per square inch; $\bar{\delta}_0 \approx$ 3.0 inches.

Figure 16.- Concluded.

Static-deflection method.

Unyawed-rolling-force method.

Unyawed rolling deflection method.

Yawed-rolling method.
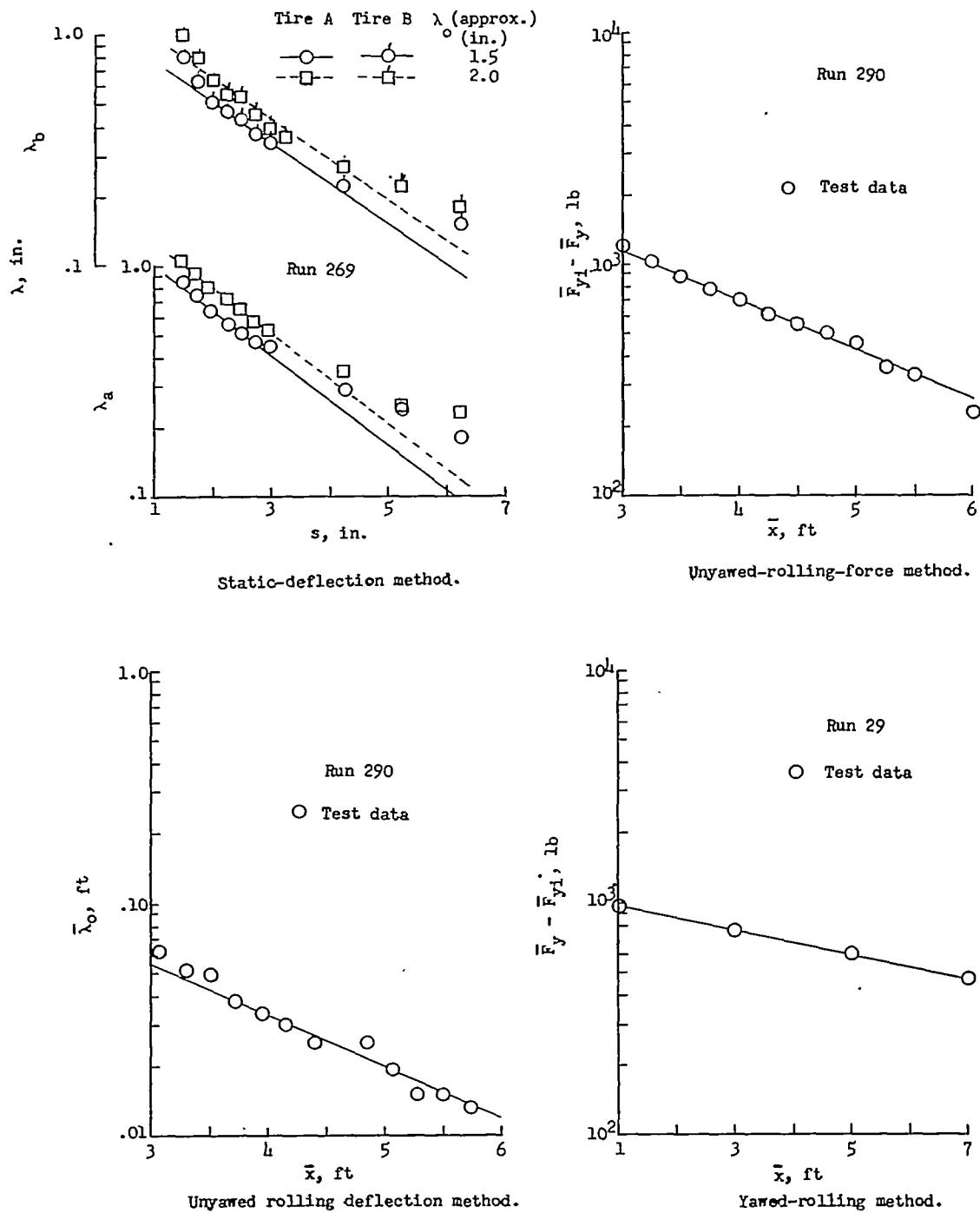
(a) Test series A: $\bar{F}_z = 17,000$ pounds; for runs 269 and 290, $\bar{p} \approx 60$ pounds per square inch and $\bar{\delta}_0 \approx 3.7$ inches; for run 29, $\bar{p} \approx 168$ pounds per square inch and $\bar{\delta}_0 \approx 1.8$ inches.

Figure 17.- Sample test data obtained from the four methods used to determine relaxation length.
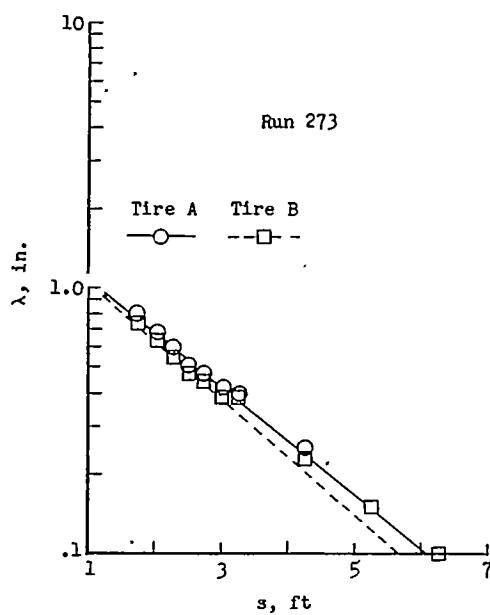
Run 273

Tire A   Tire B
───○─── ──□──

Static-deflection method.

Run 297

○ Test data

Unyawed-rolling-force method.

Run 297

○ Test data

Unyawed-rolling-deflection method.

Run 51

○ Test data
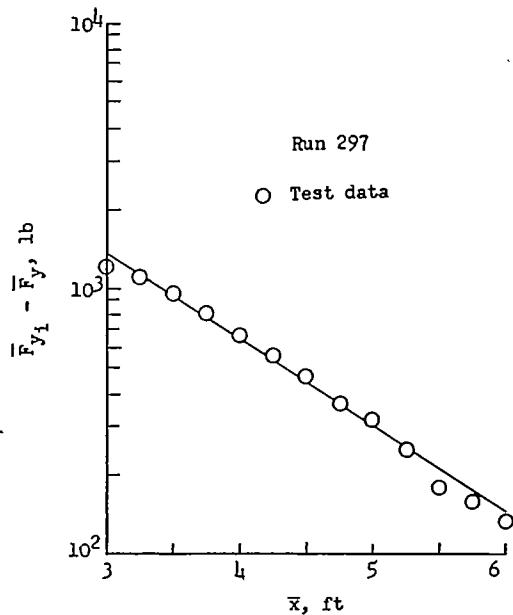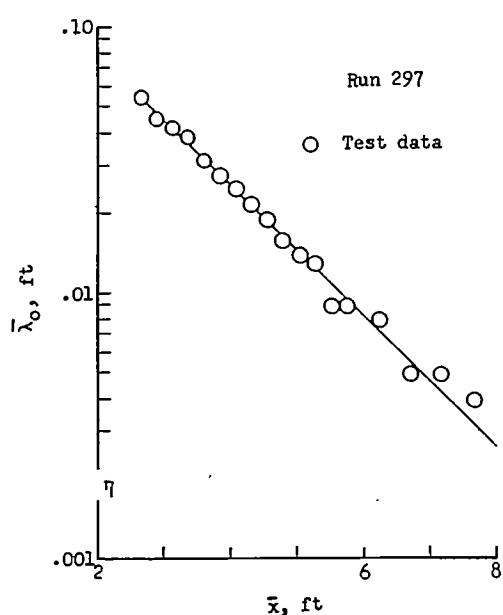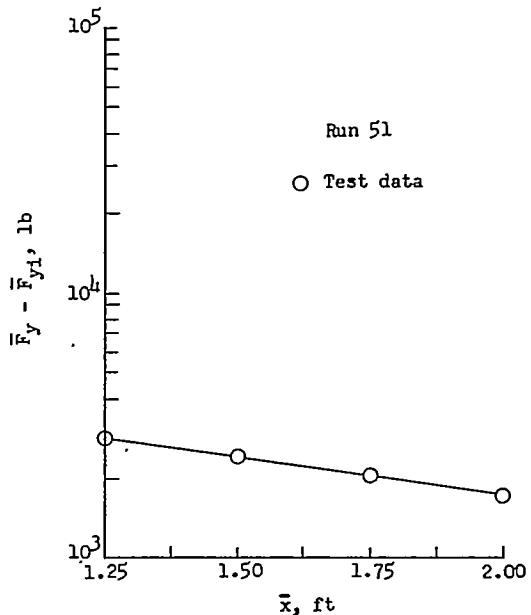
Yawed-rolling method.

(b) Test series B: $\bar{F}_z$ = 23,700 pounds; $\bar{p} \approx$ 130 pounds per square inch; $\delta_o \approx$ 2.8 inches.

Figure 17.- Continued.
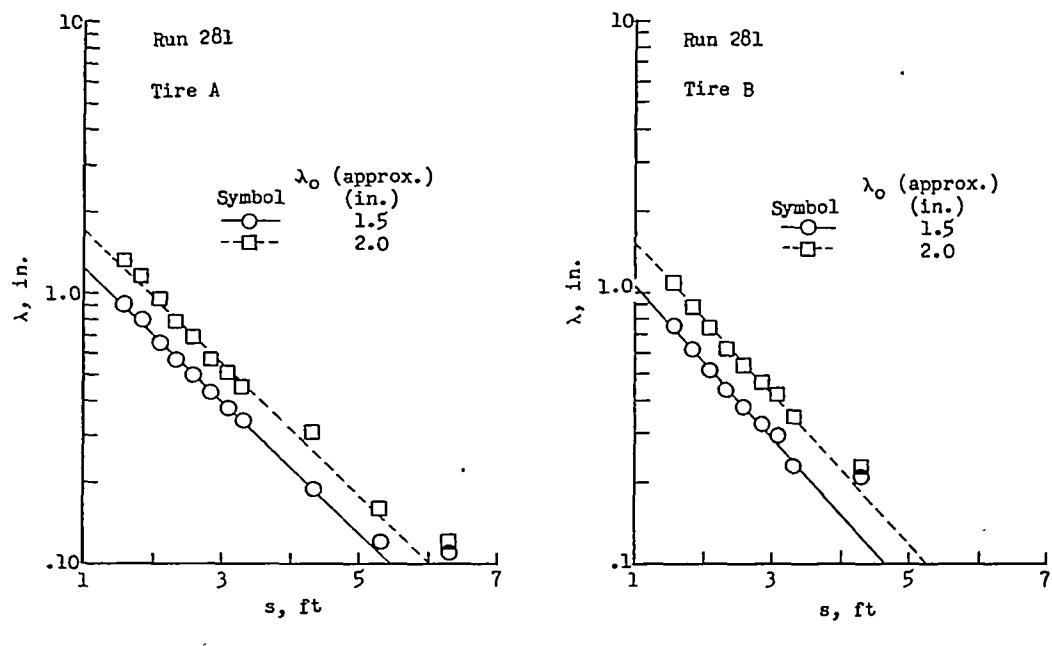
Static-deflection method.
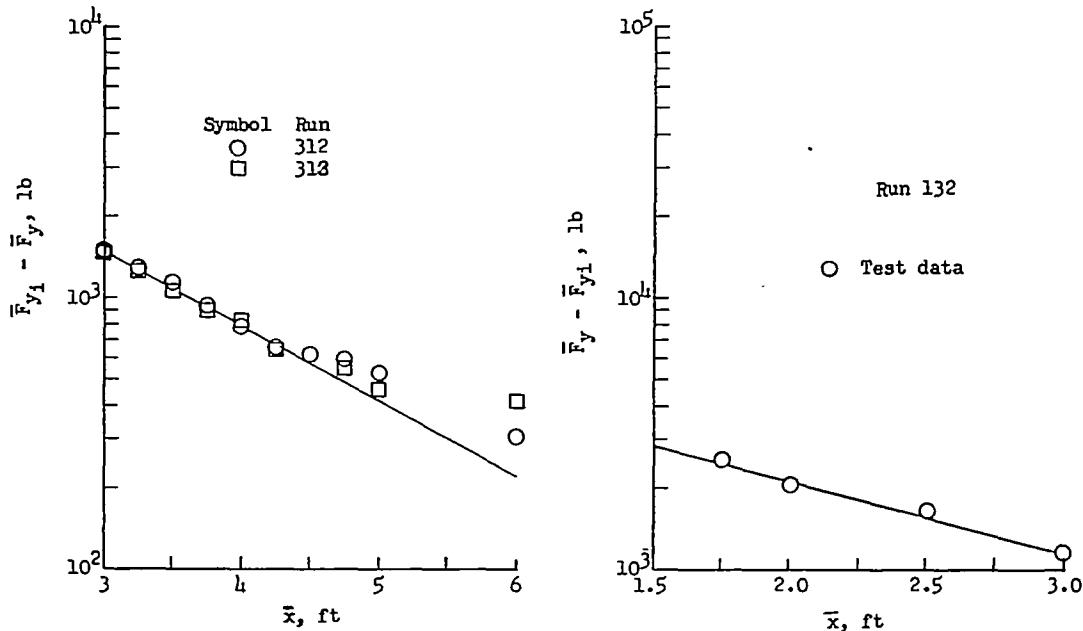
Unyawed-rolling-force method.

Yawed-rolling method.

(c) Test series E: $\bar{F}_z = 45,200$ pounds; $\bar{p} \approx 150$ pounds per square inch; $\bar{\delta}_o \approx 4.3$ inches.

Figure 17.- Continued.
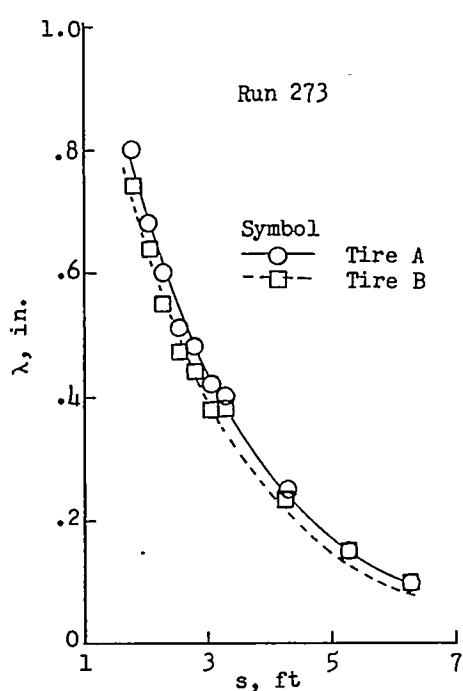
Static-deflection method.
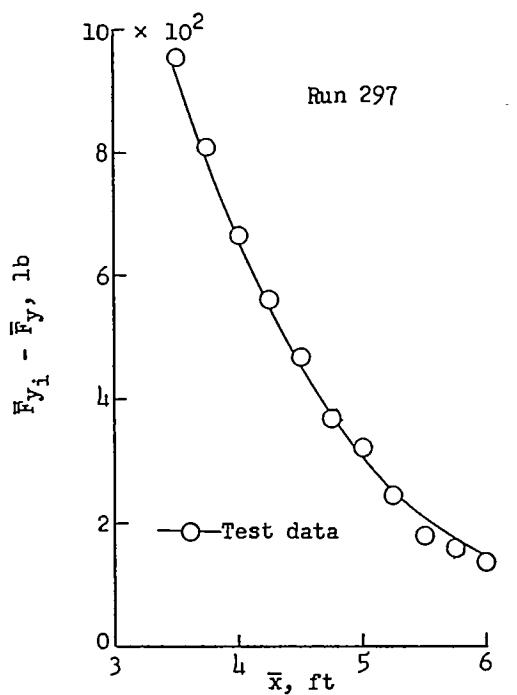
Unyawed-rolling-force method.
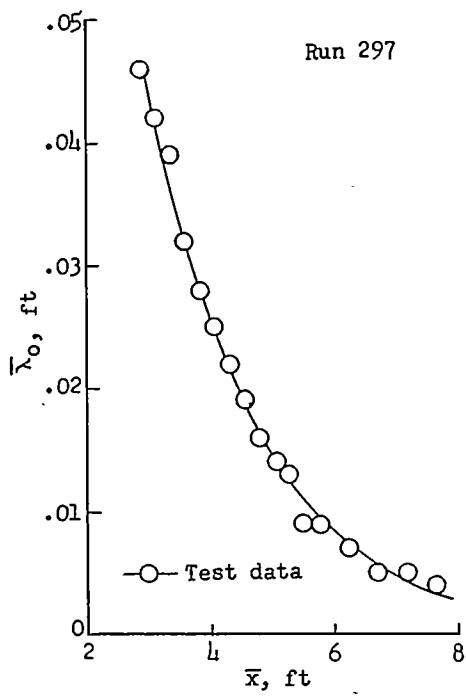
Unyawed-rolling-deflection method.
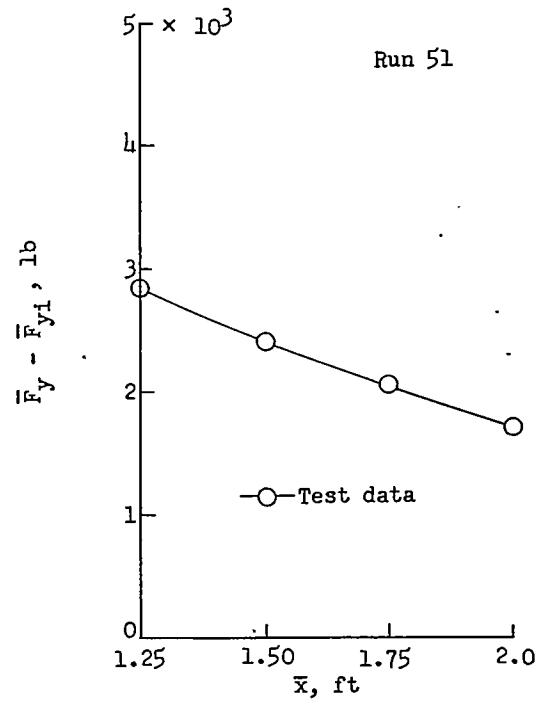
Yawed-rolling method.

(d) Data for test series B (see fig. 17(b)) replotted in linear coordinates.

Figure 17.- Concluded.
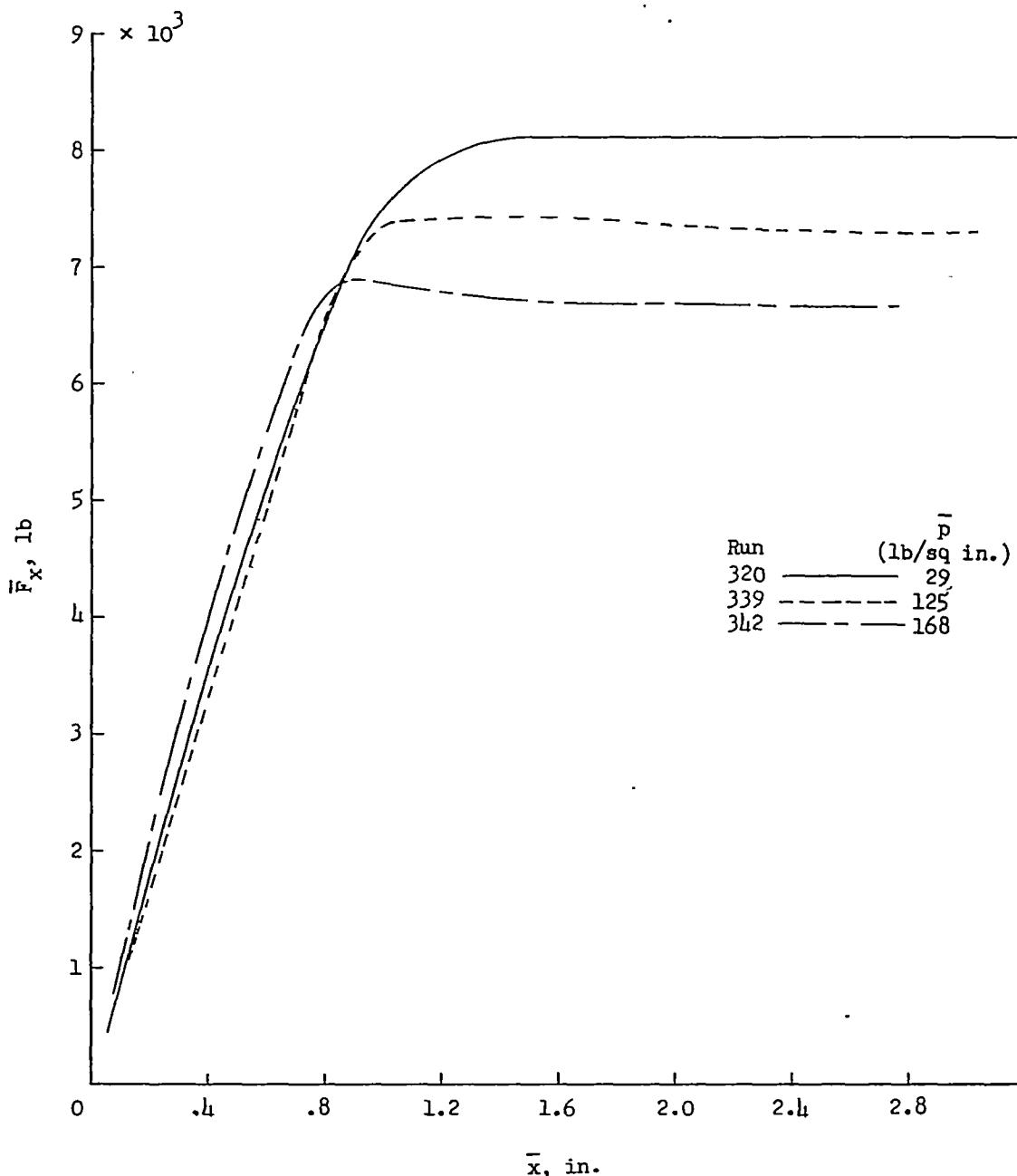
Figure 18.- Drag force buildup with horizontal distance pulled for several typical runs. Locked-wheel drag tests with $\bar{F}_z$ = 9,730 pounds for $\bar{F}_x$ = 0.
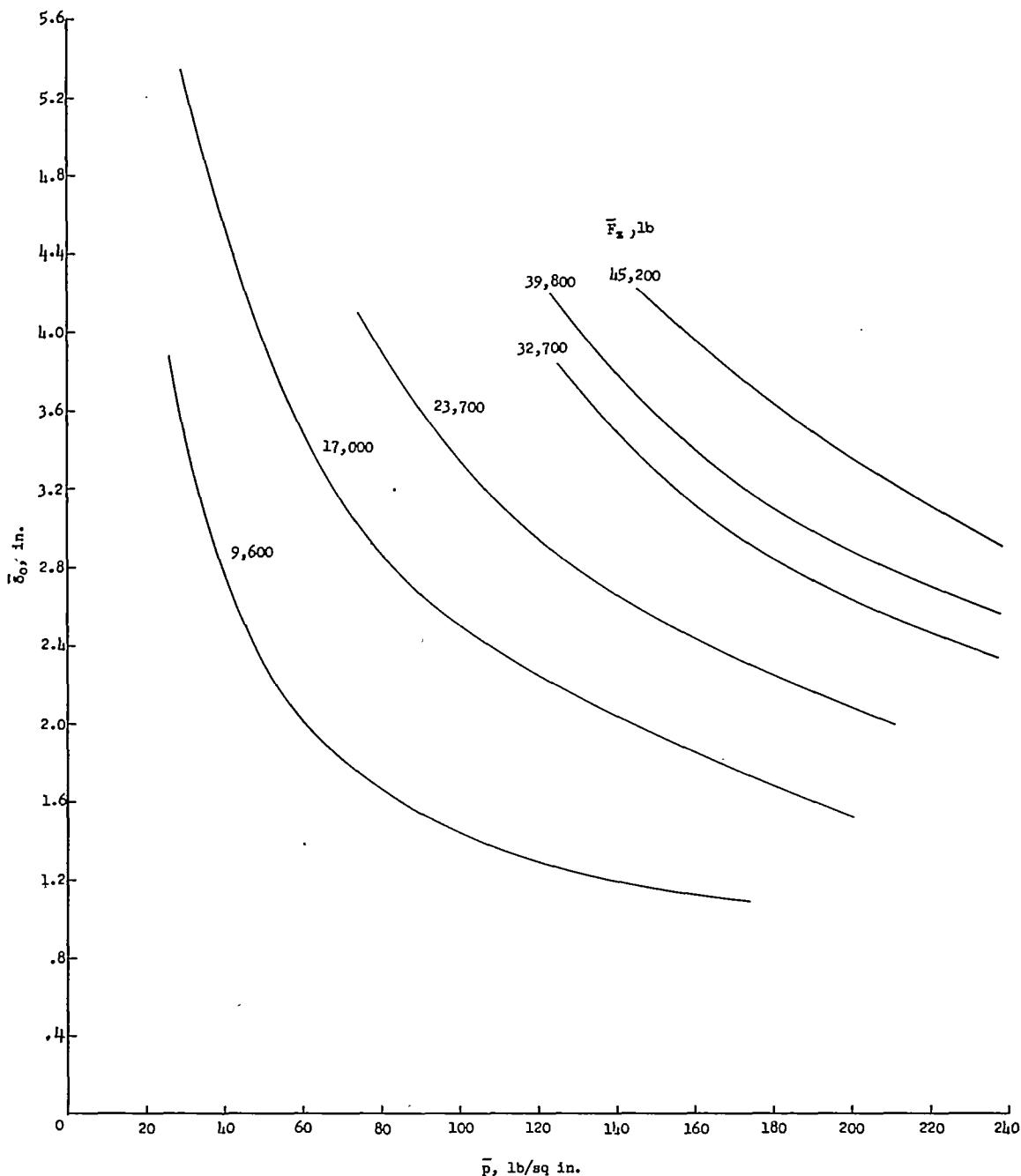
Figure 19.- Average vertical-load—vertical-tire-deflection characteristics
of tires A and B.
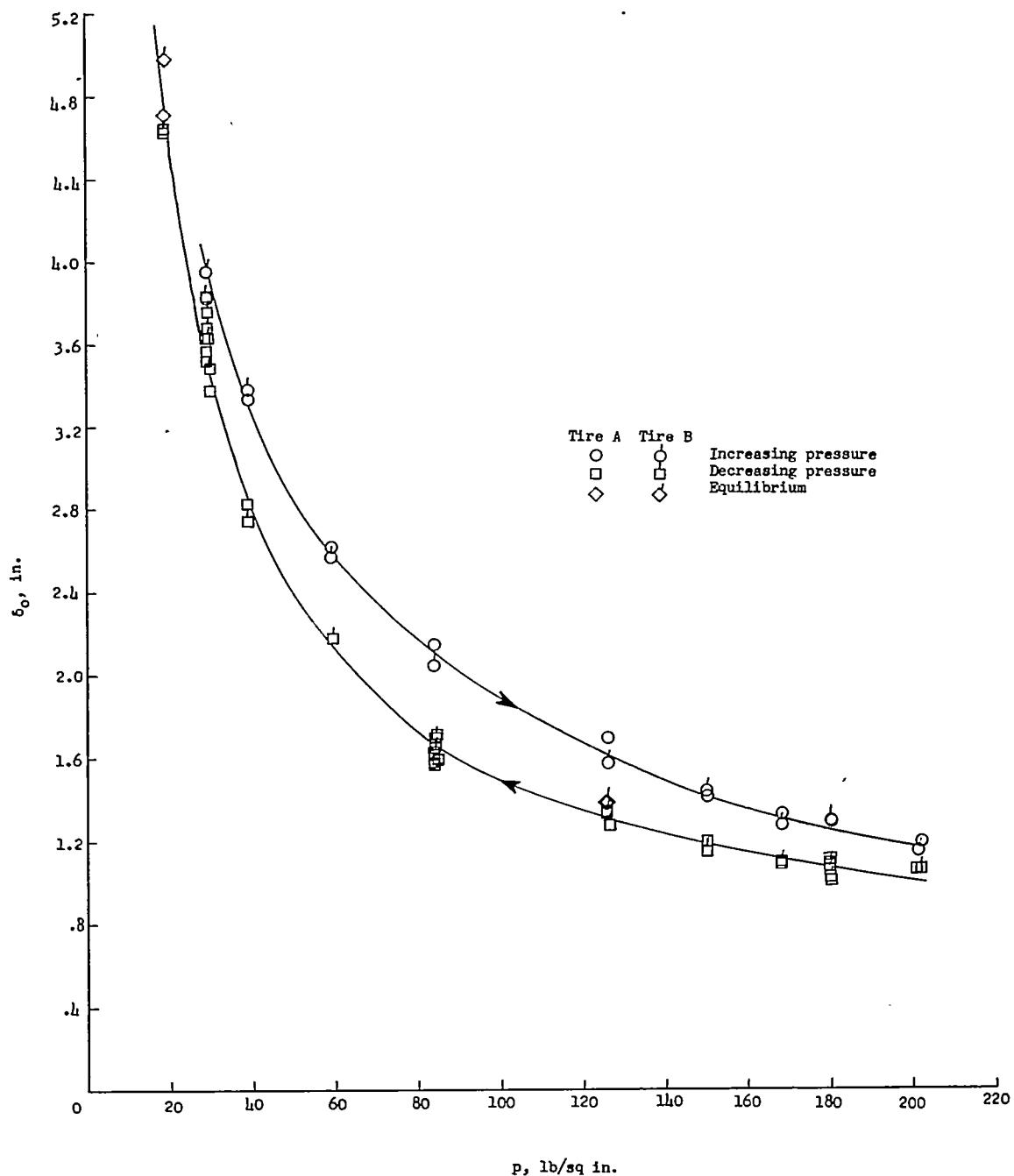
Figure 20.- Hysteresis effects on tire-pressure—vertical-deflection
   relationships (table V, locked-wheel drag tests) for $\bar{F}_Z$ = 9,730 pounds.
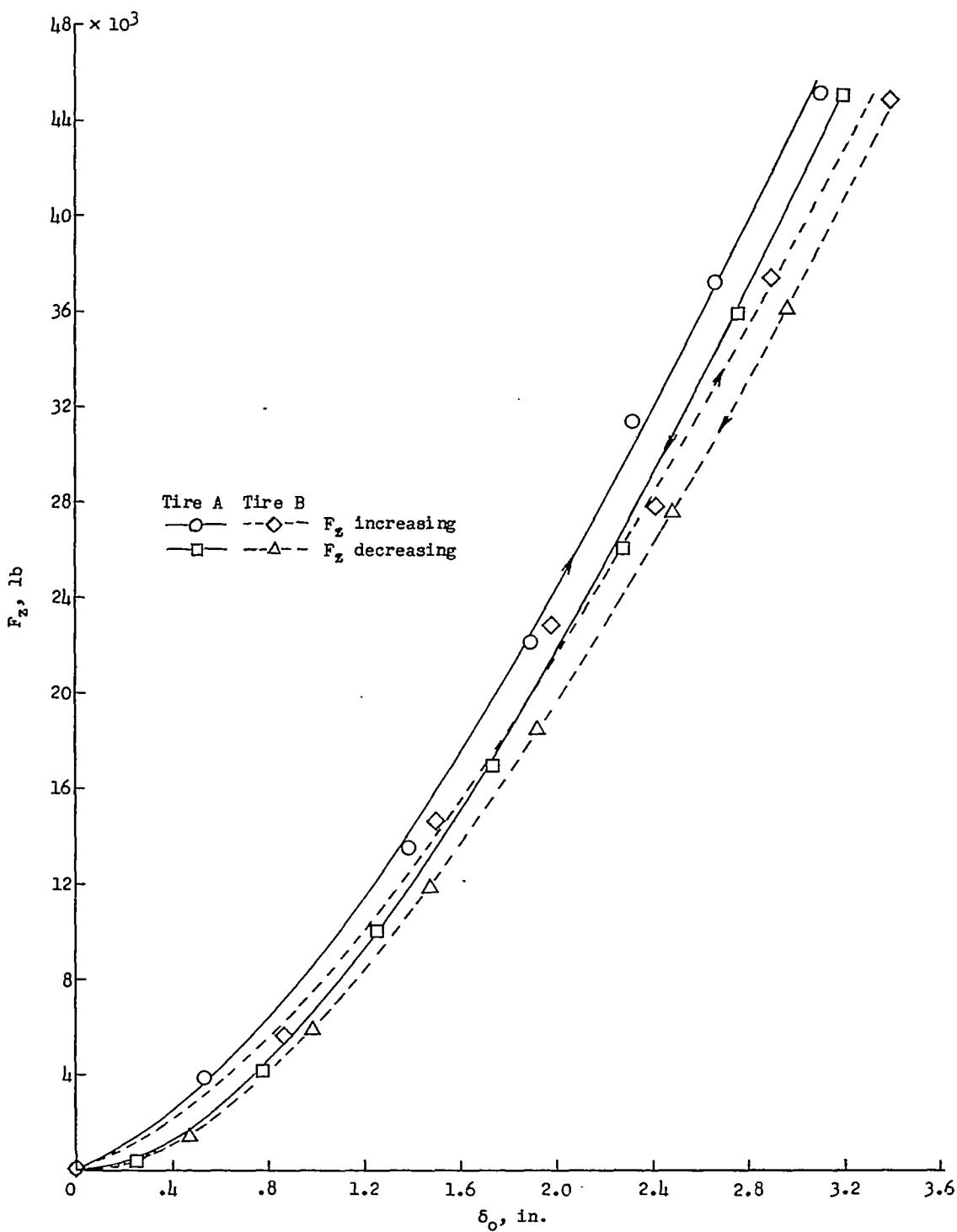
Figure 21.- Variation of vertical load with vertical tire deflection for
p_O = 219 pounds per square inch. p = 221 pounds per square inch
at $F_{z_{max}}$.
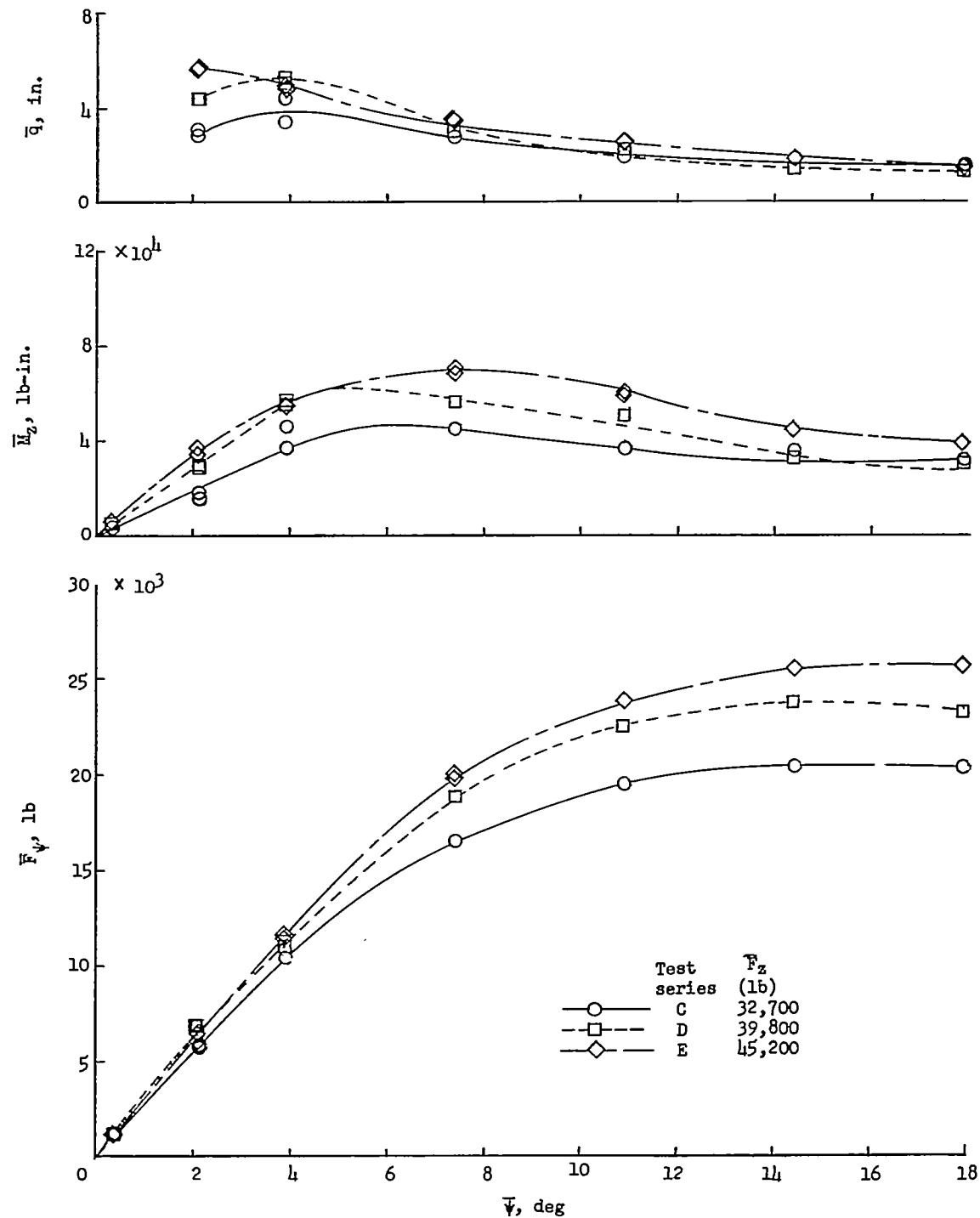
Figure 22.- Variation of normal force, self-alining torque, and pneumatic caster with yaw angle for constant inflation pressure. $\bar{p} \approx 230$ pounds per square inch.
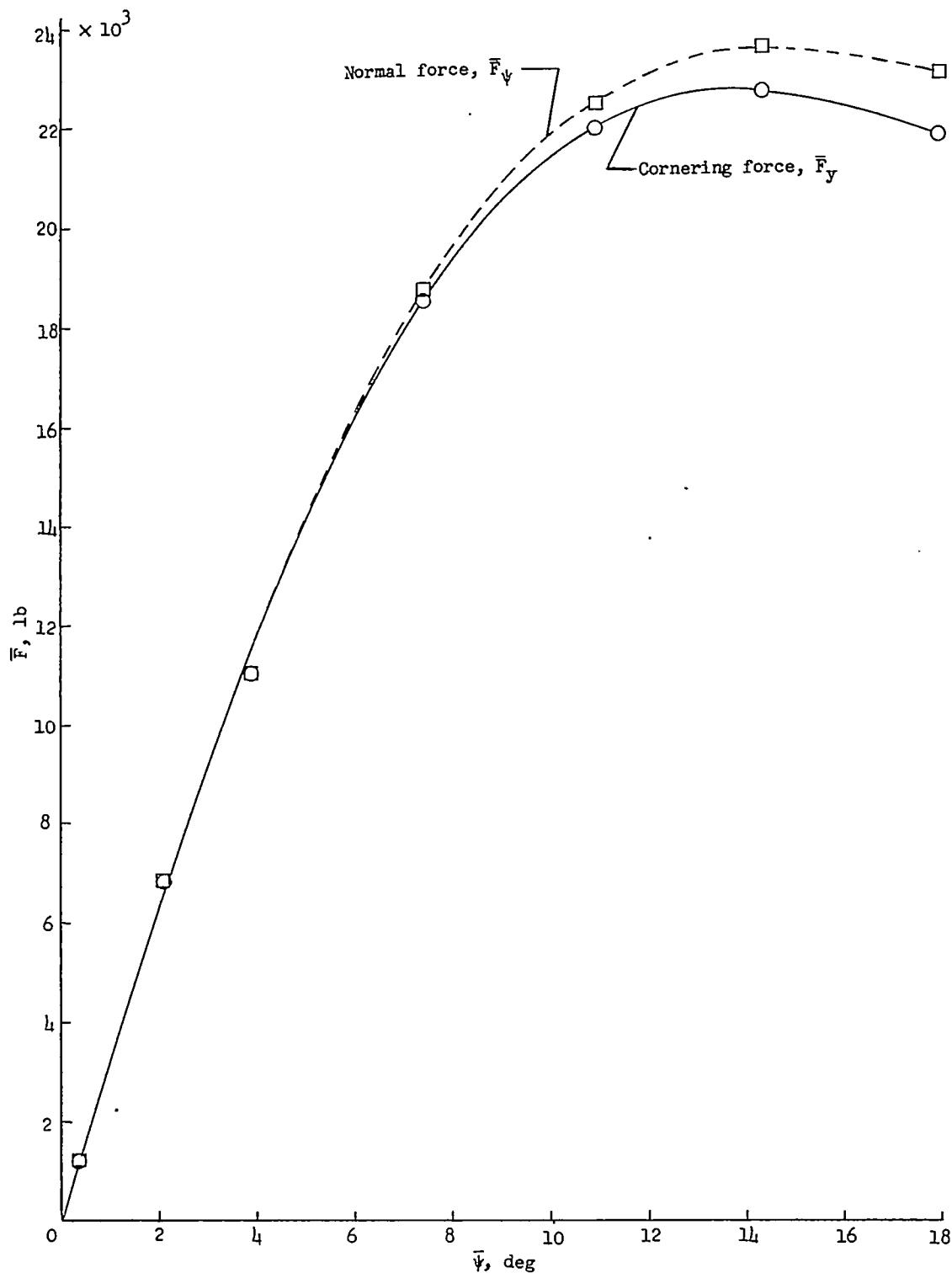
Figure 23.- Comparison of cornering-force and normal-force variations
with yaw angle for a typical loading condition. (Test series D:
$\bar{F}_z$ = 39,800 pounds; $\bar{p}$ ≈ 230 pounds per square inch; δ_o ≈ 2.7 inches.)
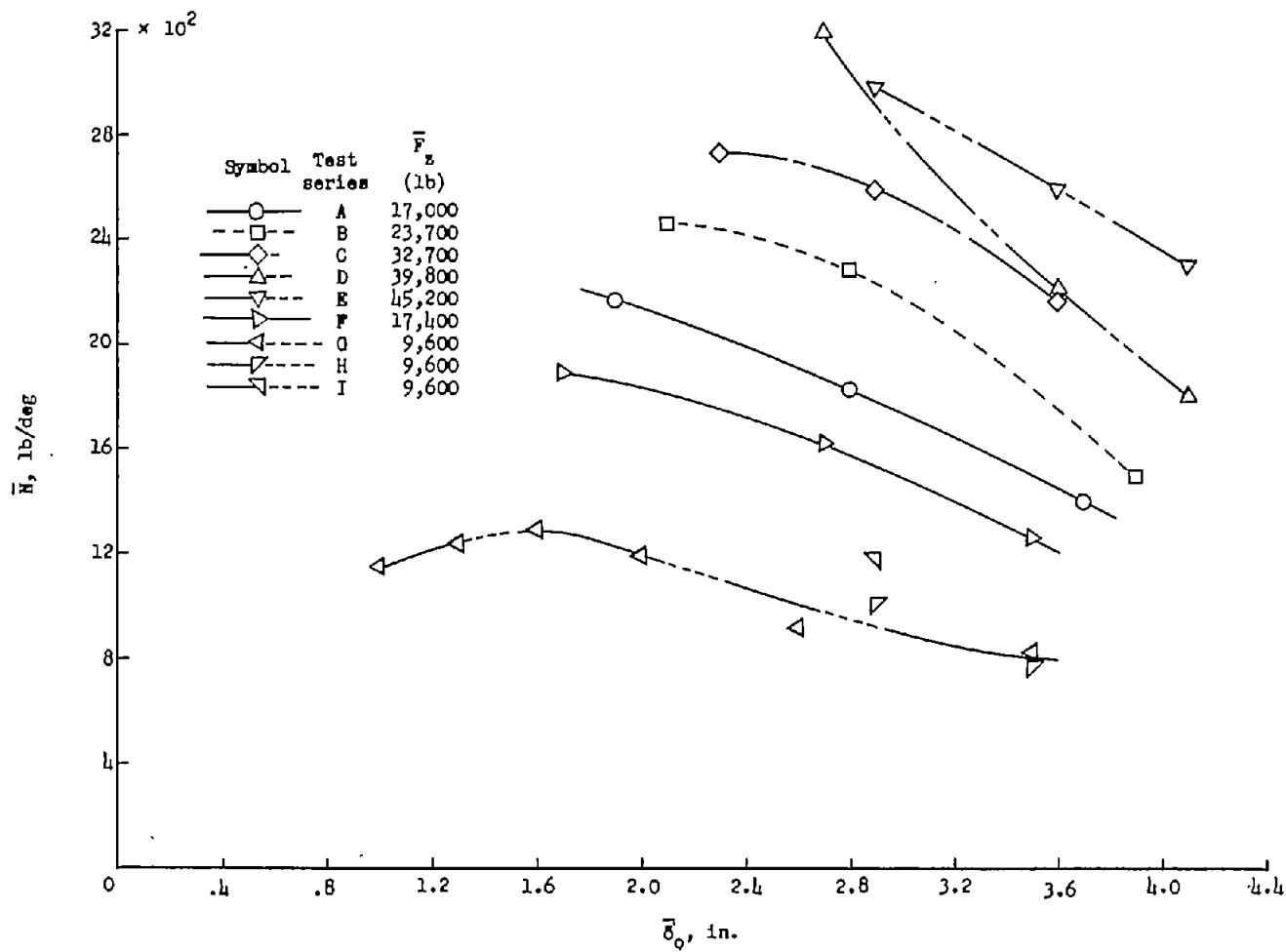
(a) Variation of cornering power with vertical tire deflection.

Figure 24.- Variation of cornering power with vertical tire deflection and inflation pressure.
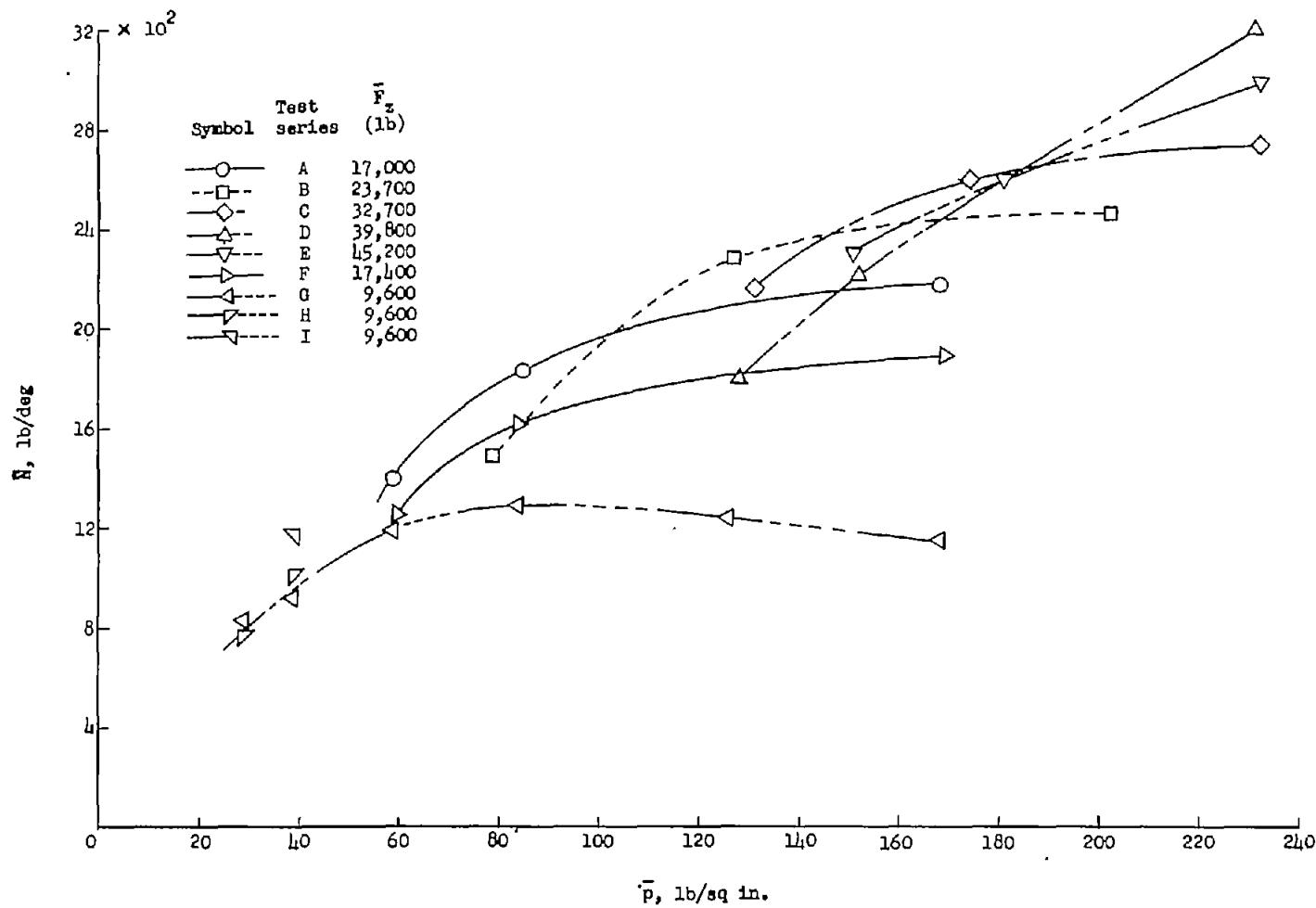
(b) Variation of cornering power with inflation pressure.

Figure 24.- Concluded.
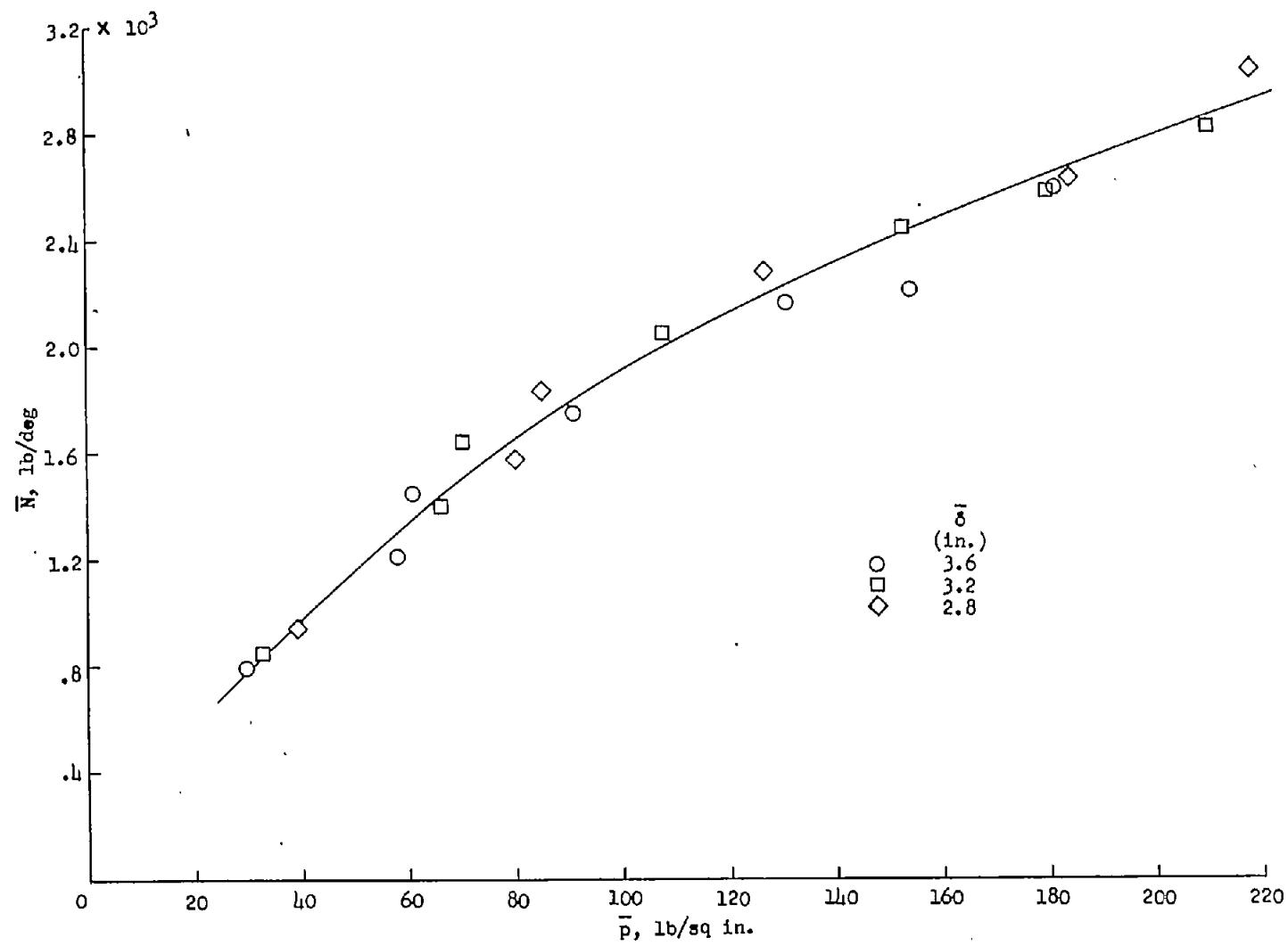
Figure 25.- Variation of cornering power with inflation pressure for
several constant vertical deflections.
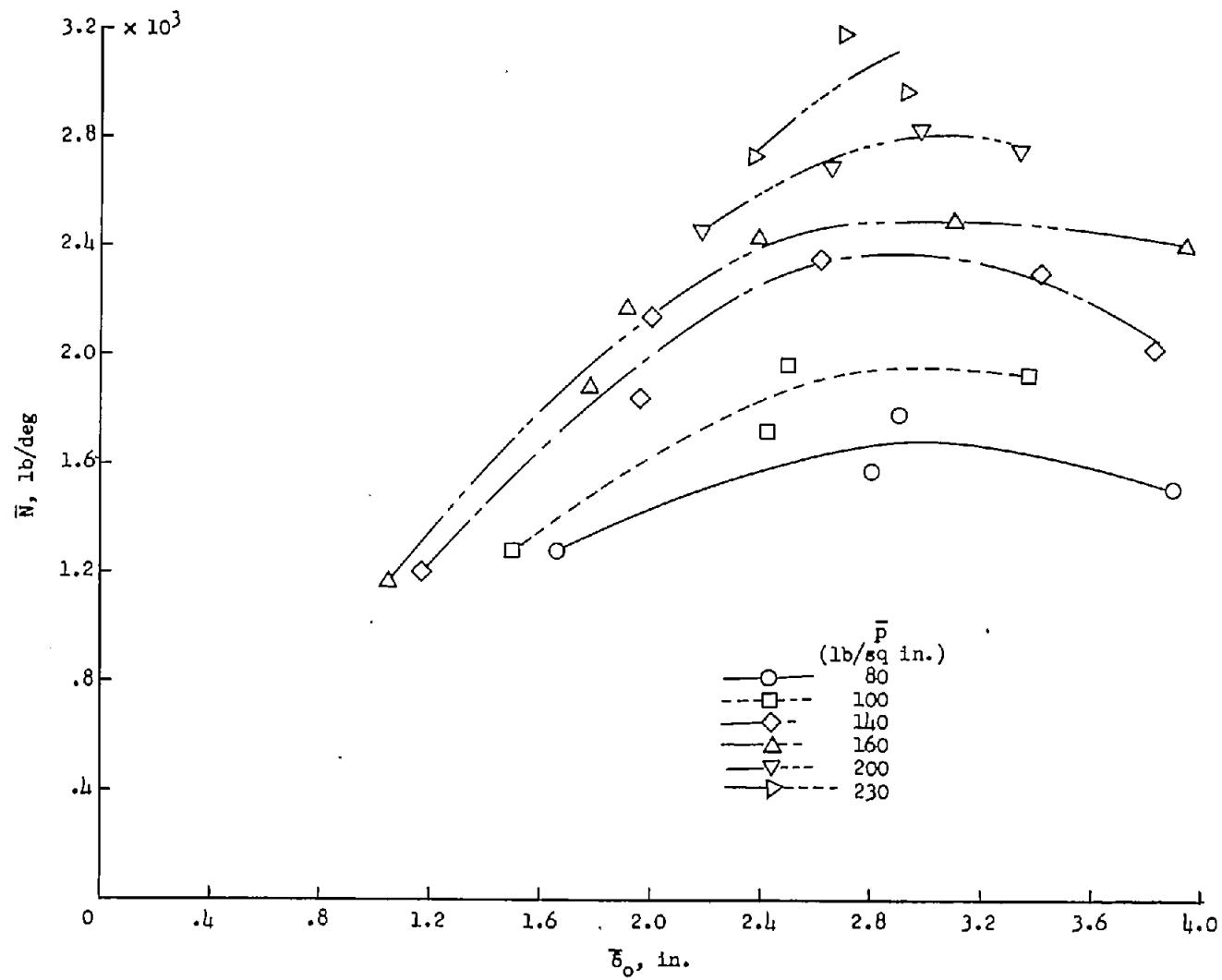
Figure 26.- Variation of cornering power with vertical tire deflection for several constant inflation pressures.
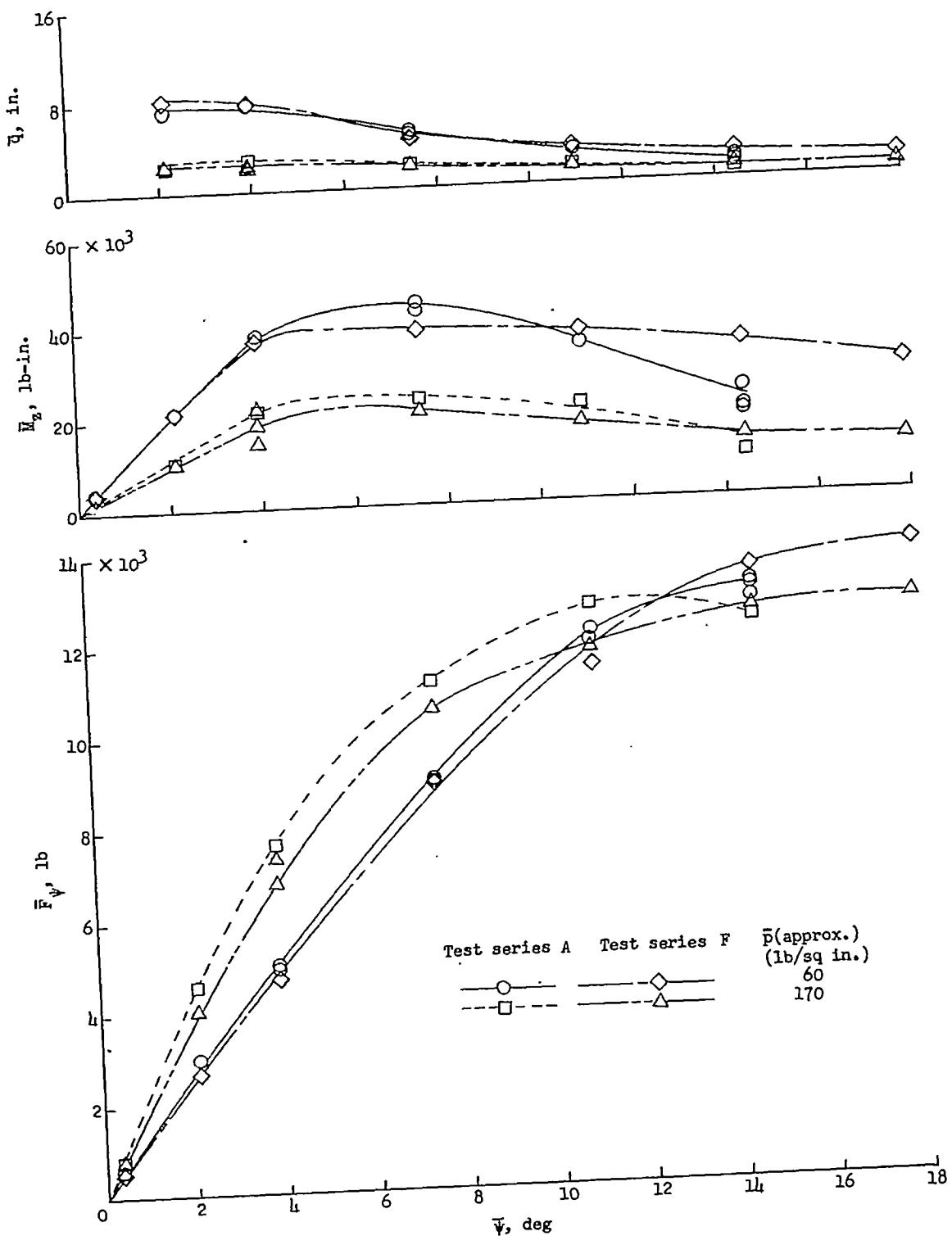
Figure 27.- Effect of tire wear on normal force, self-alining torque, and pneumatic caster for $\bar{F}_z \approx 17,000$ pounds.
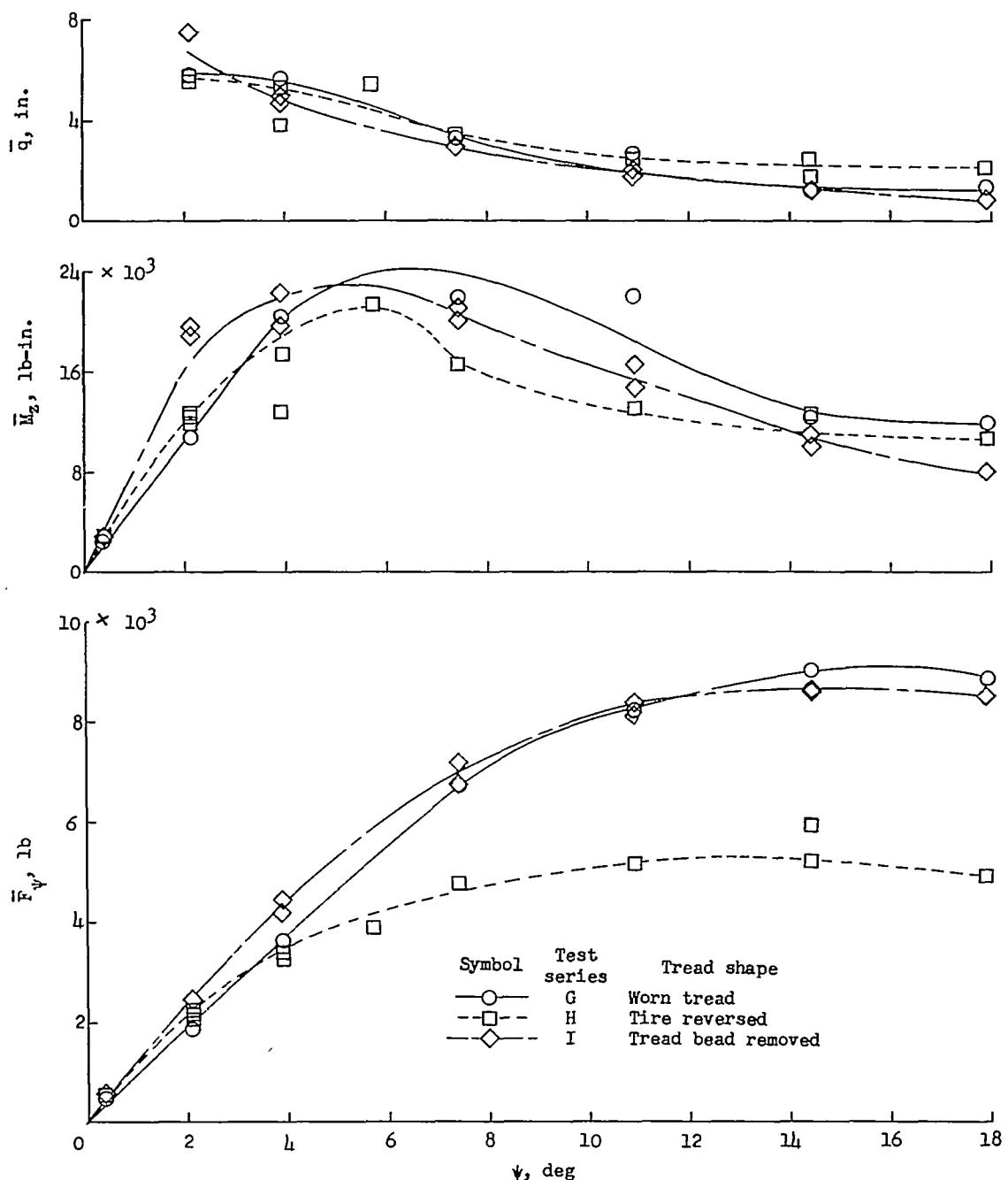
Figure 28.- Effect of tread shape on normal force, self-alining torque, and pneumatic caster for $\bar{F}_z = 9,600$ pounds and $\bar{p} \approx 39$ pounds per square inch.

(a) Tire unloaded.

(b) Tire under normal towing conditions (test series A to G).

(c) Tire under reversed towing conditions (test series H).
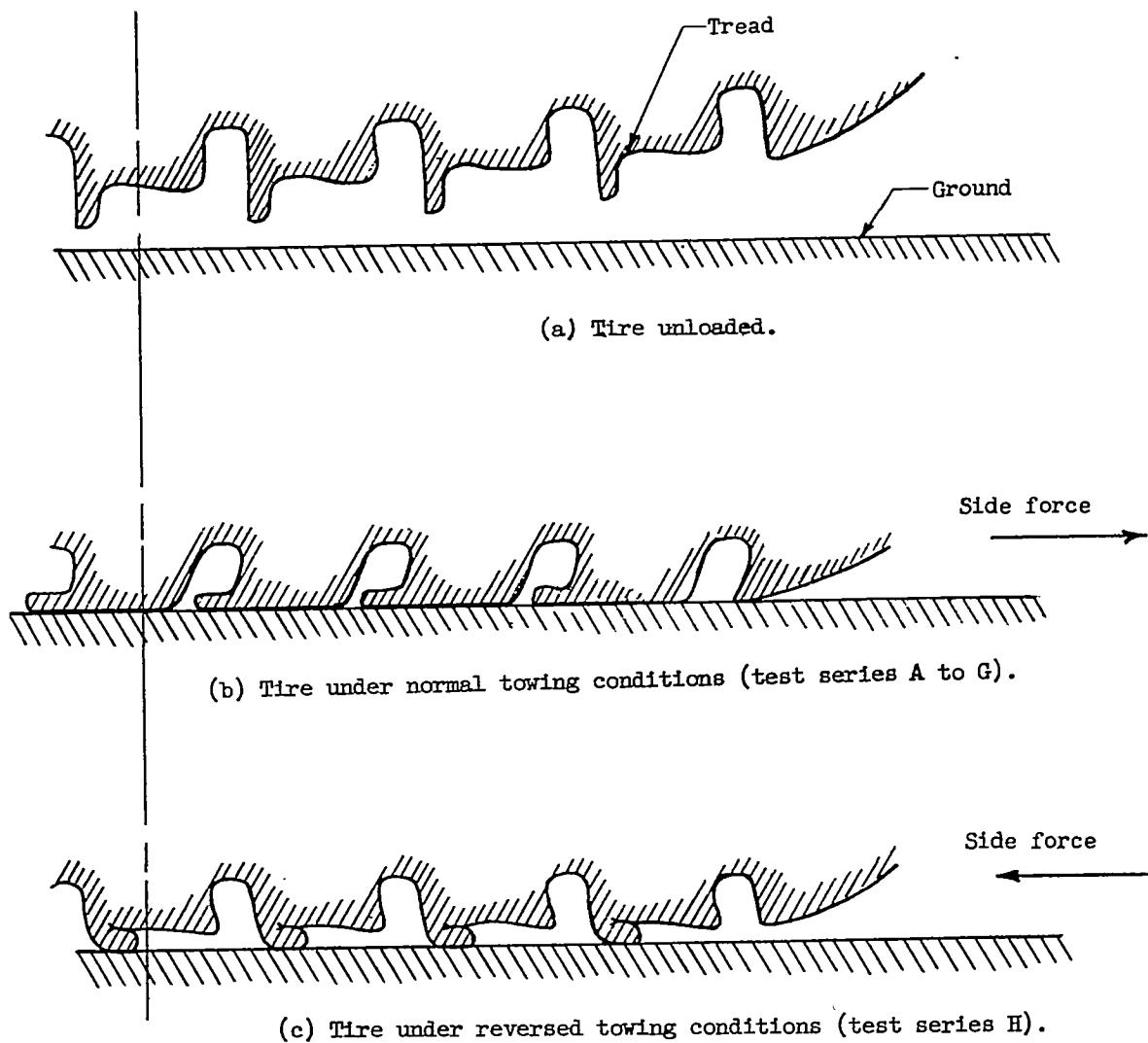
Figure 29.- Tread bead position.
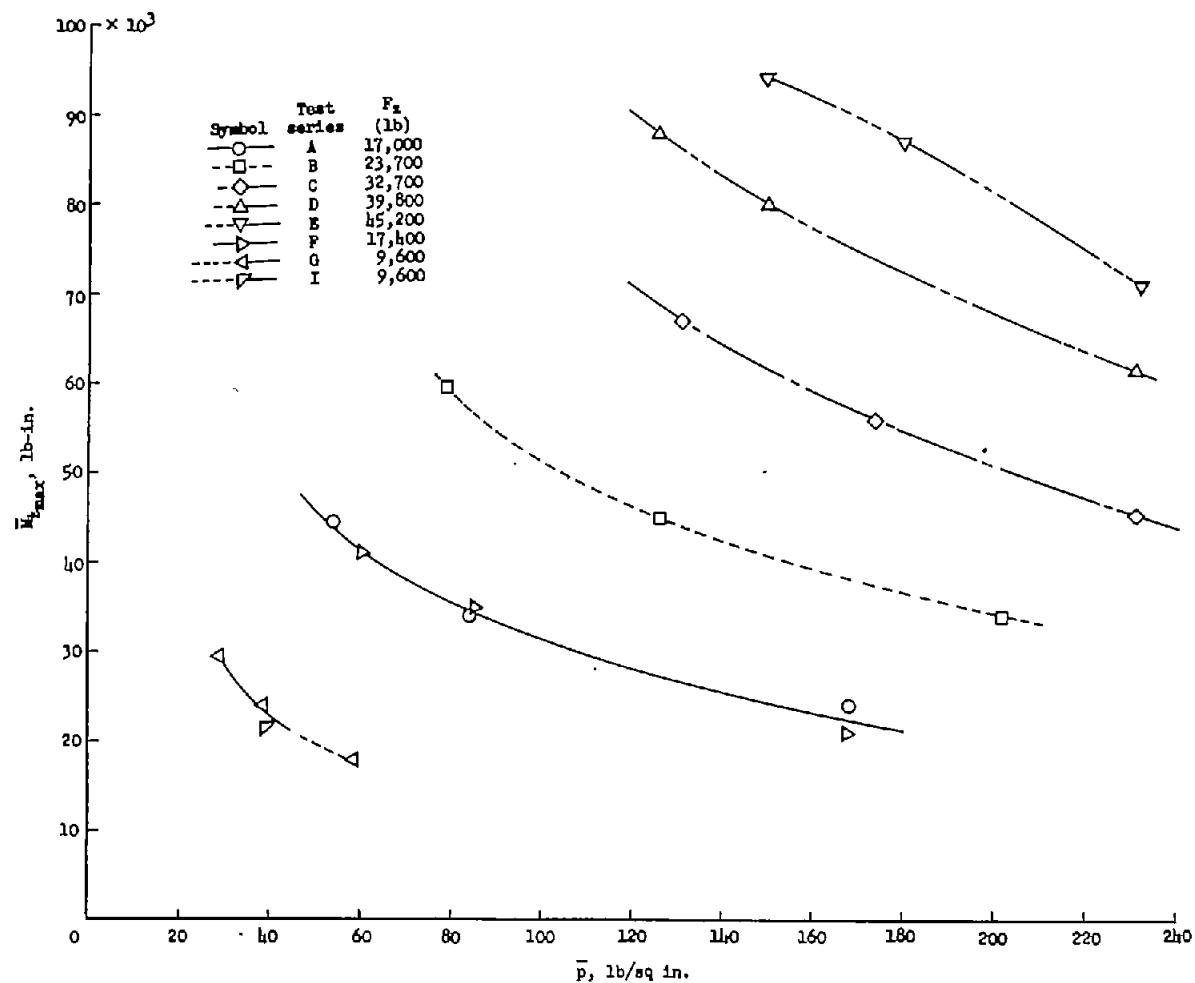
(a) Variation of maximum self-alining torque with inflation pressure.

Figure 30.- Variation of maximum self-alining torque with inflation
pressure and vertical tire deflection.
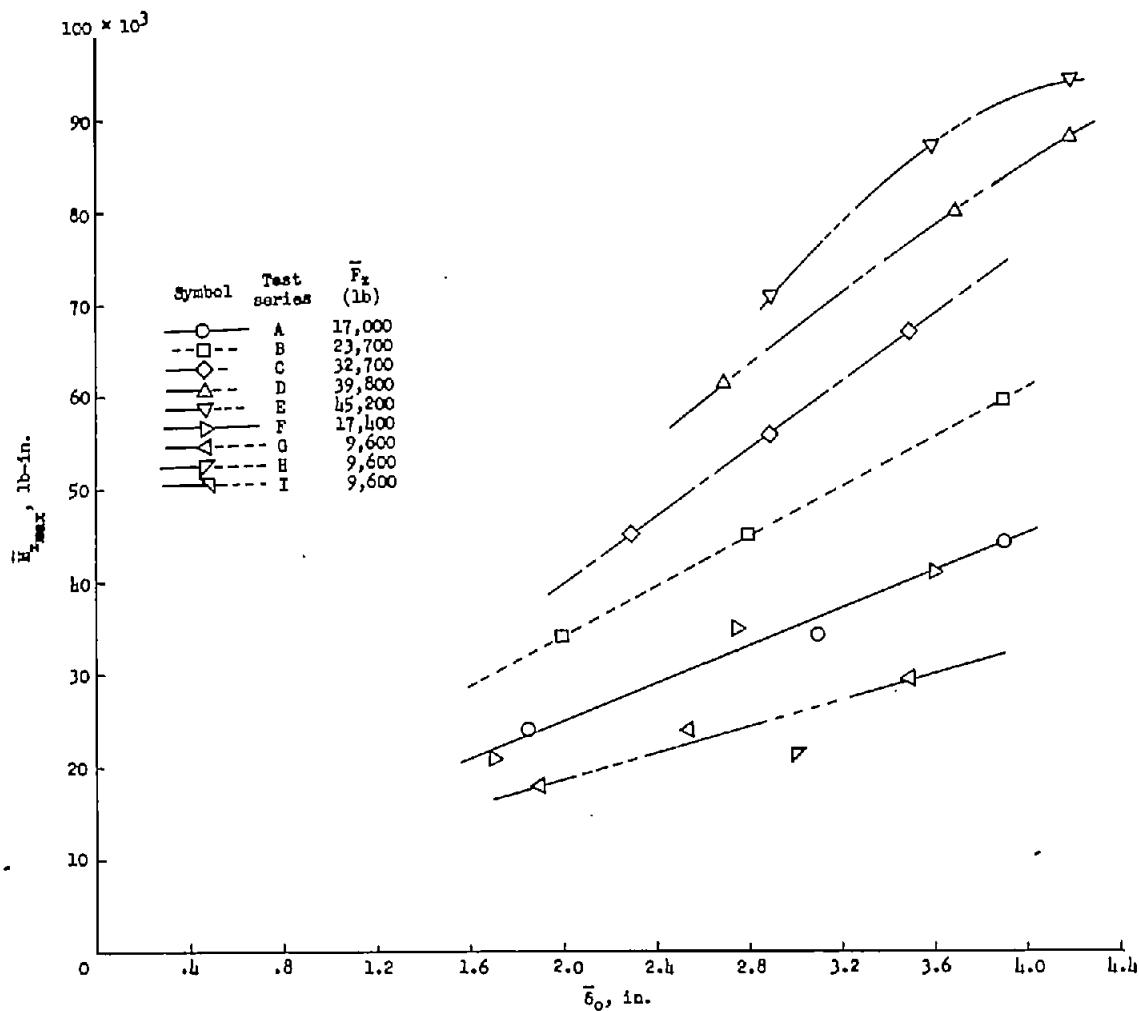
(b) Variation of maximum self-alining torque with vertical tire deflection.

Figure 30.- Concluded.
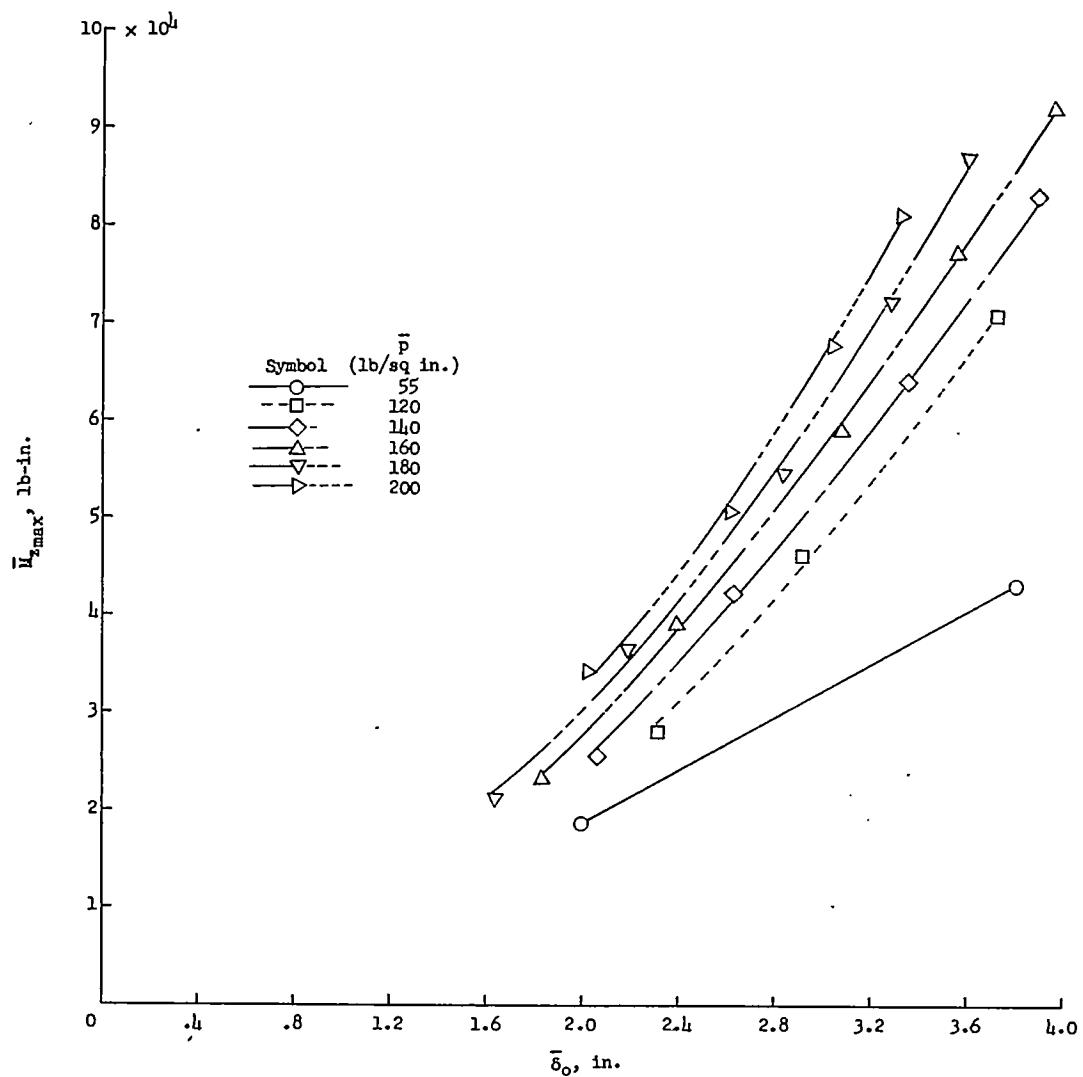
Figure 31.- Variation of maximum self-alining torque with vertical tire
deflection for several constant inflation pressures.
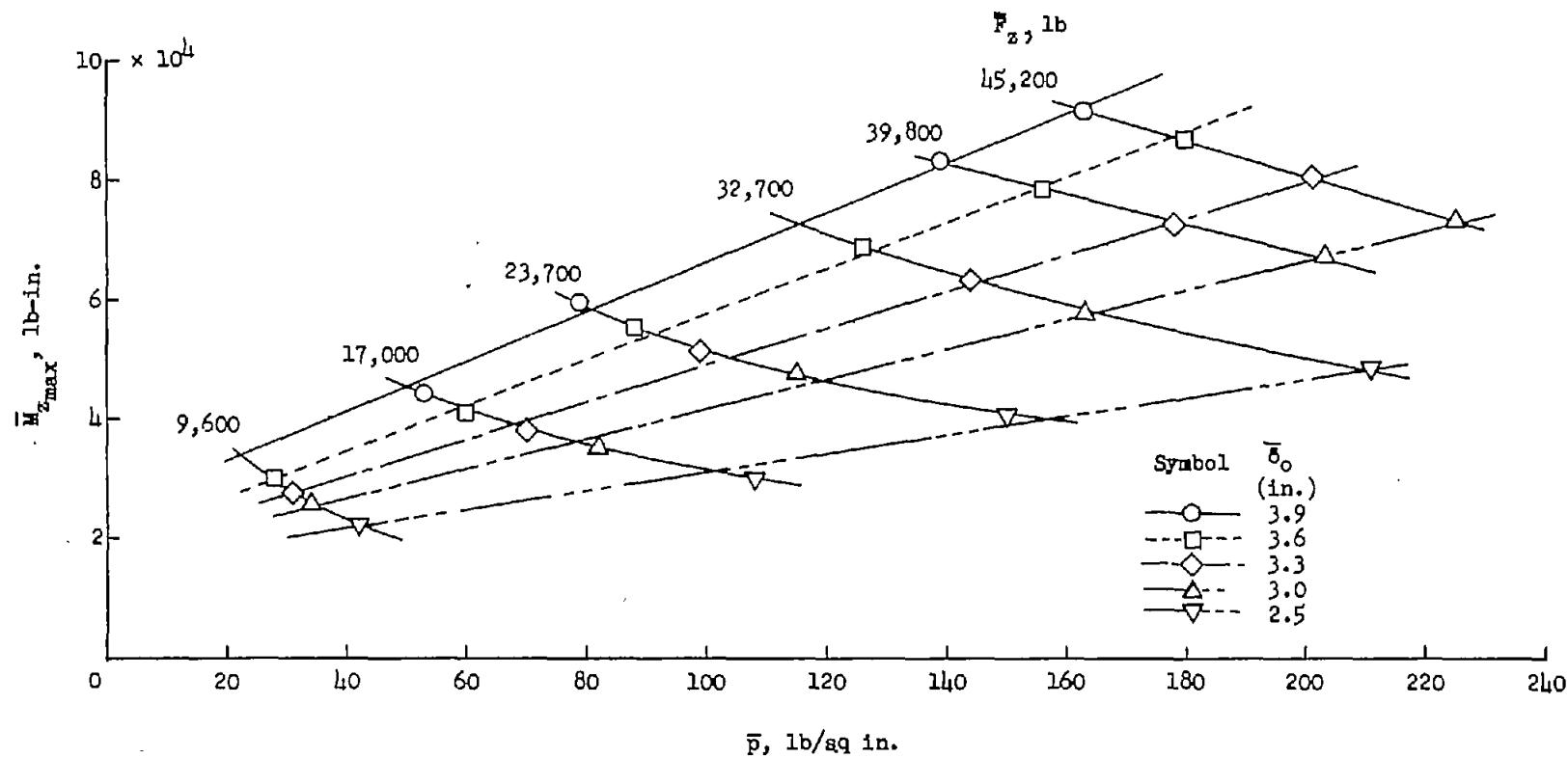
Figure 32.- Variation of maximum self-alining torque with inflation
pressure for several constant vertical tire deflections.
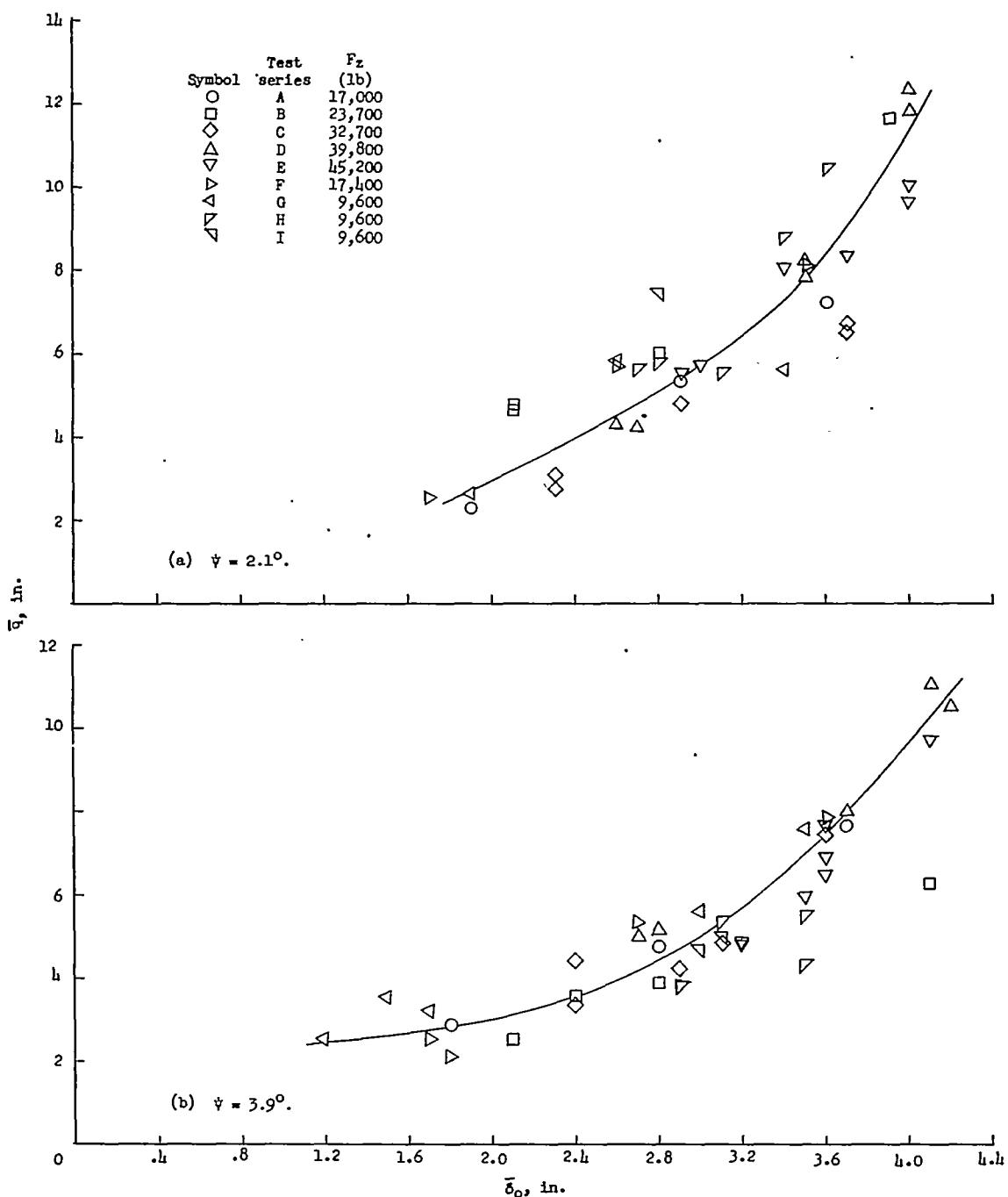
Figure 33.- Variation of pneumatic caster with vertical tire deflection
for the vertical-load and yaw-angle ranges tested.

Symbol	Test series	F_z (lb)
O	A	17,000
□	B	23,700
◇	C	32,700
△	D	39,800
▽	E	45,200
▷	F	17,400
◁	G	9,600
▽	H	9,600
◁	I	9,600

(c) $\Psi = 7.4°$.

(d) $\Psi = 10.9°$.

(e) $\Psi = 14.4°$.

(f) $\Psi = 17.9°$.
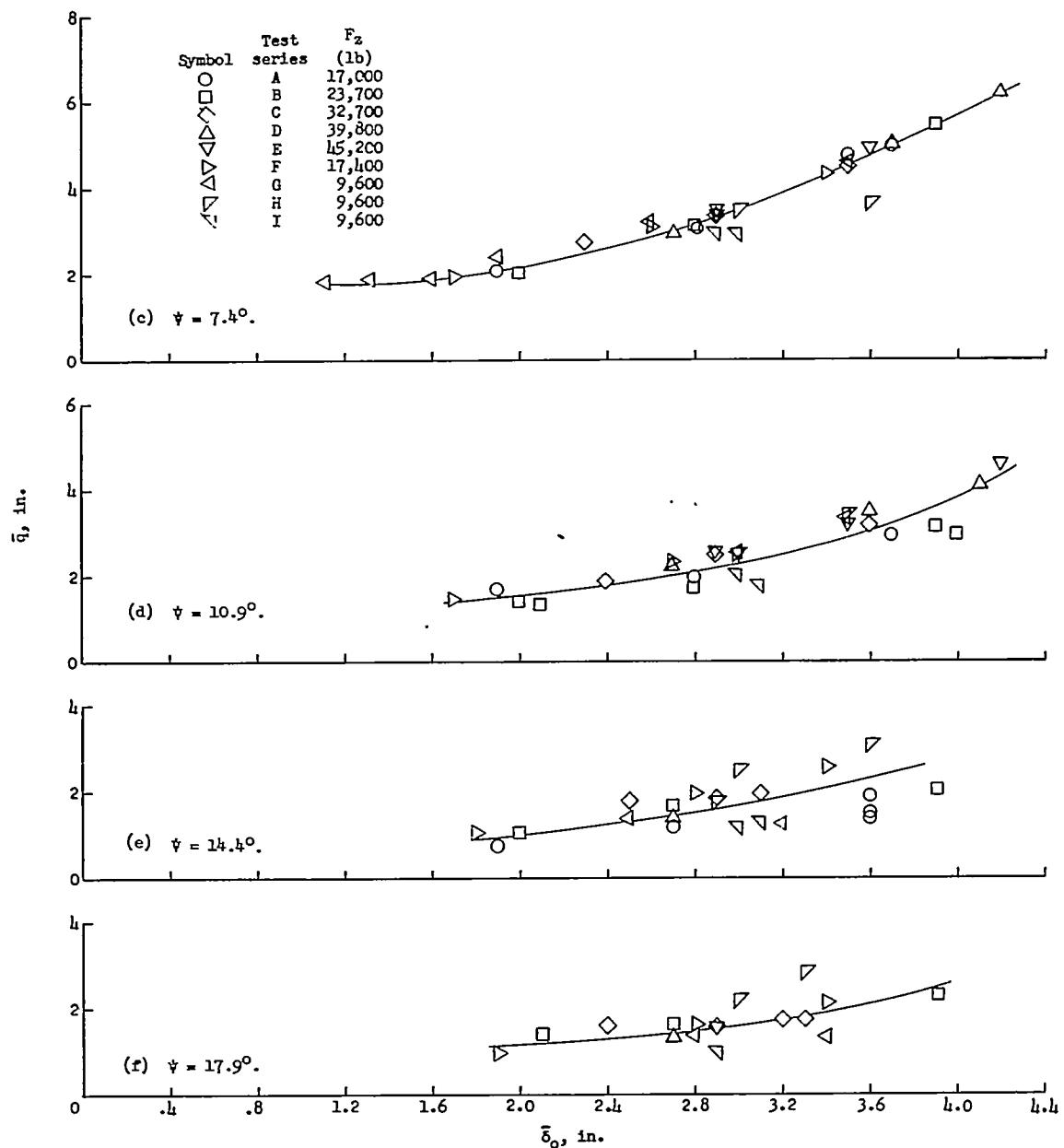
Figure 33.- Concluded.
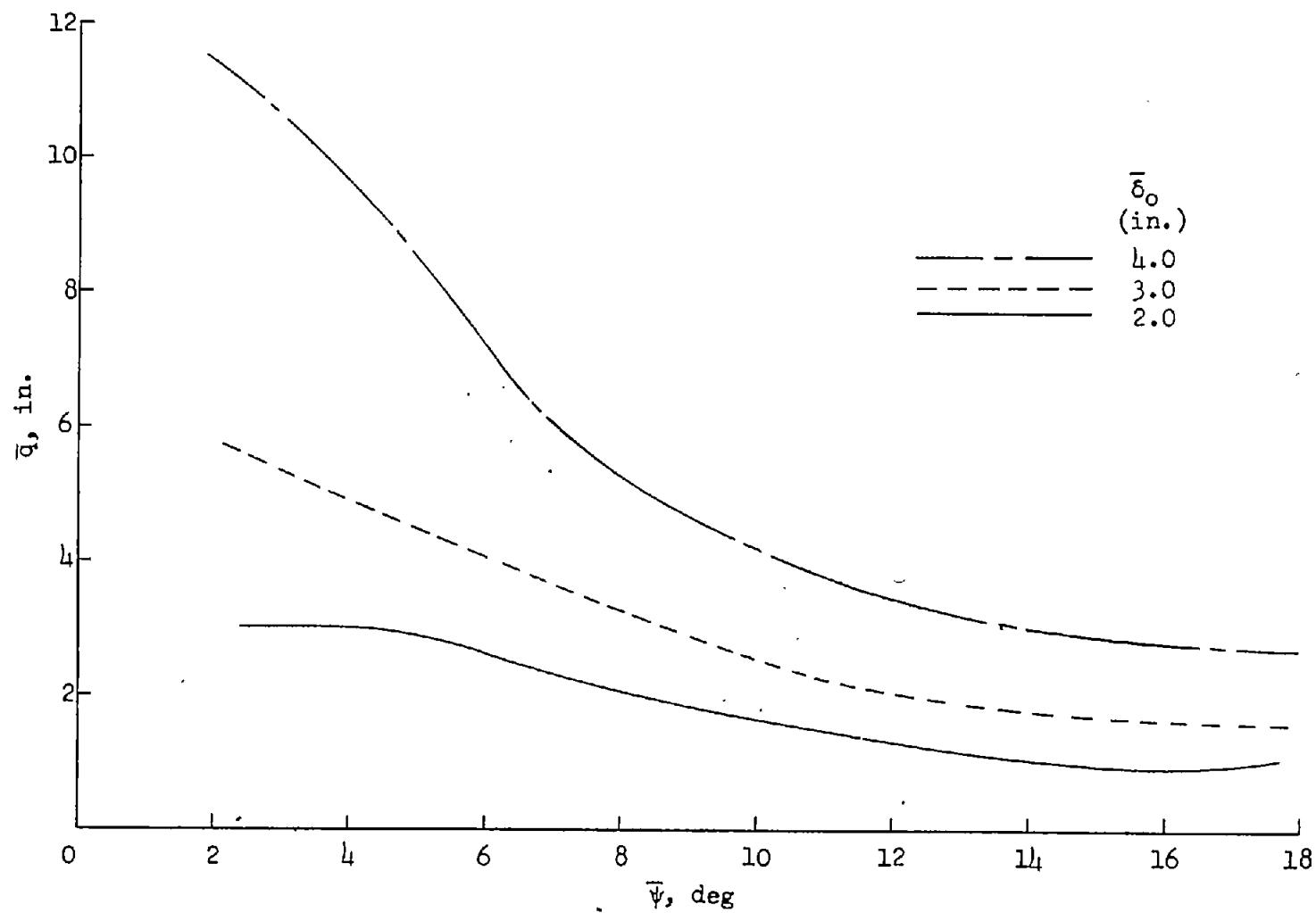
Figure 34.- Variation of pneumatic caster with yaw angle for several constant vertical tire deflections.
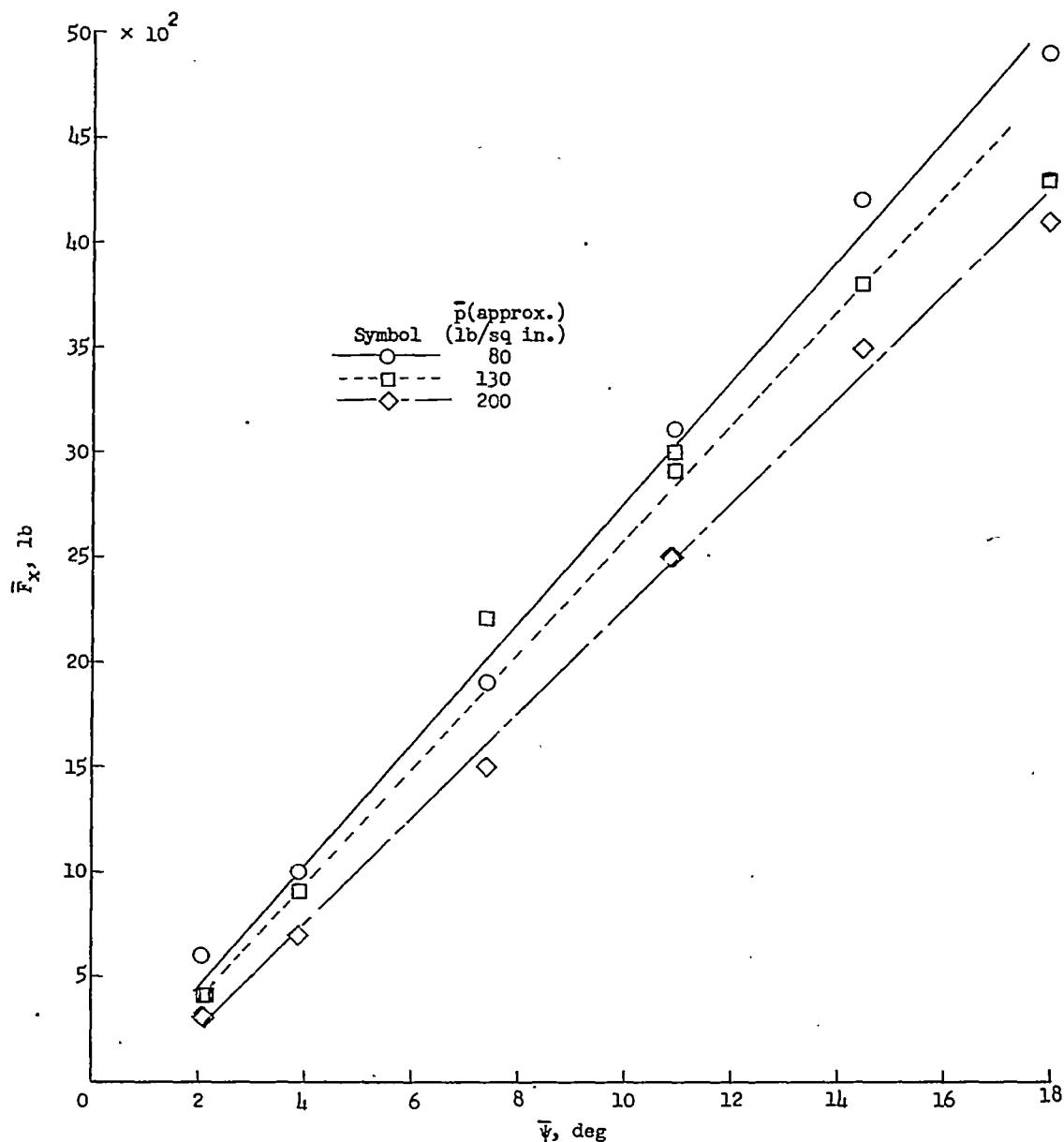
Figure 35.- Variation of drag force with yaw angle for several tire
inflation pressures. (Yawed-rolling tests, test series B;
$\overline{F}_z$ = 23,700 pounds.)
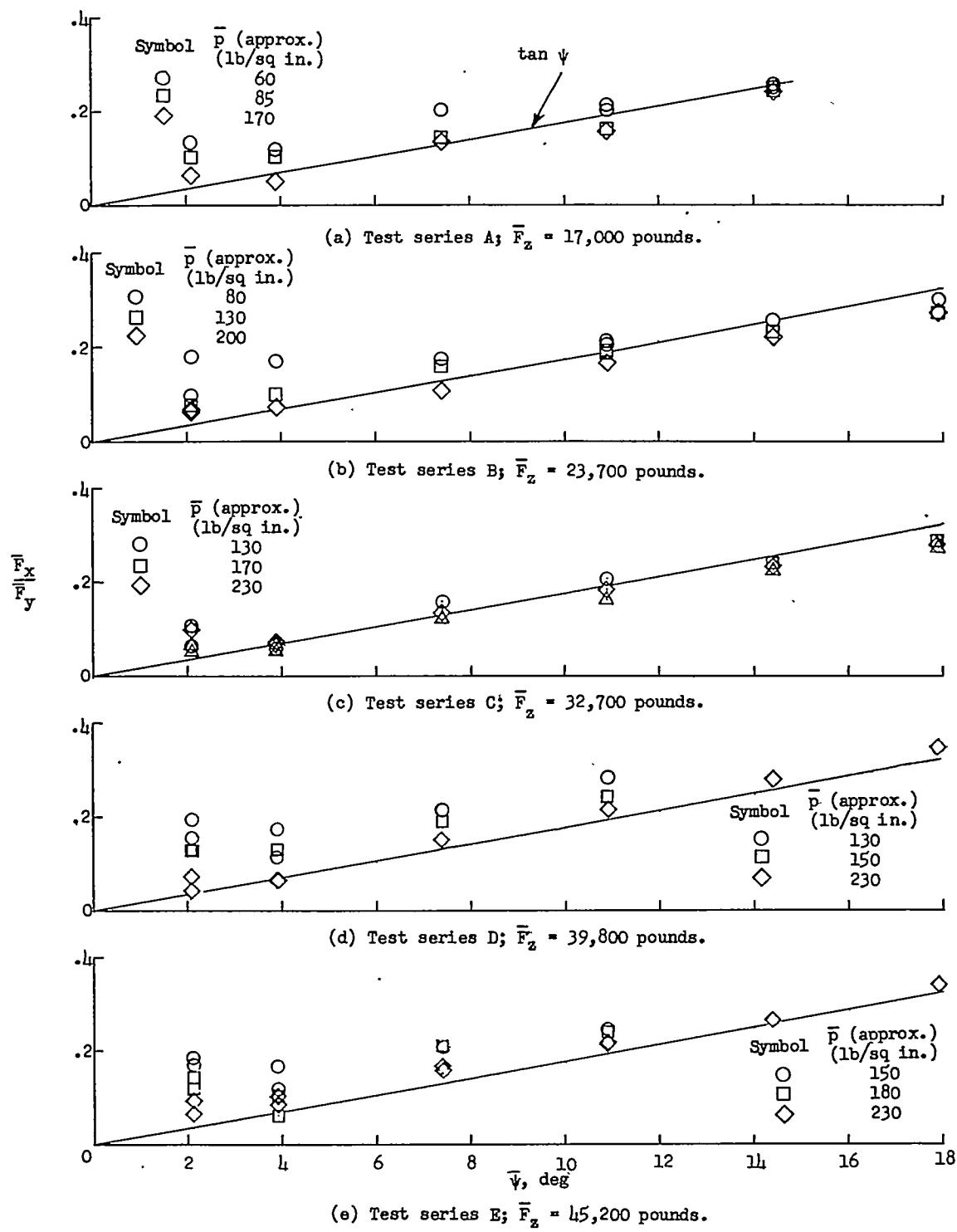
Figure 36.- Variation of the ratio of drag force to cornering
force with yaw angle.

(f) Test series F; $\overline{F}_z$ = 17,400 pounds.

(g) Test series G; $\overline{F}_z$ = 9,600 pounds.

(h) Test series H; $\overline{F}_z$ = 9,600 pounds.

(i) Test series I; $\overline{F}_z$ = 9,600 pounds.
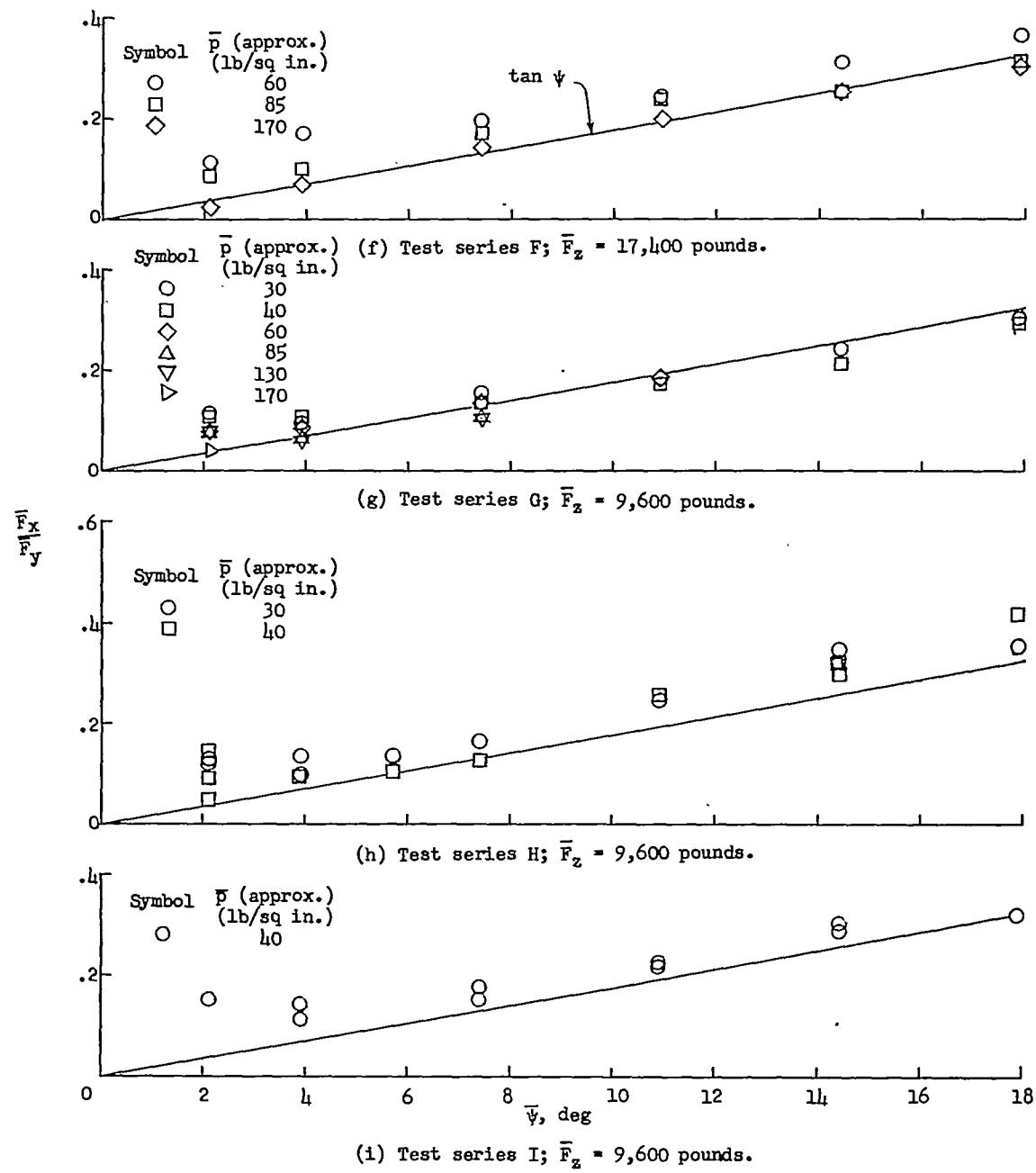
Figure 36.- Concluded.
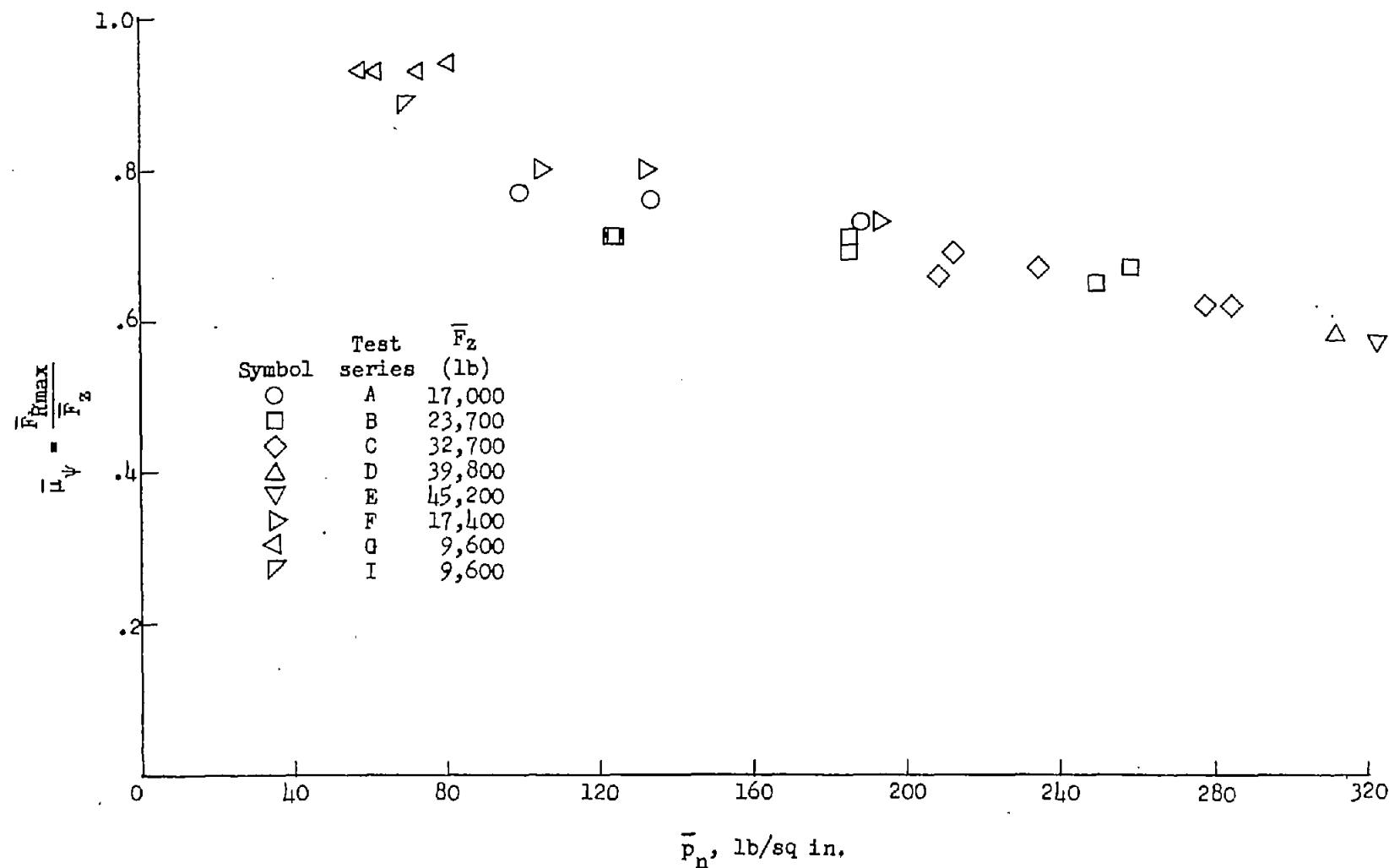
Figure 37.- Variation of yawed-rolling coefficient of friction with average bearing pressure.
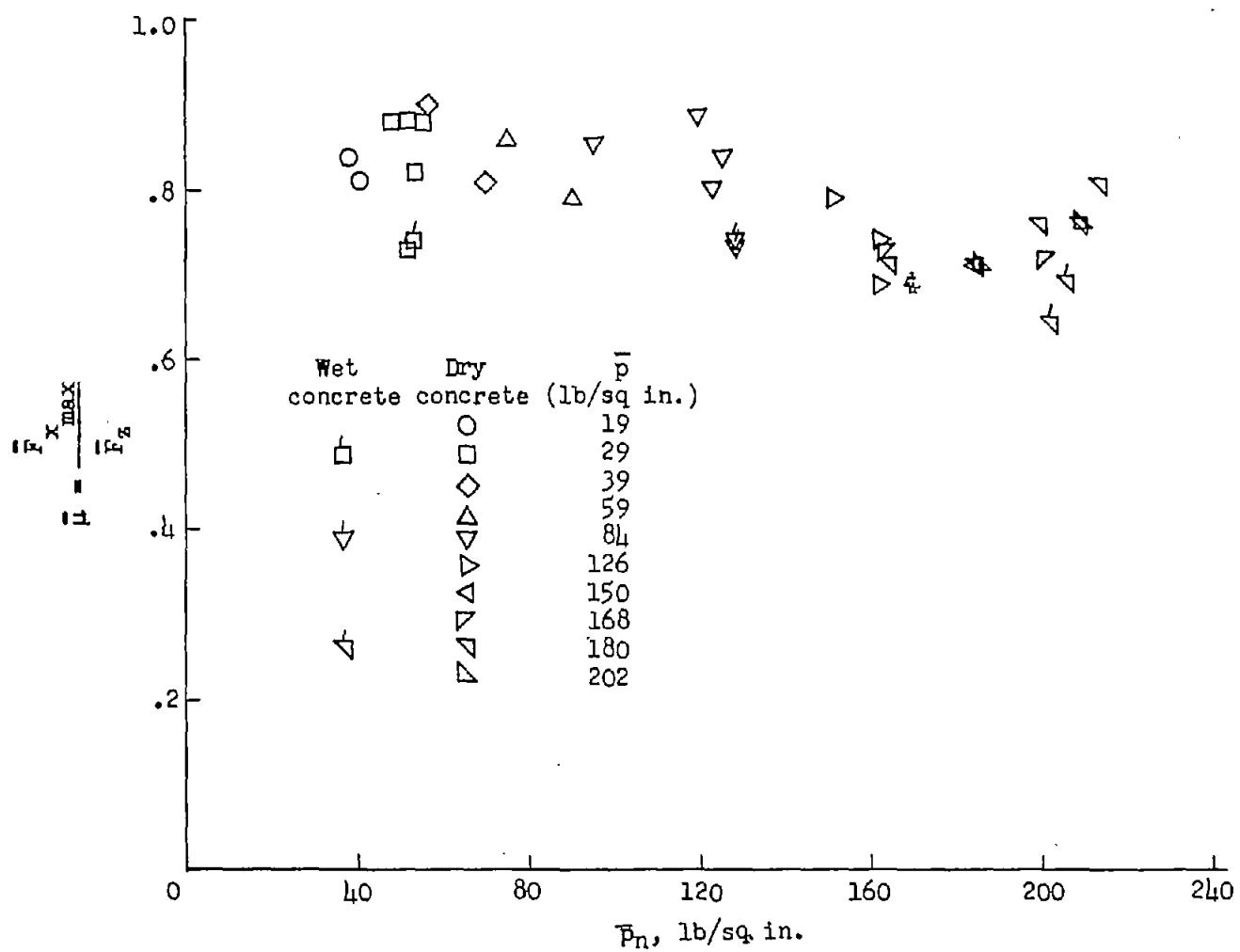
Figure 38.- Variation of sliding drag coefficient of friction with average bearing pressure. $\bar{F}_Z = 9,730 - 0.068F_{x_{max}}$ pounds.

$\bar{\mu}$

Wet
concrete

Dry
concrete

Coefficient
of friction

$\bar{\mu}_\psi$

$\bar{\mu}_x$

$\bar{p}_n$, lb/sq in.
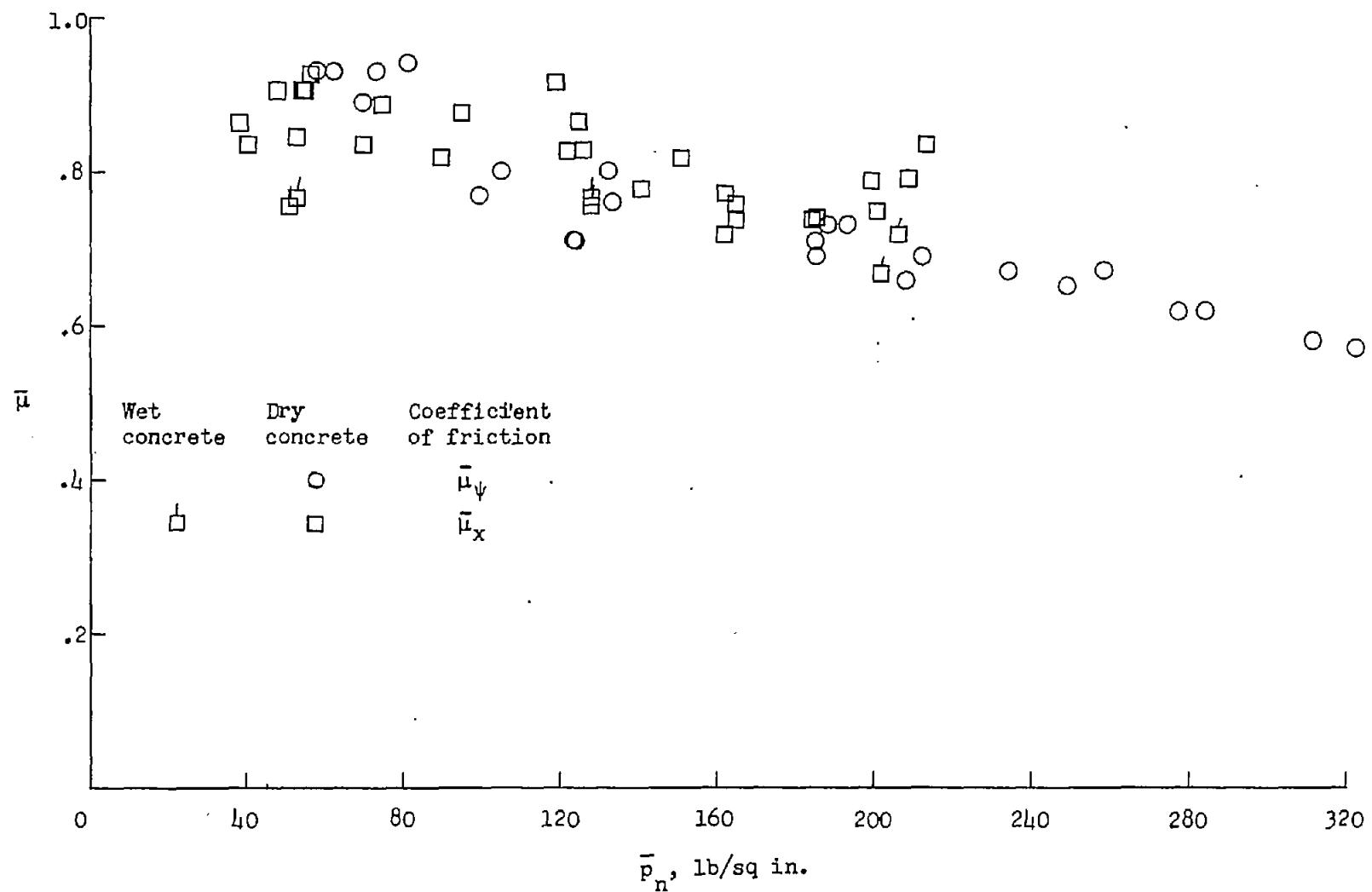
Figure 39.- Comparison of sliding drag and yawed-rolling coefficients
of friction.
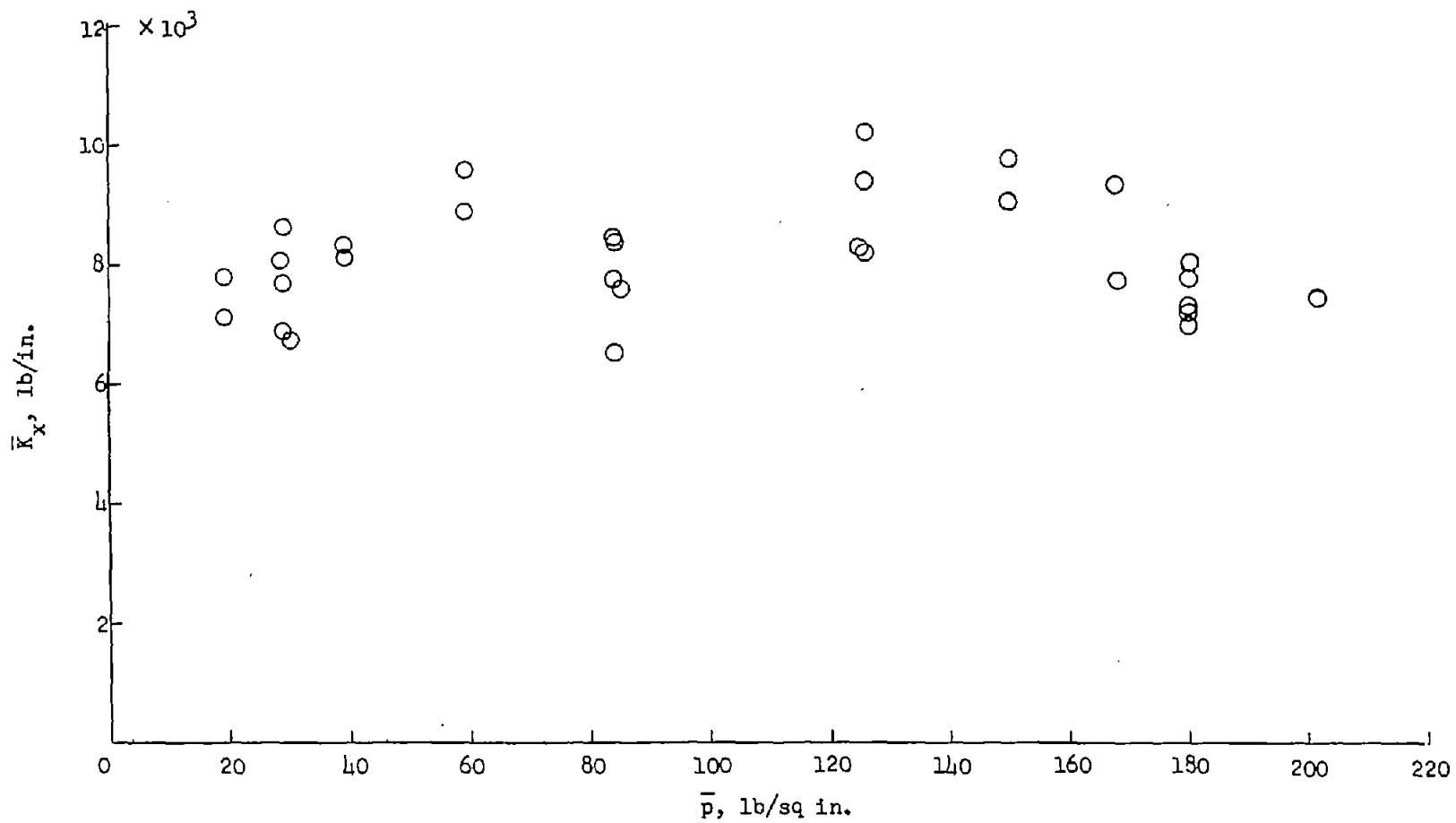
Figure 40.- Variation of fore-and-aft spring constant with tire inflation pressure.
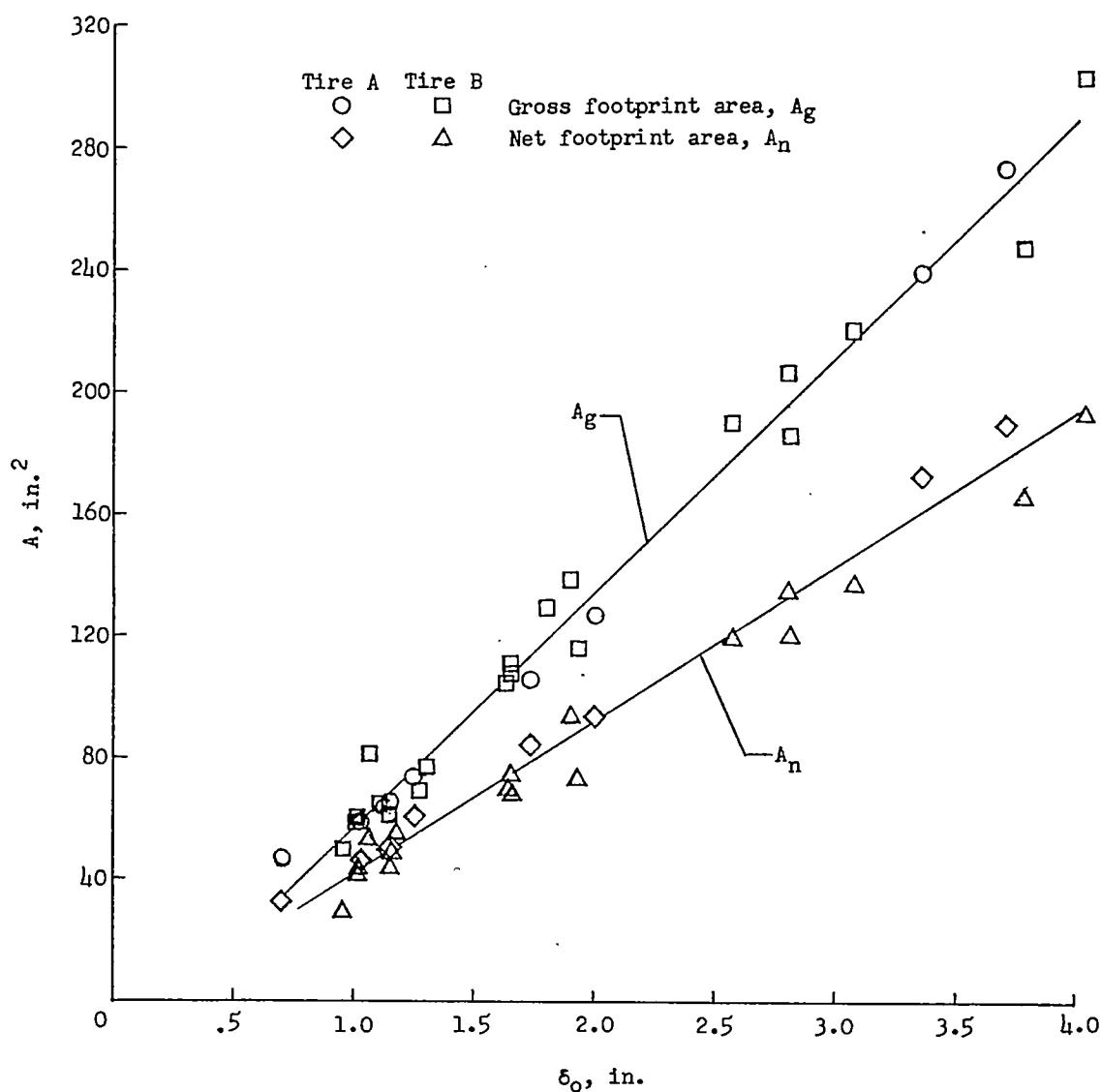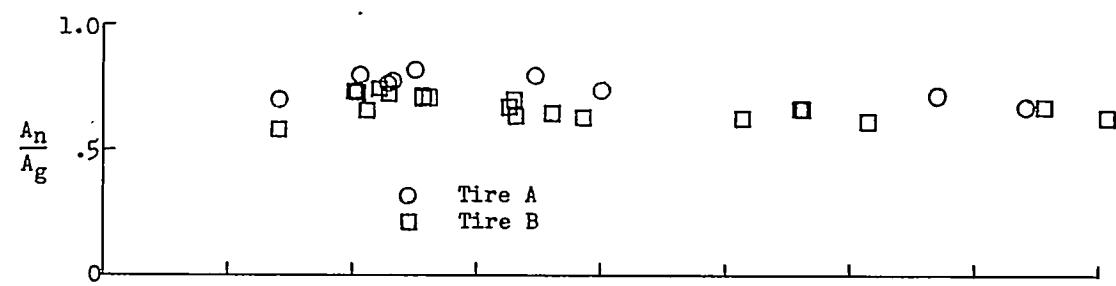
Figure 41.- Variation of gross footprint area, net footprint area, and the ratio of net footprint area to gross footprint area with vertical tire deflection for tires A and B.
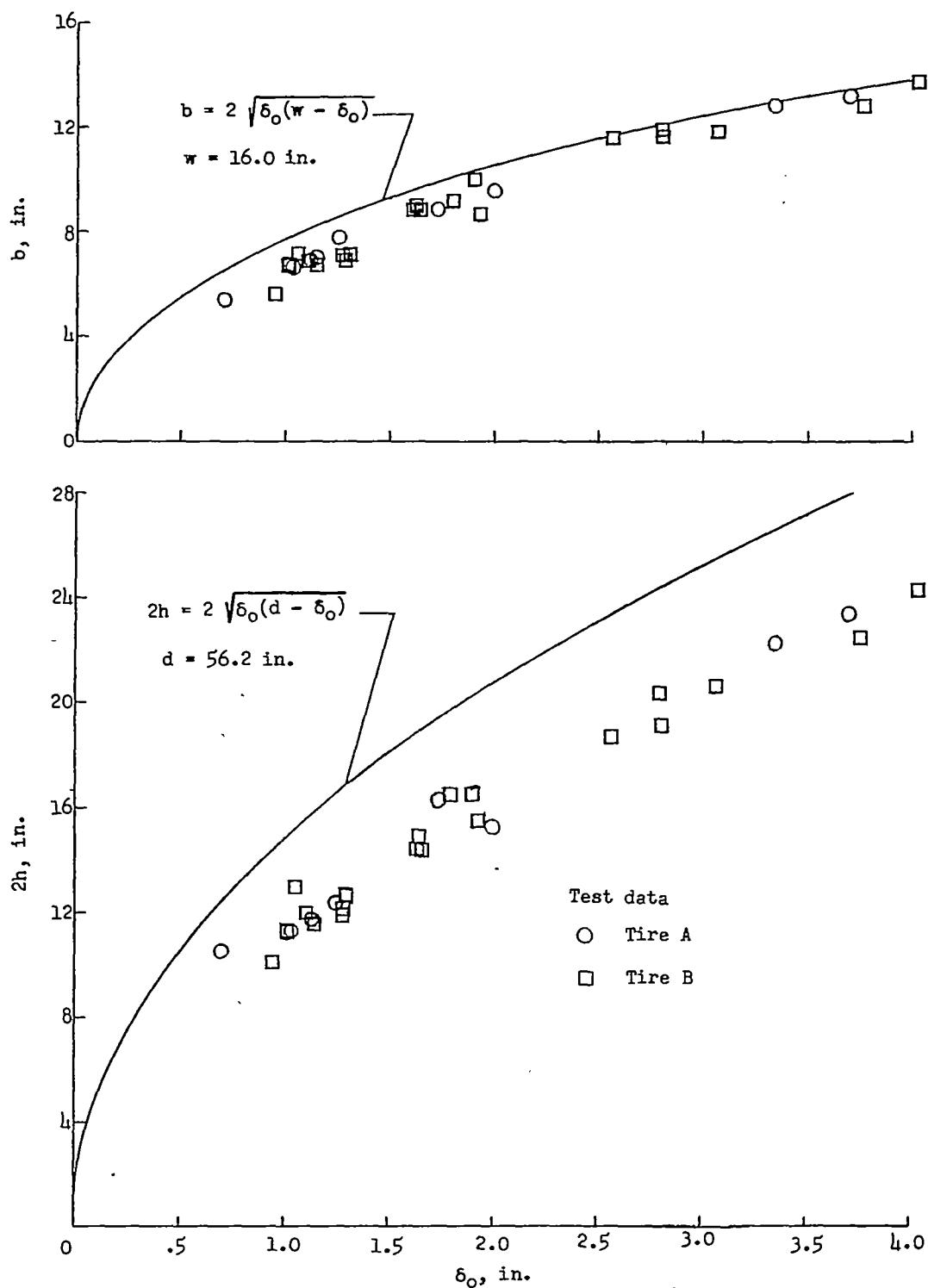
Figure 42.- Variation of footprint length and width with vertical tire deflection. (Solid lines represent chord lengths of circles having diameters equal to the diameter and width at rated inflation pressure.)
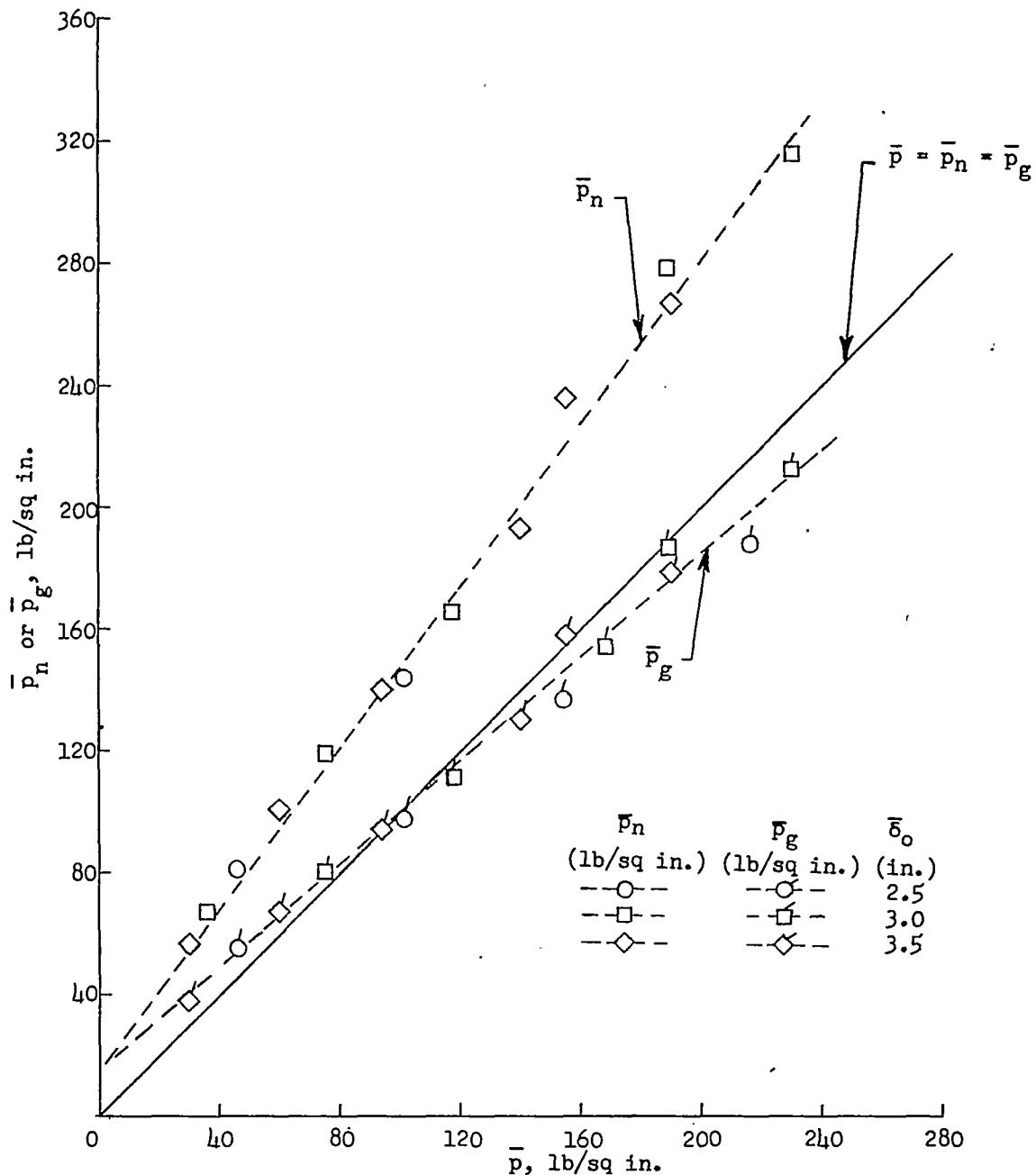
Figure 43.- Variation of average bearing and average gross footprint
    pressures with tire inflation pressure for several constant vertical
    tire deflections.
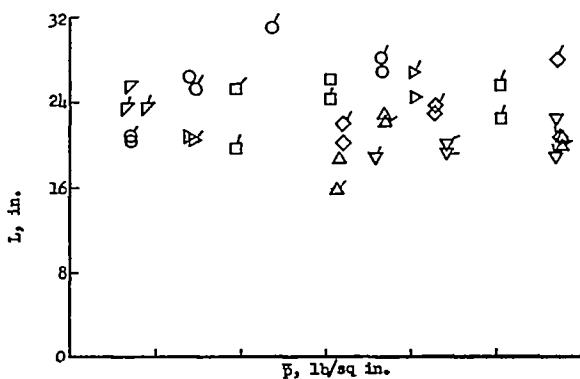
(a) Static-deflection relaxation length L_S. Symbols without flags denote
    tire A values; symbols with flags, tire B values.
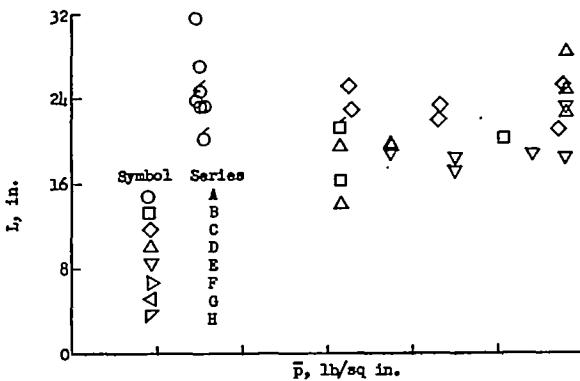
(b) Unyawed-rolling-force relaxation length $\bar{L}_f$ and unyawed-rolling-
    deflection relaxation length $\bar{L}_\lambda$. Symbols without flags are for
    the unyawed-rolling-force relaxation length; symbols with flags,
    unyawed-rolling-deflection relaxation length.
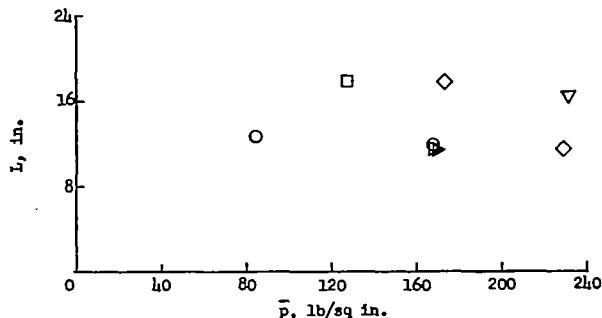
(c) Yawed-rolling relaxation length $\bar{L}_y$.

Figure 44.- Variation of the four types of relaxation length with tire
inflation pressure.
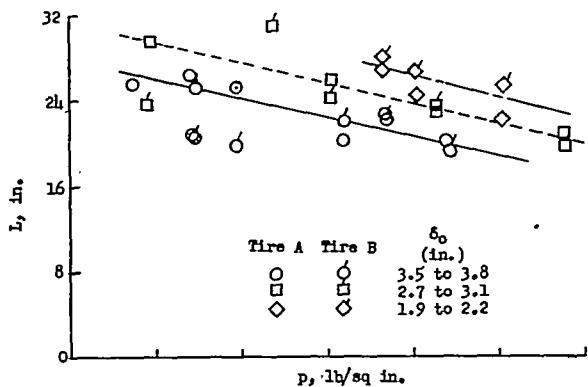
(a) Static-deflection relaxation length L_S.
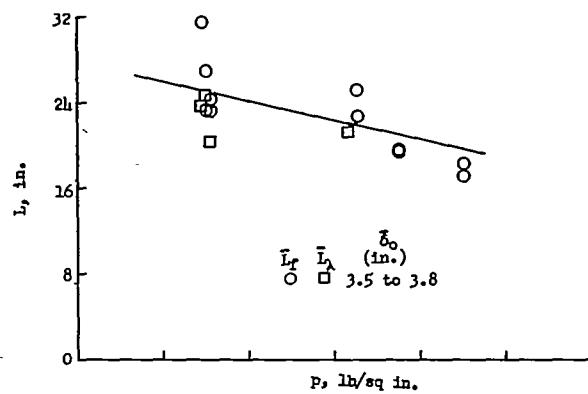
(b) Unyawed-rolling-force relaxation length $\bar{L}_f$ and unyawed-rolling-deflection relaxation length $\bar{L}_\lambda$.
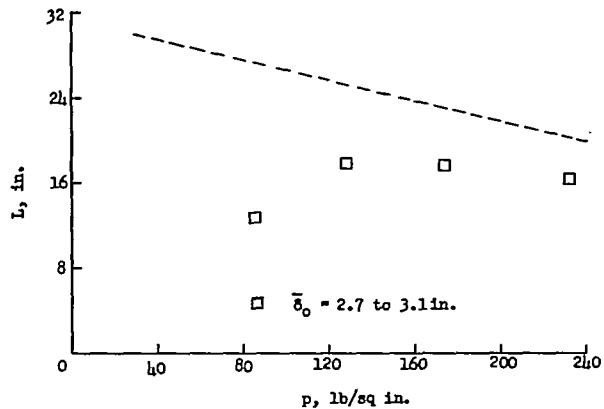
(c) Yawed-rolling relaxation length L_y.

Figure 45.- Variation of relaxation length with tire inflation pressure for several constant vertical tire deflections.
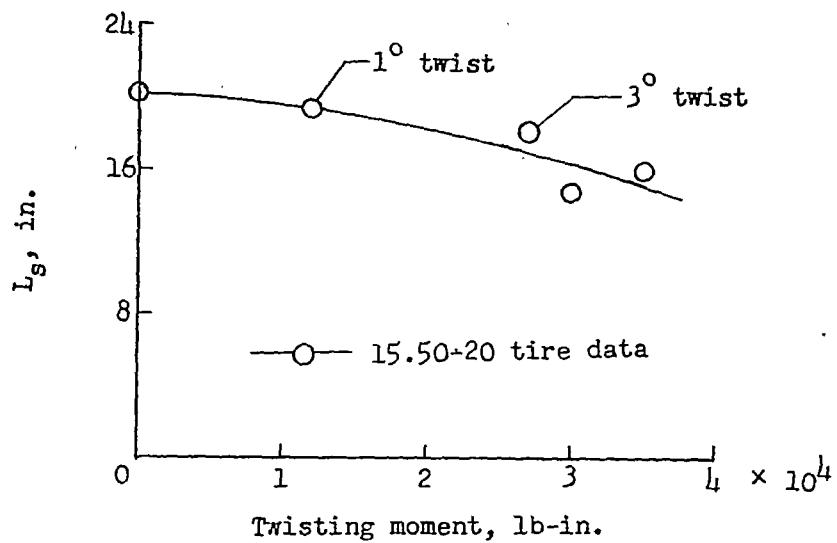
Figure 46.- Variation of static relaxation length with twisting moment
or twist for a 15.50-20, type III, low-pressure tire (tire C of ref. 2).
F_s = 3,000 pounds; F_z = 20,000 pounds; p_o = 81 pounds per square inch;
p = 84 pounds per square inch.
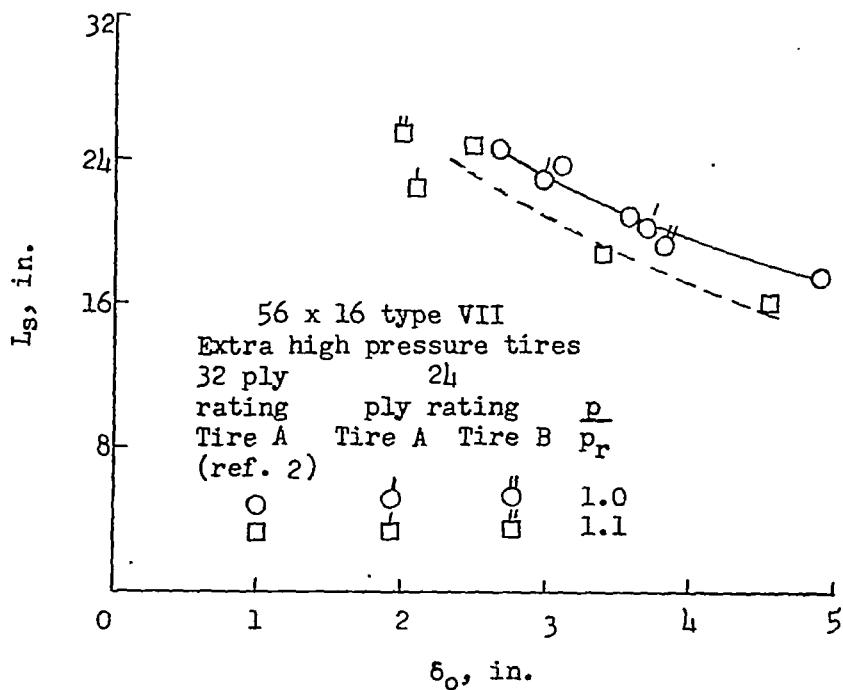
Figure 47.- Comparison of static relaxation lengths obtained from a
56 × 16, type VII, extra high pressure, 32-ply-rating tire (tire A
of ref. 2) with test data.